Cell Intrinsic Plasticity in Leech Touch Neurons

Von der Fakultät für Medizin und Gesundheitswissenschaften

der Carl von Ossietzky Universität Oldenburg

zur Erlangung des Grades und Titels eines

Doktor der Naturwissenschaften / *doctor rerum naturalium* (Dr.rer.nat)

angenommene Dissertation

Von Sonja Meiser

Geboren am 04.08.1991 in Heidelberg

Erstbetreuer: Prof. Dr. Jutta Kretzberg

Zweitgutachter: Apl. Prof. Dr. Karin Dedek

Drittgutachter: Dr. Gerrit Hilgen

Tag der Disputation: 28. Januar 2021

Für Opa

Table of Contents

Abbreviations ..... **I**

List of Figures ..... **II**

List of Tables ..... **III**

Abstract ..... **IV**

Zusammenfassung ..... **VI**

1 Introduction **1**

1.1 Sensory processing of tactile stimuli by mechanoreceptors in the leech 1

1.2 Sensory processing of tactile stimuli by the neuronal network in the leech 4

1.3 Neuronal response flexibility 5

1.4 Aim of the Study 8

1.4.1 Hypothesis 1: Repeated somatic stimulation of leech T cells leads to cell intrinsic plasticity based on Na^+/K^+ pump activity and a K_M current 8

1.4.2 Hypothesis 2: Cell intrinsic plasticity in leech T cells occurs at multiple spike initiation zones (SIZs), which interact with each other 9

1.4.3 Hypothesis 3: Timing and amount of T cell spikes effect network activity 10

2 Materials und Methods **11**

2.1 Animals and preparation 11

2.2 Electrophysiological Technique 11

2.3 Experimental Designs 13

2.3.1 Hypothesis 1: Repeated somatic stimulation of leech T cells leads to cell intrinsic plasticity based on Na+/K+ pump activity and a KM current 14

2.3.2 Hypothesis 2: Cell intrinsic plasticity in leech T cells occurs at multiple spike initiation zones (SIZs), which interact with each other 16

2.3.3 Hypothesis 3: Timing and amount of T cell spikes effect network activity 17

2.4 Data Analysis 20

2.4.1 Electrophysiological Current Clamp Recordings 20

2.4.2 Voltage Sensitive Dye Imaging 23

2.5 Neuron Modelling 24
2.5.1 Model Structure 24
2.5.2 Model Fitting 26
2.6 Cell staining 27

3 Results 28

3.1 Repeated somatic current injection induces cell intrinsic plasticity in T cells due to increased Na^+/K^+ pump activity and a slow potassium current (K_M) 29
3.1.1 Repeated somatic current injection increases SC and IR and hyperpolarizes RMP 29
3.1.2 Na^+/K^+ pump and a slow potassium current might induce cell intrinsic plasticity 31
3.1.3 Na^+/K^+ pump inhibition decreases SC in T cells after repeated stimulation 34
3.1.4 Different holding potentials triggers different SC in T cells 37
3.2 Cell intrinsic plasticity occurring at multiple spike initiation zones (SIZs) interact 39
3.3 Timing and amount of T cell spikes effect network activity 42
3.3.1 Non-synaptic plasticity effects postsynaptic responses of other T cells 42
3.3.2 Timing of T cell spikes effects response of postsynaptic interneurons 44
3.3.3 T cell spikes trigger network activity 46

4 Discussion 48

4.1 Cellular basis of non-synaptic plasticity 48
4.2 Non-synaptic plasticity might tune the relative impact of different computational tasks in T cells 52
4.3 T cell as a key player for eliciting network activity 54
4.4 Reflection 56
4.4.1 Experimental limitations 56
4.4.2 Data Analysis limitation 57
4.5 Conclusion 58
4.6 Outlook 58
4.6.1 Cellular basis of non-synaptic plasticity 59
4.6.2 T cells as key players for eliciting network activity 59

5 References 61

APPENDIX I

Publication II

Contributions of collaborators XVII

Curriculum Vitae XVIII

Danksagungen XX

Erklärung XXI

Abbreviations

μm	Micrometer
CNS	Central nervous system
IN	Interneuron
IR	Input resistance
ISI	Interspike interval
LAT	Latency
min	Minute
mM	Millimolar
ms	Millisecond
mV	Millivolt
nA	Nanoampere
PR	Postsynaptic response
PSP	Postsynaptic potential
(R)MP	(Resting) membrane potential
ROI(s)	Regions of interest(s)
SC	Spike count
sec	Sec
SIZ(s)	Spike initiation zone(s)
VSD	Voltage sensitive dye

List of Figures

Figure 1 | The central nervous system of the leech 2

Figure 2 | Neuronal activity and flexibility 6

Figure 3 | Schematic drawing of the experimental setup 12

Figure 4 | Protocol Pseudorandomized 14

Figure 5 | Protocol Pharmacology 15

Figure 6 | Protocol Different Baselines 16

Figure 7 | Protocol Tactile Stimulation 17

Figure 8 | Protocol Pulse Packages 18

Figure 9 | Protocol Interneurons. 19

Figure 10 | Protocol Intracellular stimulation in VSD recordings. 20

Figure 11 | Experimental design and data analysis 22

Figure 12| Voltage Sensitive Dye Imaging 24

Figure 13 | Repeated somatic current injection effects physiological properties of T cells. 30

Figure 14 | Modeling T cell spike responses. 33

Figure 15 | Pharmacological Block of Na+/K+ pump changes somatic SC of T cells 36

Figure 16| The same amount of somatic current injection in T cells induce different SCs on different holding potentials 38

Figure 17 | Repeated tactile stimulation of the ventral midline effects physiological properties of T cells. 42

Figure 18 | Effect of repeated somatic current stimulation on the communication between two ipsilateral T cells 44

Figure 19 | Exemplary postsynaptic responses of the local bend INs 157 and 212 to different numbers of presynaptic T cell spikes with either 1 ms ISI or 50 ms ISI 45

Figure 20| Identification of Interneurons involved in the processing of tactile stimuli based on VSD recordings 47

List of Tables

Table 1 | Experimental sets for the analysis of the effect of repeated mechanoreceptor stimulation 13

Table 2 | T cell model equations. 25

Table 3 | T cell model parameters. 26

Table 4 | Absolute values for non-synaptic plasticity effects in T cells. 31

Table 5 | Absolute SC for DHO blocking experiments 35

Table 6| Absolute values for non-synaptic plasticity effects in T cells induced by tactile skin stimulation. 40

Abstract

Behavioral reactions to sensory stimuli are based on neuronal activity. One fundamental goal in neuroscience is to understand how neurons code and process sensory information to elicit a suitable behavioral reaction. The medicinal leech produces, in response to a light touch of the skin, a precise movement away from the touch location. This behavior, which is called local bend – results from a three-layered network consisting of ~ 50 neurons. Within the first layer, three types of mechanosensory neurons: touch (T) cells, pressure (P) cells and noxious (N) cells process the information about the touch.

Previous studies indicate that besides the P and the N cell, the T cell might also play a role in eliciting reactions in response to tactile stimulation (Kretzberg et al., 2016; Frady et al., 2016; Fathiazar et al., 2018). It is already known that the position of the tactile stimulation can influence the elicited behavior (Esch and Kristan, 2002). However, it remains to be investigated whether repeated tactile stimulation affects the behavioral outcome by changes in the neuronal network. Since neuronal response flexibility might already start with changes in individual spike responses (Mozzachiodi and Byrne, 2010) this doctoral thesis investigates the biophysical properties, that underlie response flexibility in T cells and their postsynaptic targets.

The morphology and response properties of T cells suggest that they have at least two spike initiation zones, one in the periphery and one in the central ganglion. While spikes of the T cell that are generated in the periphery should faithfully represent mechanical skin stimulation, the central part of the T cell integrates synaptic inputs from all three mechanoreceptor types. Using experimental and theoretical approaches, this doctoral thesis shows that two complementary mechanisms, following repeated T cell stimulation, seem to increase the probability for centrally elicited spikes in response to synaptic inputs from the other mechanoreceptors.

An activity dependent increase in Na^+/K^+ pump activity hyperpolarizes the membrane potential, which deactivates at the same time a putative slow K^+-current. Closing of these putative M-type channels due to hyperpolarization increases the IR of the cell, leading to a larger number of spikes. By this mechanism, the response behavior of the T cell further switches from rapidly to slowly adapting spiking. This in turn increases excitatory postsynaptic potential size of coupled T cells and affects the activity of the neuronal network (Meiser et al., 2019). Stimulating a ventral T cell by repeated rhythmic touch of the skin at the ventral midline activates the peripheral spike initiation zone (SIZ). Peripherally evoked spikes propagate to the central part of the T cell and trigger there Na^+/K^+ ATPase activity. The combination of both cell-intrinsic plasticity mechanisms (peripheral habituation and central sensitization) could therefore cause a flexible shift in the relative impact of different computational tasks. This could lead to a higher sensitivity for processing synaptic inputs, but diminished responses to tactile stimulation.

Furthermore, electrophysiological and imaging results show that timing and amount of T cell spikes trigger neuronal network activity. This suggests that every single T cell spike might be important in eliciting network activity and supports the hypothesis that the T cell is a key player in eliciting different behavioral responses.

The fundamental computational principles of sensory information processing, investigated in this thesis, could be of relevance beyond the leech system. They comprise the basis for the question of how behavioral response flexibility might depend on a specific cellular mechanism. Due to the high degree of similarities between the tactile systems of the leech and human (Burrell and Li, 2008; Pirschel and Kretzberg, 2016), the insights obtained in this thesis could inspire biomedical research, e.g., for optimizing tactile interfaces for hand prostheses (Downey et al., 2020).

Zusammenfassung

Verhaltensreaktionen auf sensorische Reize basieren auf neuronaler Aktivität. Eine grundlegende Frage der Neurowissenschaften ist es herauszufinden, wie Nervenzellen sensorische Informationen kodieren und verarbeiten, um ein passendes Verhalten auszulösen. Der medizinische Blutegel erzeugt auf eine leichte Berührung der Haut eine präzise Biegung weg von der Stelle des Kontakts. Dieses Verhalten wird local bend genannt. Es resultiert aus einem kleinen dreischichtigen Netzwerk von ungefähr 50 Neuronen innerhalb eines Ganglions. Auf erster Netzwerkebene kodieren dabei drei Typen von Mechanorezeptoren (Touch/Tast (T)-Zellen, Pressure/Druck (P)-Zellen und Noxious/Schmerz (N)-Zellen) die Information über die Berührung.

Frühere Studien weisen darauf hin, dass neben den P-Zellen und den N-Zellen, auch die T-Zellen wichtig sein könnten, um Reaktionen auf verschiedene taktile Stimulationen auszulösen (Frady et al., 2016; Kretzberg et al., 2016; Fathiazar et al., 2018). Bisher ist bereits bekannt, dass die Position der Berührung das Verhalten beeinflussen kann (Esch and Kristan, 2002). Es ist jedoch noch nicht untersucht worden, ob auch eine wiederholte Hautstimulation das Verhalten beeinflusst und damit die Aktivität im neuronalen Netzwerk verändert. Da die Flexibilität in der neuronalen Antwort auf einen Stimulus bereits von der Reaktion einer einzelnen Zelle beeinflusst wird, (Mozzachiodi and Byrne, 2010) ist das Ziel dieser Doktorarbeit herauszufinden, ob sich eine wiederholte Stimulation auf die biophysikalischen Eigenschaften von T-Zellen auswirkt.

Die Morphologie und Reaktionseigenschaften der untersuchten T-Zellen legen nahe, dass sie mindestens zwei Spike-Initiationszonen (SIZs) aufweisen, eine in der Peripherie und eine im zentralen Ganglion. In der Peripherie erzeugte Aktionspotentiale sind die Antwort auf mechanische Hautstimulation. Die zentrale SIZ in der Nähe des Somas verarbeitet die synaptischen Eingänge von anderen Zellen.

Diese Doktorarbeit zeigt aus einer Kombination von experimentellen Analysen und theoretischen Ansätzen, dass zwei komplementäre Mechanismen, als Reaktion auf wiederholte Stimulation, die Wahrscheinlichkeit für im Soma ausgelöste Spikes, als Reaktion auf synaptische Eingänge anderer Zellen, zu erhöhen scheinen.

Ein aktivitätsabhängiger Anstieg der Na^+/K^+-Pumpenaktivität hyperpolarisiert das Ruhemembranpotential. Diese Hyperpolarisation führt zu einer Schließung von K^+ Kanäle vom mutmaßlichen M-Typ, was wiederum den Eingangswiderstand der Zelle vergrößert. Die daraus resultierende erhöhte passive Antwort führt zu einer größeren Anzahl von Spikes in der T-Zelle. Durch diesen Mechanismus wechselt dann das Spikereaktionsverhalten von transient zu tonisch. Diese Änderung im Spikeverhalten wirkt sich auch auf andere T-Zellen auf derselben Seite des Ganglions aus, die über eine Kombination aus elektrischen und chemischen Synapsen verbunden sind.

Die Stimulation einer ventralen T-Zelle durch wiederholte rhythmische Berührung der Haut führt zu einer Aktivierung der peripheren SIZ. Die Anzahl der generierten Aktionspotentiale nimmt hierbei mit wiederholter Berührung ab. Das zeigt, dass zellinterne Plastizitätsmechanismen an mehreren SIZs auftreten können. Weiterhin wandern peripher ausgelöste Spikes in Richtung des Somas und lösen dort eine erhöhte Na^+/K^+

Pumpenaktivität aus. Das macht sich in einem Anstieg der Spikefrequenz und des Eingangswiderstandes sowie einer Membranpotentialhyperpolarisation bemerkbar.

Die Kombination von peripherer Habituation und zentraler Sensitivierung könnte dazu führen, dass die Wichtigkeit der Verarbeitung verschiedener Informationen (taktiler Input vs. synaptischer Input) je nach vorheriger Aktivität flexibel verändert werden kann.

Weitere Ergebnisse aus elektrophysiologischen und *Imaging* Experimenten dieser Arbeit zeigen, dass der Zeitpunkt und die Anzahl von T-Zell-Spikes die neuronale Netzwerkaktivität beeinflusst. Außerdem scheint die Aktivität einer einzelnen T Zelle auszureichen, um im neuronalen Netzwerk Aktivität auszulösen. Dies stützt die Hypothese, dass die T-Zelle ein wichtiger Bestandteil bei der Aktivierung von Netzwerkaktivität ist und damit eventuell auch das Verhalten beeinflussen könnte.

Zusammengefasst können die Ergebnisse dieser Doktorarbeit als Grundlage dienen, die Frage zu beantworten, wie die Flexibilität einer Verhaltensreaktion von einem bestimmten zellulären Mechanismus abhängen kann. Aufgrund der hohen Ähnlichkeit zwischen den Tastsystemen von Blutegel und Mensch (Burrell und Li, 2008; Pirschel und Kretzberg, 2016) könnten die Ergebnisse dieser Studie auch die biomedizinische Forschung inspirieren und damit vielleicht einen Beitrag zur Optimierung von Handprothesen leisten (Downey et al., 2020).

1 Introduction

Imagine you touched a hot plate, and you realize that this is painful, but you cannot remember it the next time, you will probably end up burning your fingers again. The ability to learn is a fundamental evolutionary achievement and gives each animate being the ability to use prior experiences for adapting to their environment (Kandel and Tauc, 1965a, 1965b). Behavioral reactions to sensory, stimuli like the described reaction to a hot plate, are based on neuronal activity. Therefore, one fundamental goal in neuroscience is to understand how neurons code and process sensory information to elicit behavioral reactions. Assuming that general neuronal strategies for eliciting behaviors are the same in all animals with a central nervous system (Kristan et al., 2005) the investigation of sensory processing is of general interest. The resulting findings might be transferable to the human system and could be the basis for the understanding of neurological disorders (Downey et al., 2020).

However, most nervous systems are too large and too complex to understand. Therefore, a good experimental configuration is required, to monitor the link between stimulus and behavior. For this purpose, the reference model system should be simple to observe, maintain and prepare. For decades, the medicinal leech *hirudo medicinalis* proved to be a useful model organism in systems neuroscience for the investigation of sensory processing, network dynamics, and even behavioral choice on the level of multiple individually characterized neurons (Kristan et al., 2005; Wagenaar, 2015). Like other invertebrates – the possibly most famous example is the sea slug *Aplysia californica* with which Eric R. Kandel investigated 1965 the neuronal principles of learning – the leech has several advantages for neuroscientific studies. It exhibits several discrete behaviors that are each relatively simple and can all be studied – at least at a basal level – in the isolated nervous system, which is small and experimentally easily amenable. The following three sub-chapters provide the biological basis for this thesis. It investigates the flexibility of one specific neuron in the leech central nervous system (CNS), which is potentially important in the triggering of behaviors.

1.1 Sensory processing of tactile stimuli by mechanoreceptors in the leech

The leech CNS consists of about 10 000 neurons and contains a highly repetitive ventral nerve cord with one ganglion in each of the 21 midbody segments (Figure 1 A). Each of these ganglia contains an ensemble of around 400 large, mostly paired and stereotypically arranged neurons (Figure 1 C) serving as the basis of multiple comparatively relatively simple sensory-input motor-output networks (Kristan et al., 2005). Because leeches love nothing more than a juicy blood meal, they first have to find a victim with their senses before they can sink their jaws into a succulent snack. The leech uses different sensory systems to localize their prey. Besides the visual system, the medicinal leech has five pairs of eyes, each with about 50 photoreceptors (Peterson, 1984), the chemical and the tactile sense is mainly used (Harley et al., 2011).

However, the leech is an escape animal (Wagenaar, 2015), the tactile sense is also important for avoidance behavior (Kristan et al., 2005). Depending on the position of the touch, leeches respond either with whole-body shortening, local bending, swimming, or crawling to tactile stimulation of the body wall (Esch and

Kristan, 2002). One of the most impressive behavior is the *local bend*, because the animal produces a bend away from the contact location with a surprisingly high accuracy comparable to the human fingertip (Johnson, 2001; Baca et al., 2005; Thomson and Kristan, 2006; Pirschel and Kretzberg, 2016).

However, the number of mechanoreceptor cells in the leech skin is an order of magnitude lower than in the human fingertip, which is innervated by more than 200 mechanoreceptors per cm (Vallbo and Johansson, 1984; Kretzberg et al., 2016). In fact, the leech system only possesses 14 mechanoreceptors per ganglion, which can be subdivided into three different types of cells [touch (T), pressure (P), and nociceptive (N) cells]. Though, they share several fundamental properties with the human tactile receptors (Baca et al., 2005; Burrell and Li, 2008; Smith and Lewin, 2009; Pirschel and Kretzberg, 2016).

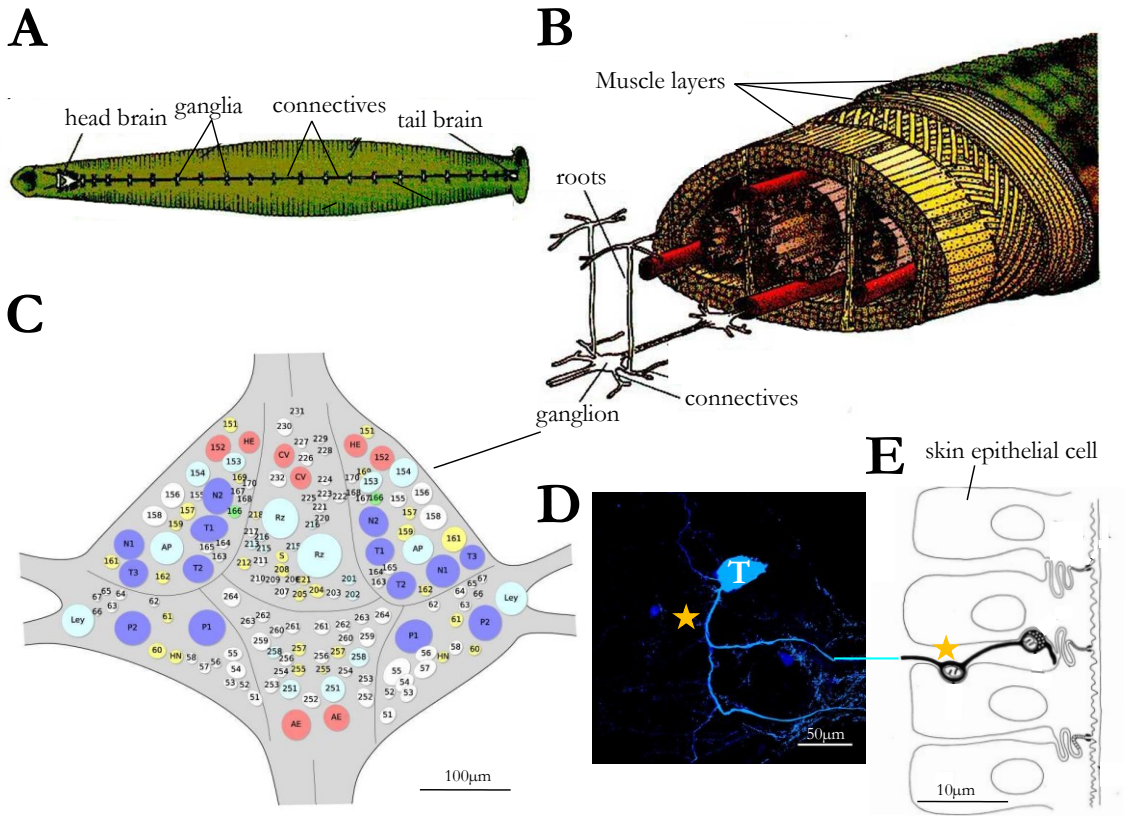

Figure 1 | The central nervous system of the leech. (A) Sketch of the ventral nerve cord of a leech with 21 midbody or segmental ganglia and an anterior and posterior brain. The interganglionic connectives connect ganglia in adjacent segments. **(B)** Cross section of a leech. Ganglia are connected with each other via connectives and each segmental ganglion sends also roots into the skin. The leech body is formed by (from outside): skin followed by layers of circular, oblique, and longitudinal muscles. The ends of the dorsoventral muscles are fixed in the longitudinal muscle layer. The ventral nerve cord is surrounded by the ventral sinus (in red brown). Additionally, the leech possesses a lateral and dorsal sinus. Modified from: Nicholls et al., 2001, "From Neuron to Brain", p. 294. **(C)** Sketch of a segmental ganglion with connectives, roots, and cell bodies. Circular edges inside the ganglion contour the somata of the neurons (named with letters / numbers). Sensory neurons in the sketch are labeled in purple, interneurons in yellow, endocrinological neurons in blue and motoneurons in red. Modified from: D. A. Wagenaar, 2017. An interactive map of the segmental ganglia of *Hirudo verbana*. **(D)** Neurobiotin injection into a T cell revealed its unipolar morphology and putative electrically coupled cells. **(E)** Schematic diagram showing a T cell terminal between skin epithelial cells, ending immediately beneath the junctional area at the outer ends of the cell. Modified from Blackshaw et al. 1981. Yellow stars indicate SIZs in the T cell.

Early studies on sensory processing of touch focused mostly on P cells because stimulation of a single P cell is sufficient to elicit muscle movements for behavioral responses like local bending or swimming (Kristan, 1982; Kristan et al., 1982). Though, several studies suggested that T cells might play a substantial role in the sensory processing, especially of the local bend response (Frady et al., 2016; Pirschel and Kretzberg, 2016; Tomina and Wagenaar, 2017; Fathiazar et al., 2018) Hence, an in-depth investigation of the low threshold, rapidly adapting T cells was necessary. T cells primarily encode the temporal qualities, especially velocity, of applied mechanosensory stimuli during the onset and offset phases of the stimulation (Nicholls and Baylor, 1968; Carlton and McVean, 1995). One ganglion contains three bilateral pairs of T cells (Figure 1 D), which form both electrical and chemical synaptic connections with each other (Nicholls and Baylor, 1968; Baylor and Nicholls, 1969a; Burrell and Li, 2008). Moreover, T cells receive polysynaptic input from the other mechanoreceptor type (P cells) and nociceptors (N cells), leading to a combination of excitatory and inhibitory potentials (Burgin and Szczupak, 2003). This might play a role in localization of the local bend response (Baltzley et al., 2010).

The classical picture of neuronal information processing is that a neuron receives inputs onto its dendrites, integrates them at the soma and transforms the integrated signal into a sequence of action potentials at the axon hillock. However, like most other invertebrate neurons, T cells are (pseudo)unipolar (Figure 1 D), meaning that dendrites and axon are not clearly separated, but form a continuum of processes (Rolls and Jegla, 2015). Moreover, like several invertebrate neurons (Calabrese, 1980; Meyrand et al., 1992), leech T cells were found to have at least two distinct spike-initiation zones (Figure 1 D, E). A peripheral spike initiation zone near the skin conveys information about touch stimuli, and a central one close to the soma processes synaptic inputs within the ganglion (Burgin and Szczupak, 2003; Kretzberg et al., 2007).

The receptive fields of each T cell strongly overlap in anterior-posterior as well as in lateral directions, so that fields of one cell type cover the whole circumference of either the dorsal, lateral, or ventral skin area on one side (Nicholls and Baylor, 1968; Yau, 1976). The entire extent of arborization of one T cell spans three segmental ganglia, because each cell responds to touch of the skin at its own and the adjacent anterior and posterior segments (Yau, 1976). However, the sensitivity of each T cell is highest in the receptive field center and decreases with distance from the center. The reason for that is the density of the nerve endings, which the cells develop as receptors on the skin (Nicholls and Baylor, 1968; Blackshaw, 1981; Blackshaw et al., 1982). The long-range dendritic processes of T cells run through the ipsilateral nerve roots (Figure 1 D) in the body wall to branch extensively in the base of the layer of epithelial cells and end at a few micrometers before the skin surface (Blackshaw, 1981).

The rapidly adapting Meissner corpuscles, a type of human mechanoreceptors, which are not sensitive to static touch but to movement and vibration, show similar response properties, elicited by encapsulated unmyelinated nerve endings with stretch-sensitive ion channels in the tip (Abraira and Ginty, 2013). Potentially, the nerve endings of T cell may also contain similar mechanosensitive channels, which may change opening probability after repeated stimulation, like in human hair cells during stimulation with a high sound pressure level (Peng et al., 2011; Hakizimana et al., 2012).

1.2 Sensory processing of tactile stimuli by the neuronal network in the leech

Leeches respond to identical stimulation on different parts of the body wall with multiple distinct reactions, which inspired the discussion of behavioral choice (Kristan et al., 2005; Baljon and Wagenaar, 2015). These behavioral alternatives are triggered by different patterns in neuronal activity. Due to the small number of neurons of the leech CNS, multifunctional cells play a particular role in shaping response patterns (Kristan et al., 2005; Briggman and Kristan, 2006; Frady et al., 2016). The functional maps determined with a special imaging technique (voltage sensitive dye) indicate which neurons are active during a specific behavior. This revealed that a large percentage of multifunctional neurons are members of functional networks for more than one behavior (Briggman and Kristan, 2006; Frady et al., 2016; Tomina and Wagenaar, 2017). T cells, which are not capable of eliciting a behavior on their own (Kristan, 1982; Fathiazar et al., 2018), might activate a modulatory network with their very fast responses, that later can tune the behavior. This supports the idea of a "preparatory network", the first step in sequential decision making (Esch and Kristan, 2002). The preparatory network was defined as a set of neurons that respond to sensory stimulation after a very short latency with rapid depolarization before any of the motion-specific neurons are activated. Several studies suggest that T cells might trigger the activity of the preparatory network because among other things they elicit interneuron responses, probably via gap junctions, before P cell spikes reach the ganglion (Kretzberg et al., 2016; Pirschel et al., 2018).

Imaging methods can be used to measure the electrical activity of such multiple spatially resolved neurons simultaneously (Peterka et al., 2011). The most popular method is the calcium imaging due to its high status of development (Russell, 2011). Even though this method is highly sensitive (Tada et al., 2014) the optical measurement of the calcium status of an isolated cell or tissue can only provide limited information. For example, hyperpolarization and subthreshold events are temporally low-pass filtered from the initial depolarization (Peterka et al., 2011; Miller et al., 2012). However, the voltage-sensitive dye (VSD) imaging technique allow a direct measurement of the membrane potential and thus provide improved information on timing and location of voltage changes (Miller et al., 2012). Therewith, it addresses the problems associated with calcium imaging and is an optimal method for imaging leech networks because the neurons generate slower and smaller spikes compared to the vertebrate system. Despite the possibilities, VSDs were struggling with issues like insensitivity to voltage changes (González and Tsien, 1995), slow dye kinetics (Cacciatore et al., 1999) or high phototoxicity (Akemann et al., 2009). Only a new generation of dyes using an improved technique greatly enhanced the availability of VSD imaging (Miller et al., 2012). These VSDs detect voltage changes with larger and faster responses compared to any other VSDs before, making this an attractive tool for isolated ganglion recordings of the leech (Briggman and Kristan, 2006; Fathiazar et al., 2013; Fathiazar et al., 2016; Kretzberg et al., 2016; Fathiazar et al., 2018). VSD recordings, in a body wall preparation of the leech, were used to analyze network responses to sensory skin stimulation (Fathiazar et al., 2013; E. Fathiazar and J. Kretzberg, 2015; Fathiazar et al., 2016; Fathiazar et al., 2018). However, it is not clear if repeated skin stimulation can change the network responses, which then may be can result in changes of the behavioral reaction.

Moreover, a recent voltage-sensitive-dye (VSD) study showed that several members of the preparatory network are active, when network activation by individually stimulated T cells is compared with tactile skin stimulation (Fathiazar et al., 2018). To be specific, tactile skin stimulation elicits significantly stronger network activity than the activation of one single P cell (Fathiazar et al., 2018), because soft touch in the midbody region causes the concerted firing of four cells: two P cells and two T cells with overlapping receptive fields. They encode touch location and pressure intensity of tactile skin stimulation in a multiplexed way, combining spike count and temporal response features (Pirschel and Kretzberg, 2016; Kretzberg et al., 2016). Pressure intensity is represented well by spike counts in particular, if spike counts of two receptors are integrated (Pirschel and Kretzberg, 2016). Concurrently, stimulus location is encoded best by the difference in response latencies of two T cells or two P cells with overlapping receptive fields (Pirschel and Kretzberg, 2016). The activity of T cell pairs encodes touch location more precisely than that of P cell pairs (Lewis and Kristan, 1998; Pirschel and Kretzberg, 2016) since T cell responses have a shorter latency than P cell responses and are temporally more precise (Pirschel and Kretzberg, 2016; Kretzberg et al., 2016). Subsequent studies by Kretzberg et al., (2016) and Pirschel et al., (2018) supported this hypothesis by showing that postsynaptic interneurons receive synaptic inputs from all types of mechanoreceptors and that their graded membrane potential changes allow the estimation of tactile stimulus intensity and location. Furthermore, some of the postsynaptic interneurons integrate all mechanoreceptor inputs with a long time constant, while others responded more specifically to precisely timed inputs.

1.3 Neuronal response flexibility

Like all nervous tissue, the leech nervous system is plastic and allows flexible adaptation to external or internal conditions and their changes. Neuroplasticity is the ability of a particular part of the brain or specific region of a neuron to change in strength over time (Fuchs and Flügge, 2014). It can occur in response to previous activity (activity-dependent plasticity) to acquire memory (Ganguly and Poo, 2013) or in response to malfunction or damage of neurons (reactive plasticity) to compensate a pathological event (Geddes et al., 1990). Repeated skin stimulation of the leech might result in modification of ion channel function, like the change of opening probability of human hair cells during stimulation with a high sound pressure level (Peng et al., 2011; Hakizimana et al., 2012) or in changes in the strength of the connection between two neurons.

The term synaptic plasticity describes changes in the strength of the connection between two neurons, including the amount of neurotransmitter released from the presynaptic neuron, and the response generated in the postsynaptic neuron (Bear et al. (2018) and see Figure 2 B lower panel). Persistent activity-dependent changes in synaptic transmission, such as long-term potentiation (LTP) or long-term depression (LTD), are thought to play a critical role in learning and subsequent memory formation (Bear and Linden, 2001). The presence of LTP and LTD in leeches was examined at synapses formed by the T and P cell onto the interneuron S. The S cell was chosen as postsynaptic partner, because of its role in learning-related behavioral plasticity of the whole-body shortening reflex. The S cell is critical for the induction and maintenance of sensitization and contributes to dishabituation of this reflex (Sahley et al., 1994).

In contrast, changes in the number and properties of ion channels is called non-synaptic plasticity. However, non-synaptic plasticity is considered a separate entity it interacts with synaptic plasticity (Mozzachiodi and Byrne, 2010). The modification of the intrinsic excitability of the neuron, including spike generation, subthreshold propagation and synaptic integration (Figure 2 B upper panel), plays a role in many aspects of plasticity from homeostatic plasticity to learning and memory itself (Mozzachiodi et al., 2008; Mozzachiodi and Byrne, 2010). Non-synaptic plasticity can have short-term or long-term effects (O'Dell and Kandel, 1994; Lin et al., 2000).

One possibility these effects occur is through modification of voltage-gated channels in the dendrites and axon, which for example can change their opening probability (Mozzachiodi and Byrne, 2010). The most important voltage-gated ion channels are initially characterized by Alan Lloyd Hodgkin and Andrew Huxley in their Nobel Prize-winning studies of the physiology of the action potential (Hogkin and Katz, 1949; Hogkin and Huxley, 1952). These so-called *standard Na^+_v and K^+_v channels* (the v stands for the voltage dependency) are essential in the formation of an action potential (Bear et al., 2018). As the membrane potential is increased over a specific threshold (Figure 2 A1), Na^+_v channels open, allowing the entry of sodium ions into the cell (depolarization, Figure 2 A2). This is followed by the opening of K^+_v ion channels that permit the exit of potassium ions from the cell (repolarization, Figure 2 A3).

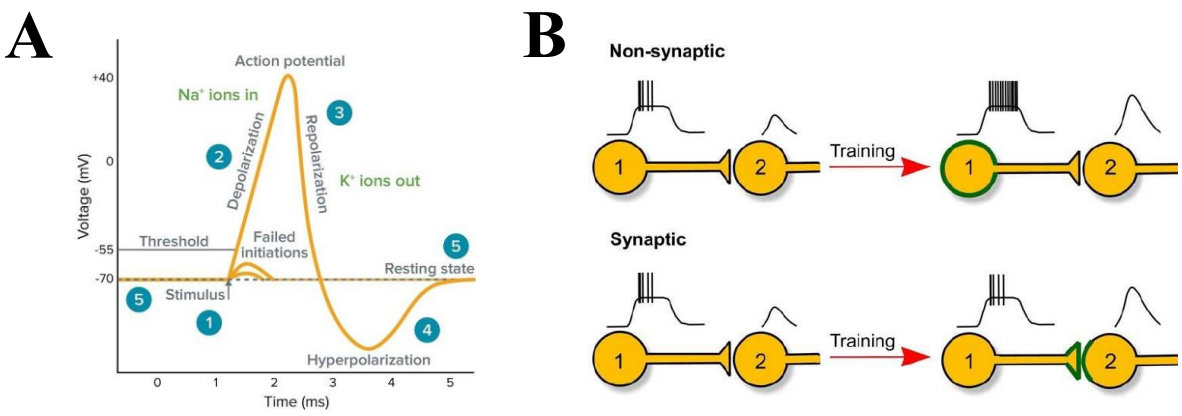

Figure 2 | Neuronal activity and flexibility (A) An action potential is a rapid rise and subsequent fall in voltage or membrane potential across a cellular membrane with a characteristic pattern. If sufficient current through Na^+ channels is required to depolarize the membrane to the threshold level, an action potential is fired. This leads to an outward K^+ current, which again repolarizes the membrane below rest before a slow Ca^{2+} channel brings the potential back to rest. Adapted from (Molecular Devices, 01.10.2020) **(B)** Schematic comparison of non-synaptic and synaptic plasticity. Upper inset: As a result of training, the intrinsic excitability of the pre-synaptic neuron (1) increases, which leads to a higher rate of action potential firing in response to a depolarizing stimulus and causes an enhanced response in the post-synaptic neuron. Lower inset: Training results in a strengthening of the synapse between the pre- and post-synaptic cell, which leads to an enhanced response in the post-synaptic cell even though the action potential firing rate of the pre-synaptic cell remains unchanged. Bold green outlines in A and B indicate sites of plastic changes that can be pre- and/or post-synaptic. Modified from (Benjamin et al., 2008).

However, a leech neuron expresses as the most other neurons not only the Na^+_v and K^+_v channels but also several different ion channels (Johansen, 1991; Kleinhaus and Angstadt, 1995; Gerard et al., 2012). For example, leech sensory cells exhibit four different types of Na^+ channels (Johansen and Kleinhaus, 1986) defined by their relative sensitivity to Tetrodotoxin (TTX), a potent neurotoxin produced by symbiotic bacteria like *Pseudoalteromonas tetradonis* (Simidu et al., 1990; Lee and Ruben, 2008). These Na^+ channels have in the leech, just as in other excitable cells, the function to carry the positive charges, which are necessary to induce an action potential (Kleinhaus and Angstadt, 1995).

Sodium-dependent K^+ channels as they were found in leech pressure cells (Klees et al., 2005), for example, might affect spiking in an activity dependent manner as well as the K_M-channel. It is a voltage-gated K^+ channel (Kv7/KCNQ family) that is named after the receptor it is influenced by (Brown and Adams, 1980). When the muscarinic acetylcholine receptor is activated, the probability of closed K_M channel increased (Brown and Adams, 1980). Furthermore, the M-type potassium current is slowly activating at subthreshold potentials important and therefore important in shaping of the action potential firing properties (Madison and Nicoll, 1984; Bordas et al., 2015). This current was found to be present besides in vertebrates in other invertebrate model systems like the fruit fly *drosophila melanogaster* or the nematode *Caenorhabditis elegans* (Wei et al., 2005; Cavaliere and Hodge, 2011). However, it is not known if these K_M channels exist in the leech system.

Moreover, the review from Kleinhaus and Angstadt (1995) indicates that there are more voltage dependent K^+ channels carrying repolarizing K^+ conductances. Besides there is a growing body of evidence documenting the existence of multiple types of Ca^{2+} channels that can be separated by virtue of their voltage dependence, kinetics, and pharmacological properties. It is likely that they play different roles in regulating the excitability of neurons and transmitter release (Eaton, 1985).

High frequency spiking in touch mechanoreceptors triggered by somatic electrical stimulation or peripheral skin stimulation (Baylor and Nicholls, 1969a) induces a long term afterhyperpolarization (AHP, Figure 2 A), arising from the activation of this Na^+/K^+-pump and an additional Ca^{2+}-dependent K^+ current (Nicholls and Baylor, 1968; Baylor and Nicholls, 1969a; Jansen and Nicholls, 1973; Scuri et al., 2002; Scuri et al., 2007). Previous studies pointed out that modulation of the Na^+/K^+-pump activity is involved in activity-dependent synaptic plasticity between two ipsilateral T cell (Catarsi and Brunelli, 1991; Catarsi et al., 1993; Scuri et al., 2002; Lombardo et al., 2004; Scuri et al., 2007). Additionally, high-frequency stimulation of a T cell elicits long-term depression in the activated pathway and potentiation in the non-activated T cell synapses (Burrell and Sahley, 2004). Furthermore, low-frequency stimulation of T cells can depress synapses through an endocannabinoid-dependent mechanism (Burrell and Li, 2008; Li and Burrell, 2009, 2010). This indicates that T cell activity is adjustable and affects network activity.

In this thesis it is shown that T cell activity is not only influenced by synaptic plasticity as described by (Scuri et al., 2007), but also influenced by non-synaptic plasticity. It would make this sensory neuron to an optimal candidate in behavioral choice because decision making relies on neuronal response flexibility (Esch and Kristan, 2002).

1.4 Aim of the Study

Depending on several intrinsic and extrinsic factors like the neuromodulator concentration, the water depth and the position of the stimulation leeches show different behavioral responses to tactile simulation of the body wall (Esch and Kristan, 2002). This so called behavioral choice is based on different neuronal network states (Gaudry and Kristan, 2009; Palmer et al., 2014). Previous studies of tactile skin stimulation were restricted to steady-state responses with stimuli separated by recovery periods as long as 3.5 minutes to prevent habituation or sensitization (Baca et al., 2005; Pirschel and Kretzberg, 2016). Hence, the question arises if and how repeated skin stimulation might also change intrinsic properties of the neuronal network. Previous studies indicate that besides the P and the N cell, the T cell might also play a role in eliciting reactions in response to tactile stimulation (Kretzberg et al., 2016; Frady et al., 2016; Fathiazar et al., 2018). Since response flexibility already start with changes in individual spike responses (Mozzachiodi and Byrne, 2010) this thesis is based on the following research question:

Which biophysical properties cause response flexibility in T cells and their postsynaptic targets?

Because previous studies (Burgin and Szczupak, 2003; Kretzberg et al., 2007) have shown that T cells have at least two spike initiation zones (see chapter 1.2), it needs to be determined if and how repeated stimulation influences both spike initiation zones. Therefore, the first part of the thesis contains the investigation of the neuronal flexibility of the central spike initiation zone by combining experimental and theoretical approaches. In the second part the effect of repeated skin stimulation on the peripheral spike initiation zone was experimentally examined. The last chapter shows how individual T cell spikes effects the response of postsynaptic target neurons.

1.4.1 Hypothesis 1: Repeated somatic stimulation of leech T cells leads to cell intrinsic plasticity based on Na^+/K^+ pump activity and a K_M current

High frequency spiking in touch mechanoreceptors induces a long term afterhyperpolarization (AHP), arising mainly from the activation of the Na^+/K^+-pump (Nicholls and Baylor, 1968; Baylor and Nicholls, 1969a; Jansen and Nicholls, 1973; Scuri et al., 2002; Scuri et al., 2007) and thereby providing a mechanism for intrinsic, activity dependent regulation of excitability (Gulledge et al., 2013; Duménieu et al., 2015). Therefore, in the first part of this thesis intracellular current clamp recordings of single T cells were performed in isolated ganglia by stimulating the cell soma with repeated series of current pulses (simulating synaptic inputs) (see Figure 2 and chapter: 2.2). The neuronal responses were analyzed based on the features SC, RMP and cell IR (see chapter 2.4.1). A Hodgkin–Huxley (HH) type neuron model, adjusted to physiological T cell properties, suggests a combination of cellular-level mechanisms for this non-synaptic plasticity. To focus on the

fundamental biophysical mechanisms a minimalistic description of ion channels and pumps was used, although the leech T cell may express several other ionic conductances (Johansen, 1991; Kleinhaus and Angstadt, 1995; Gerard et al., 2012). The HH type neuron model comprises in addition to the standard Na^+, K^+ and leak currents an additional Na^+/K^+-pump and an M-type slow potassium current. Repetitive spiking leads to an increase of intracellular Na^+. This in turn activates the pump, which exchanges three intracellular Na^+ ions with two extracellular K^+ ions. The resulting net negative current hyperpolarize the membrane potential (Forrest, 2014; Bear et al., 2018). The M-type K^+ conductance, whose kinetics are much slower than the spike-generating conductances, might cause the cessation of spiking during current injection in a voltage dependent manner (Benda and Herz, 2003). The opening probability of the K_M-channels increases with depolarized membrane potential, causing spike responses to stop before the end of the stimulation. The hyperpolarized membrane potential due to increases Na^+/K^+ pump activity closes K_M channels, which increases IR and lead in combination with a smaller M-type potassium current to a higher SC.

As a next step blocking of Na^+/K^+-pumps was done to experimentally confirm the model assumptions and verify the second hypothesis. Inhibiting the Na^+/K^+- pump leads to an increase of intracellular sodium and extracellular potassium (see chapter 1.3 and Jacob et al. (1987)). Therefore, we applied dihydrouabain (DHO), a plant derived toxic substance, which reversible inhibits the Na^+/K^+ pump. This should lead to a slight depolarization of the RMP in T cells. Additionally, the increased intracellular sodium should reduce the activity of the sodium-calcium exchanger (NCX), which elevates intracellular calcium and thereupon depolarizes the membrane potential (Terracciano, 2001). Therewith the ionic concentrations are out of balance and we expected an increase in SC, because the membrane potential of the cell is closer to the spiking threshold (Bear et al., 2018). However, if K_M channels are present in leech T cells the SC as well as the IR should decrease because at a depolarized membrane potential the probability of open K_M channels is lower. In a final step we artificially set the membrane potential of a T cell to different holding potentials to open and close the putative voltage dependent K_M channels. We expected a decrease in SC at a depolarized holding potential, because more open K_M channels decrease IR and change the firing pattern from sustained to transient.

1.4.2 Hypothesis 2: Cell intrinsic plasticity in leech T cells occurs at multiple spike initiation zones (SIZs), which interact with each other

The second part of the thesis contains the investigation of the neuronal plasticity of the peripheral spike initiation zone. T cells respond transiently to changes in tactile stimulation and are very sensitive to stimulus velocity (see chapter 1.2). Therefore, it was expected that sinusoidal up- and down movements of a lever arm at the ventral midline activate peripheral spike initiation zone and elicit high spike counts. It is technically not possible to record the membrane potential in the periphery. However, spikes can travel from the periphery to the soma. Therefore, we recorded the membrane potential of the T cell intracellularly in the soma while eliciting spikes in the periphery of a body wall preparation (see chapter 2.1).

If the number of spikes, which were initiated in the skin and recorded in the soma, increase with repeated stimulation, it can be narrowed down where cell-intrinsic plasticity could happen:

If the spike initiation site in the skin is the only place of cell-intrinsic plasticity, T cell spikes should not trigger Na^+/K^+ ATPase activity everywhere in the cell membrane. In this case, the somatic recorded activity only is the reflected activity from the periphery. Changes in intrinsic properties as the resting potential or the IR should not be visible, because only spikes can travel this long distance from the skin to the soma.

If the number of spikes, which were initiated in the peripheral SIZ and recorded in the soma, decreases with repeated stimulation this only indicates that both initiation zones react differently but not independently. If both spike generation sites would act independently, it is expected that somatic current injections lead to the same responses, no matter if they are applied before or after skin stimulation. However, peripheral spikes can propagate to the central part of the T cell to trigger there Na^+/K^+ ATPase activity. Hence, the somatically recorded membrane potential should hyperpolarize, the input resistance should increase, and more spikes should be generated in response to the same current pulse as applied before the tactile stimulation.

1.4.3 Hypothesis 3: Timing and amount of T cell spikes effect network activity

Behavioral responses are based on muscle movements, which are controlled by a population of motor neurons, which receive synaptic inputs from a network of interneurons connecting both the motor neurons and the sensor neurons (Bear et al., 2018). In the last part of this thesis, the hypothesis that T cells could activate the preparatory network is further investigated (see chapter 1.2) by examining how timing and amount of T cell spikes affect response behavior of postsynaptic cells. As described in chapter 1.2 soft touch at any position on the body surface causes the concerted firing of four cells: two P cells and two T cells with overlapping receptive fields (Pirschel and Kretzberg, 2016; Kretzberg et al., 2016). Because all six T cells within one ganglion form both electrical and chemical synaptic connections with each other (Nicholls and Baylor, 1968; Baylor and Nicholls, 1969b; Li and Burrell, 2008) and receive polysynaptic input from the other mechanoreceptor type (P cells) and nociceptors (N cells) (Burgin and Szczupak, 2003) it was first investigated how somatically induced T cell spikes could influence the response behavior of another T cell by intracellular double recordings. Additionally, it is shown how the activity changes that were induced by non-synaptic plasticity in an electrically stimulated T cell (presynaptic) affects the responses of the non-stimulated T cell (postsynaptic).

The studies of Kretzberg et al. (2016) and Pirschel et al. (2018) showed that the postsynaptic interneuron 157 receives synaptic inputs from all types of mechanoreceptors but responded more specifically to precisely timed inputs. This indicates that T cells play a major role as presynaptic partner. Therefore, the effect of precisely timed T cell spikes was additionally tested on the postsynaptic interneurons 212 and 157 by intracellular double recordings. To investigate the effect of T cell activation on the network and to further support the third hypothesis voltage-sensitive dye recordings (see chapter 2.3.3.2) were performed. They can be used to measure the electrical activity of multiple spatially resolved neurons simultaneously (Peterka et al., 2011) and allow a direct measurement of the membrane potential and provide improved information on timing and location of voltage changes of different (inter)neurons at the same time (Miller et al., 2012).

2 Materials und Methods

The content of the following chapters 2.1, 2.2, 2.3.1, 2.3.3.1, 2.4.1 and 2.5 is published in Meiser et al. 2019.

2.1 Animals and preparation

The experiments were performed on adult hermaphrodite medicinal leeches (*Hirudo verbana*) obtained from the Biebertaler Leech Breeding Farm (Biebertal, HE, Germany). According to German regulations, no approval of an ethics committee was required for the work on these invertebrates. The animals were kept at room temperature in tanks with ocean sea-salt diluted with purified water (1:1000). All experiments were performed at room temperature. The leeches were anesthetized with ice-cold saline (mM: 115 NaCl, 4 KCl, 1.8 CaCl2, 10 Glucose, 4.6 Tris-maleate, 5.4 Tris base and buffered at pH 7.4 with NaOH, modified after (Muller and Scott, 1981) before and during dissection.

Two types of preparations (see Figure 11 A) were used for the experiments:

I. **Isolated ganglia,** dissected from segments 7-13 and pinned, ventral side up, to a plastic petri dish, coated with the silicone elastomer *Sylgard* (Dow Corning Corporation, Midland, MI, USA).

II. **Body-wall preparation,** consisted of mid-body segments of either 7-9, 9-11 or 10-12 with corresponding ganglia. Innervations of segment 8, 10 or 11 remained unscathed. The body-wall was flattened and pinned out, with the epidermis upwards, in a petri dish coated with *Sylgard*. In the area of 5th annulus (counted from anterior) of the 8th, 10th or 11th segment, a hole was cut into the skin to provide access to the ganglion. The skin was stimulated at the ventral midline of the middle annulus (3rd annulus of segment 8, 10 or 11), which was identified by location of the sensilla.

2.2 Electrophysiological Technique

Based on observations on "animal electricity" by Luigi Galvani in the late 18th century, Emil Heinrich Du Bois-Reymond became the founder of experimental electrophysiology. He described instruments such as multipliers (galvanometers), slide inductors and other measuring devices that are now part of the modern equipment of physiological laboratories.

In order to be able to record the membrane potential of a cell and its fluctuations, the principle of the current clamp is used today (Hermey, 2011). To address both the measure points inside and outside the cell, the method uses two recording electrodes (Figure 3 A). One is inserted to the cell and a second one, the reference electrode, stays inside the surrounding bath and is grounded (Müller et al., 2015). The main principle of the current clamp method is to fixate the current in the way that no current flows between both parts of the electric circuit, and the potential of the recording electrode and the cell is equal (Hermey, 2011).

The experimental rig for the experiments to the cellular plasticity in T cells consisted of either one or two mechanical micromanipulators type MX-1 (Narishige Group), and up to two amplifiers from NPI Electronic (model SEC-05X and BA1S). The data were acquired via an interface BNC-2090 with NI PCI-6036E board

from National Instruments. The neuronal responses were recorded (sample rate 100 kHz, 10 kHz) and analyzed using MATLAB software (MathWorks). For applying pressure stimuli onto the skin, a Dual-Mode Lever Arm System (Model 300 B, Aurora Scientific, Aurora, ON, Canada) with a poker tip size of 1 mm^2 was used (Kretzberg et al., 2016; Pirschel and Kretzberg, 2016; Fathiazar et al., 2018).

Intracellular single and double recordings were performed at room temperature from mechanosensory touch cells and interneurons, while either injecting current into one T cell soma or stimulating the skin mechanically (see Figure 3 B). For these current clamp recordings, the cell soma was impaled with borosilicate microelectrodes (TW100F-4, World Precision Instruments Inc., Sarasota, FL, United States) which were pulled with the micropipette puller P97 Flaming Brown (Sutter Instruments Company, Novato, CA, United States). The glass electrodes were filled with 3 M potassium acetate and had resistances of 15–30 MΩ. The neurons were identified by the size and the location of their cell bodies with a binocular microscope (Olympus szx7, Olympus, Tokyo, Japan) or a microscope (Examiner D1, Zeiss, Oberkochen, BW, Germany) as well as by their firing pattern (Nicholls and Baylor, 1968).

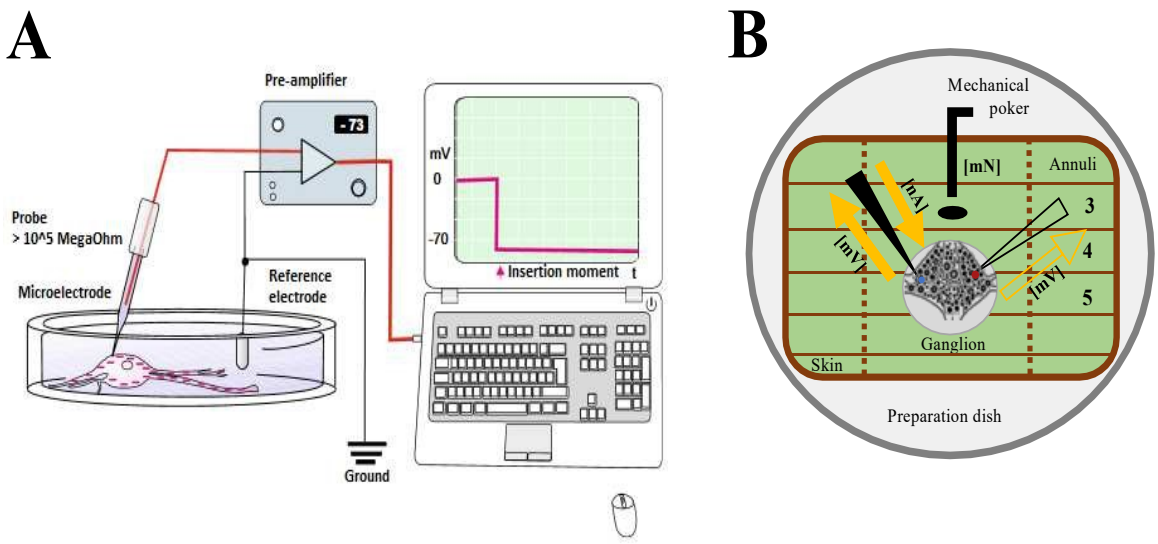

Figure 3 | Schematic drawing of the experimental setup: (A) Microelectrode inside the cell, reference electrode inside the bath and grounded, high-impedance probe, amplifier and PC, recording shows the neuronal response as the potential difference between the microelectrode and the grounded reference electrode. Modified from (Müller et al., 2015). **(B)** Sketch of the preparation and the principle of the current-clamp recording. In the body-wall preparation, the skin was flattened and pinned with the epidermis upwards in the dish. A hole in the skin provided access to the ganglion. While stimulating the skin mechanically with the poker, we recorded the membrane potential of one of the T cells (blue) with an inserted electrode (black arrow). In the isolated ganglia preparation, only the single ganglion was pinned on the dish. While injecting current with the inserted electrode into the T cell soma, we recorded the membrane potential of either only the stimulated T cell (blue) or an additional postsynaptic cell (red) with a second intracellular electrode (black rimmed white arrow).

2.3 Experimental Designs

The focus of this thesis was to investigate the effect of repeated mechanoreceptor stimulation on the intrinsic physiological properties of T cells and their synaptic partners respectively neuronal network (see chapter 1.4). Therefore, different experimental designs, with either somatic current injection or tactile skin stimulation or both in combination, were applied. Additionally, pharmacological blocking of Na^+/K^+ pump by Dihydrouabain (DHO) as well as voltage-sensitive dye (VSD) imaging were performed. In total 82 cells of 57 ganglia out of 36 preparations were selected for analysis (see chapter 2.4 for selecting criteria).

Table 1 | Experimental sets for the analysis of the effect of repeated mechanoreceptor stimulation on the intrinsic physiological properties of T cells as well as the response properties of their synaptic partners. One experimental set contains all recordings with the same stimulation protocol. Since I did not all of the recordings, the column experimenter shows who of my supervised students and colleagues did the recordings, which then I analyzed for this thesis. The experimenter is also given in the following subchapters, which explain the experiments more in detail. The analysis of the VSD recordings was done by B.Sc. Jimin Roh. The recordings were done by myself.

Experimental set	Leeches	Ganglia	Stimulated Cells	Experimenter
Pseudorandomized	8	17	20	M.Sc. Sonja Meiser
Pharmacology	4	9	9	M.Sc. Ihor Arkhypchuk
Baseline	4	5	16	M.Sc. Sonja Meiser M.Sc. Jens-Steffen Scherer
Double Recordings current step	6	10	13	M.Sc. Sonja Meiser
Double Recordings single pulses	4	5	12	M.Sc. Sonja Meiser
Tactile Experiments	7	8	8	B.Sc. Maren Prelle
Interneuron Recordings	2	2	2	M.Sc. Sonja Meiser
VSD Recordings	1	1	2	M.Sc. Sonja Meiser

2.3.1 Hypothesis 1: Repeated somatic stimulation of leech T cells leads to cell intrinsic plasticity based on Na+/K+ pump activity and a KM current

In the first part of this thesis a T cell in an isolated ganglion preparation (see 2.1) was stimulated repeatedly with a series of 12 current pulses in a pseudo-randomized order (see Figure 4). To get an impression if and how repeated somatic stimulation acts on intrinsic response properties of T cells, each experiment consisted of 15–20 identical trial repetitions. The amplitude of the pulses varied between -2 and +1.5 nA. The duration of each pulse was 500 ms and the inter-pulse-interval was 2.5 s long to prevent cell regeneration. The inter-trial-interval was 5 s long. While injecting current into the T cell soma with the intracellular electrode, the membrane potential of the stimulated T cell was recorded with the same electrode (see Figure 2 C). The neuronal responses of the stimulated T cells were quantified by the following response features SC, RMP and cell IR (see chapter 2.4.1)

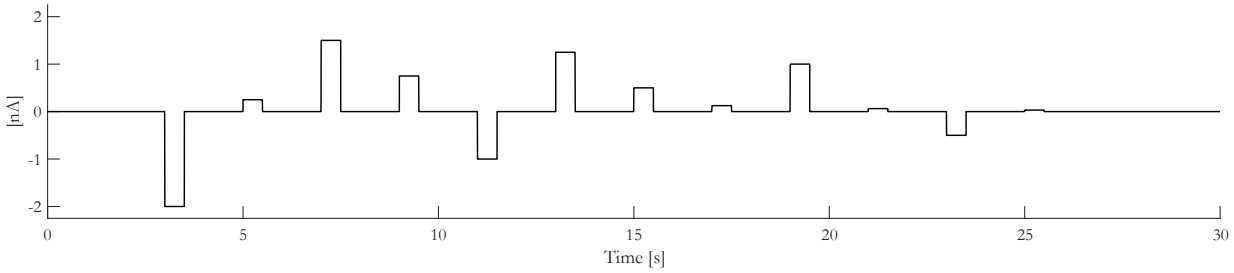

Figure 4 | Protocol Pseudorandomized. Each trial consists of a series of 12 current pulses (amplitude varied between -2 and +1.5 nA). The duration of each pulse was 500 ms and the inter-pulse-interval was 2.5 s long. The inter-trial-interval was 5 s long and each experimental set consisted of 15–20 identical trial repetitions.

Next, the cellular basis of the neuronal response behavior of T cells due to repeated somatic stimulation was investigated. First a single-compartment Hodgkin-Huxley-type neuron model, comprising in addition to the standard Na^+, K^+ and Leak current an additional Na^+/K^+-pump and an M-type slow potassium current was created (based on the studies from Nicholls and Baylor (1968) and Baylor and Nicholls (1969a) see chapter 2.5). To experimentally confirm the model assumptions pharmacological blocking of Na^+/K^+-pumps was done. Furthermore, an artificial setting of the membrane potential to different baselines should support the hypothesis of K_M involvement.

2.3.1.1 Pharmacological blocking of Na^+/K^+ pump

The evaluation of Na^+/K^+ pump involvement in the proposed cell intrinsic plasticity of leech T cells was experimentally verified by inhibiting pump activity using Dihydrouabain (DHO, Carl Roth, Karlsruhe, BW, Germany). An isolated ganglion preparation was kept under constant perfusion (1.5 mL / min) by using a peristaltic pump (Masterflex, Cole-Parmer Instrument Co., Chicago, IL, USA). First, five identical trial repetitions of the protocol *Pharmacology* were applied to the T cell. Each trial consists of 20 current pulses of 1nA and one pulse of 2.5 nA, each of them 500ms long and with an inter-pulse-interval of 2.5 s (see Figure 5).

Additionally, a negative current pulse of 0.25 nA was applied to allow an easy calculation of the cell input resistance (IR) because these responses are not superimposed by spikes.

Treatment condition starts by adding DHO to ringer at a final concentration of 10 nm. Then the stimulation protocol *Pharmacology* was repeated five times again. After replacing DHO solution with ringer solution the washout condition starts by repeating the protocol five times again. RMP analysis was not done for this experimental set, because the recordings were superimposed by an electric drift (see chapter 4.4). Therefore, the neuronal responses of the T cells were only quantified by the response feature SC (see chapter 2.4.1).

The recordings shown in this thesis were performed and kindly provided by M.Sc. Ihor Arkhypchuk, a Master Student of the Neuroscience program at University of Oldenburg, who I supervised from July 2020 – September 2020. In addition, I also did such blocking recordings, but they were not analyzed because of different amount of repetitions of the stimulation protocol.

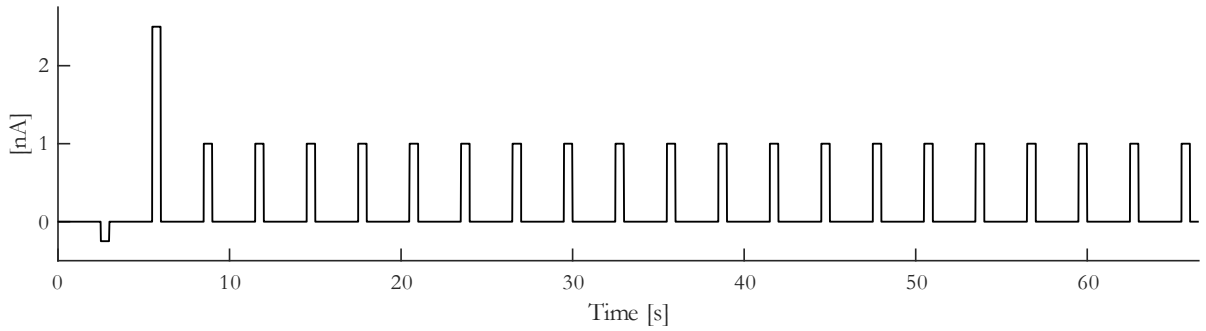

Figure 5 |Protocol Pharmacology: Each trial consists of a series of 22 current pulses (1 pulse with an amplitude of 2.5 nA and 20 pulses with an amplitude of 1 nA). One negative current pulse of 0.25 nA was applied to calculate the input resistance. The duration of each pulse was 500 ms long and the inter-pulse-interval was 2.5 s long. The inter-trial-interval was 5 s long.

2.3.1.2 Different Membrane Potential Baselines

Repetitive spikes lead to the activation of the Na^+/K^+ pump, which exchanges three intracellular Na^+ ions with two extracellular K^+ ions. The resulting net negative current hyperpolarizes the membrane potential (Forrest, 2014). This might lead to the suppression of a slow K^+ current, which channels have a higher opening probability during rest. When the cell hyperpolarizes, this slow K^+ channel closes and can affect intrinsic response properties (Madison and Nicoll, 1984; Bordas et al., 2015).

However, the existence of K_M- channels in leeches is not proved, and the known blocker XE-991 and Linopirdine are mainly used in vertebrates (Greene et al., 2017). Therefore, we try to simulate the different opening states of K_M by setting the membrane potential artificially to a hyperpolarized and a depolarized baseline by applying ± 0.5 nA current in intracellular single recordings in an isolated ganglia preparation (Figure 6). From these baselines on we applied short current pulses to analyze the response properties SC and IR. While injecting current into the T cell soma with the intracellular electrode, the membrane potential of the stimulated T cell was recorded with the same electrode. In each condition (resting level (unstimulated),

hyperpolarized and depolarized) the neuron was stimulated with two pulses of different amount of current. The duration of each pulse was 500 ms and the inter-pulse-interval was 2.5 s long. Each experimental set consisted of 20 identical trial repetitions.

The recordings of this experimental set were also superimposed by an electric drift. This leads to the fact that the results of the RMP analysis could not be interpreted (see chapter 4.4). Therefore, the neuronal responses of the T cells were only quantified by the response feature SC and IR (see chapter 2.4.1).

Half of these recordings (8 out of 16) were performed and kindly provided by M.Sc. Jens-Steffen Scherer, a PhD Student in the Computational Neuroscience Division at University of Oldenburg.

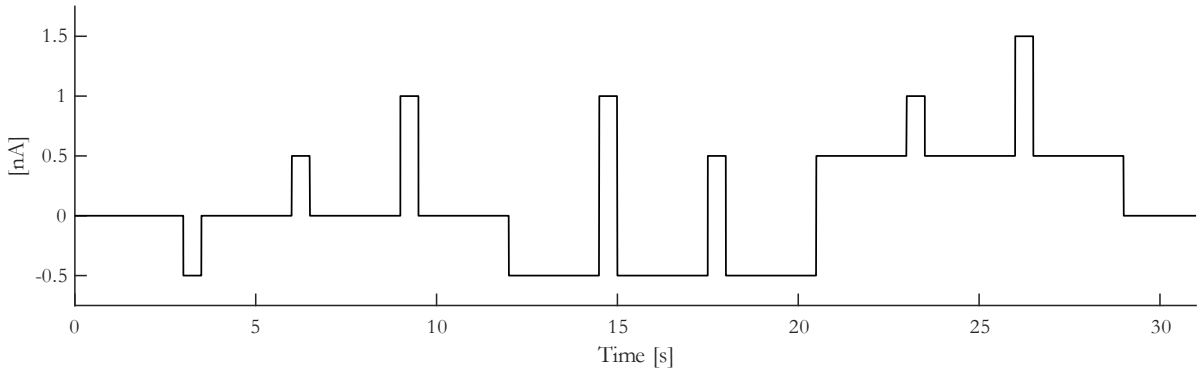

Figure 6 | Protocol Different Baselines. Each trial was 31 seconds long and split up in three baseline conditions (resting level (unstimulated), hyperpolarized, and depolarized). Each condition consists of two current pulses with a duration of 500 ms. The inter-pulse-interval was 3 s long. The inter-trial-interval was 5 s long. Each experimental set consisted of 20 identical trial repetitions.

2.3.2 Hypothesis 2: Cell intrinsic plasticity in leech T cells occurs at multiple spike initiation zones (SIZs), which interact with each other

To determine if and how the spike initiation zone in the skin is influenced by repeated stimulation a ventral T cell was stimulated by repeated rhythmic touch. T cells respond transiently to changes in tactile stimulation and are very sensitive to stimulus velocity (see chapter 1.2). Therefore, it is expected that sinusoidal up- and down movements of a lever arm on the skin elicit high spike counts. If the T cell responses to tactile stimulation cause cell-intrinsic plasticity, we expected the effect to be most clearly visible for stimuli that (at least initially) lead to massive spike responses.

As an additional step, the tactile stimulation triggering spikes in the skin is alternated with somatic current injection, leading to spike generation in the central ganglion. If both spike generation sites act independently of each other, it is expected that somatic current injections lead to the same responses, no matter if they are applied before or after skin stimulation.

A T cell was treated in a body-wall preparation (see 2.1), with the following stimulation protocol (see Figure 7): One trial consisted of two depolarizing current injections (+1 nA), each 1 s long, before and after the tactile

stimulations (Figure 7 A). Each tactile 10 Hz stimulation pulse within a poker interval lasted 2 s, whereby the skin was stimulated with 20 sinusoidal up and down movements of the poker (Figure 7 B, blue). The stimulus was varied in intensity between 8-50 mN. Between two poker intervals was a stimulation pause lasting 4 s. Adapted stimulation protocols also consisted of a hyperpolarizing current injection (-1 nA or -0.2 nA) applied before the first depolarizing current. While injecting current into the T cell soma with the intracellular electrode, the membrane potential of the same T cell was recorded with the same electrode.

These tactile stimulation recordings were performed and kindly provided by B.Sc. Maren Prelle, a Master Student from University of Cologne, who I supervised from January 2020 – March 2020.

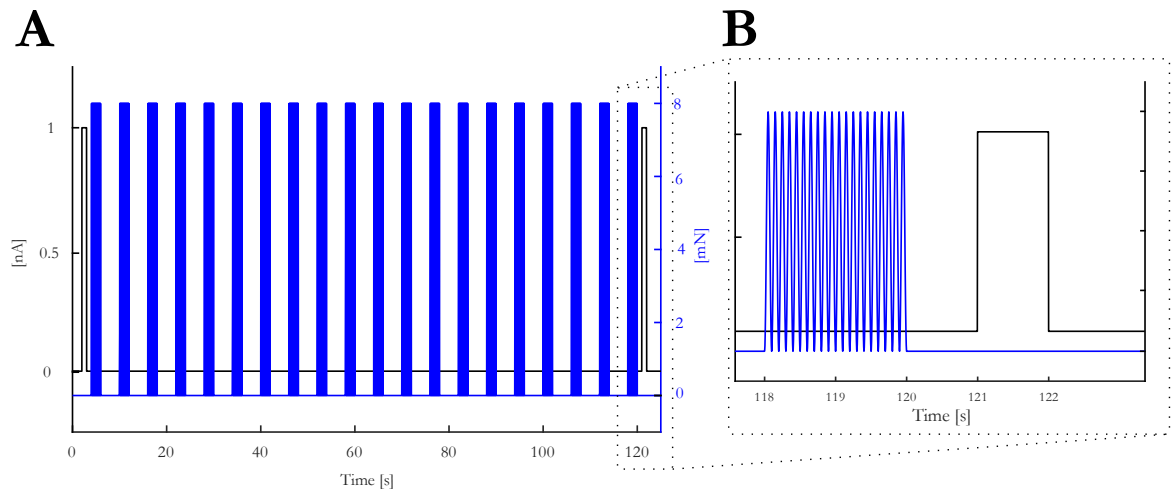

Figure 7 | Protocol Tactile Stimulation. (A) One trial consists of 20 tactile 10 Hz stimulation pulse packages with the poker (blue) framed with two somatic current injections of 1nA intensity and 1 s duration (black). (B) Each tactile 10 Hz stimulation pulse within a poker interval lasted 2 s and comprised 20 sinusoidal up and down movements of the poker. The intensity of the poker varied between 8-50 mN, because for each experiment the lowest intensity, which produces spikes was chosen.

2.3.3 Hypothesis 3: Timing and amount of T cell spikes effect network activity

Analysis of the effect of T cell spikes on the neuronal network was done by performing double recordings between T cells and putative postsynaptic partners (T, 157, 212) in an isolated ganglion preparation. While injecting current into the presynaptic T cell soma with one electrode, we recorded the membrane potential of the unstimulated postsynaptic cell with a second electrode (see chapter 2.3.3.1) or additionally the activity of the whole network by using a CCD camera (see chapter 2.3.3.2.).

2.3.3.1 Double Recordings

Since all T cells within one ganglion are electrically coupled, ipsilateral double recordings from two of the three T cells in all combinations were performed. First, the pseudorandomized stimulation protocol, presented in Figure 4, was applied into the presynaptic T cell. This shows if and how the activity changes that were induced by non-synaptic plasticity in the electrically stimulated T cell (presynaptic) affected the responses of the non-

stimulated T cell (postsynaptic). Furthermore, a pulse-package protocol (see Figure 8) was applied to examine if putative changes found in postsynaptic cell are not due to synaptic plasticity. One pulse-package comprised a fixed number (1–7) of short current pulses (2 nA, 5 ms), which were injected into the T cell soma to trigger one action potential each. In consequence, the pulse-package protocol elicited the same number and timing of presynaptic action potentials in each trial. I only analyzed recordings in which the number of elicited spikes were the same as the number of applied current pulses.

Each trial consisted of five pulse packages and each sub-experiment was composed of 25 trial repetitions. The pause between the single pulses in a package was 30 ms and the starting times of the packages were always separated by 1 s (independent of the number of pulses in the package).

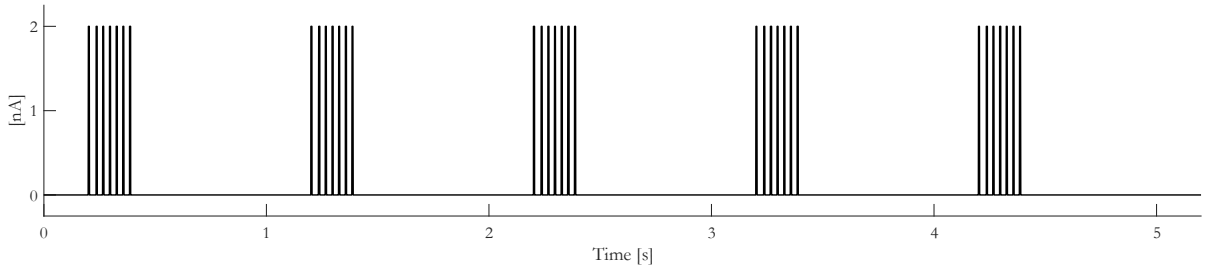

Figure 8 | Protocol Pulse Packages: One pulse-package comprised a fixed number (1–7) of short current pulses (2 nA, 5 ms), which elicited the same number and timing of presynaptic action potentials in each trial.

The effect of precisely timed T cell spikes on the postsynaptic interneurons 157 and 212 was investigated by applying a second pulse-package protocol to presynaptic T cell (see Figure 9). One pulse-package comprised two (see Figure 9 A) or five (see Figure 9 B) short current pulses (2 nA, 5 ms), which were injected into the T cell soma to trigger one action potential each. Each trial consisted of eight pulse packages, but the inter-pulse-interval varied between 1 to 50 ms in a pseudorandomized order (20, 5, 30, 50, 25, 1, 2, 10). In consequence, the protocol might not elicit the same number and timing of presynaptic action potentials in each pulse package to allow the investigation of changes in postsynaptic response behavior. The starting times of the packages were always separated by 5 s (independent of the number of pulses in the package).

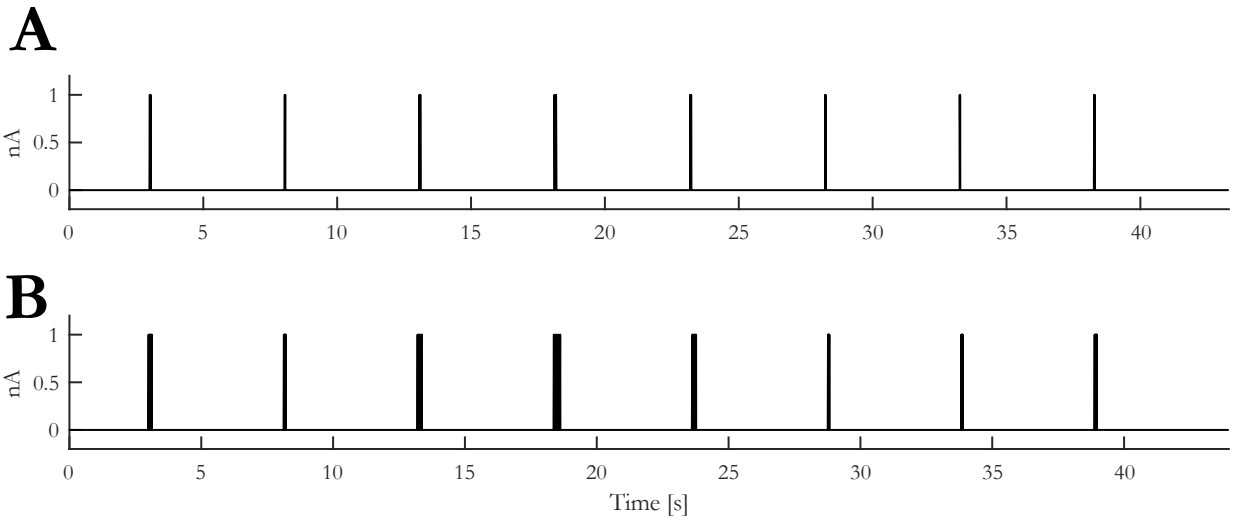

Figure 9 | Protocol Interneurons: One pulse-package comprised two (A) or five (B) short current pulses (2 nA, 5 ms). Each trial consisted of eight pulse packages, but the inter-pulse-interval varied between 1 to 50 ms in a pseudorandomized order (20, 5, 30, 50, 25, 1, 2, 10). In consequence, this pulse-package protocol might not elicit the same number and timing of presynaptic spikes.

2.3.3.2 Voltage Sensitive Dye Imaging

In this thesis VSD recordings were performed in isolated ganglia preparations (see chapter 2.1) simultaneously to a double intracellular recording from a P and a T cell. Additionally, the glia sheath on the ventral side of the ganglion was removed, and the ganglion was stained with 200 nM VF2.1.CL dye (lmax = 522 nm, lem = 535 nm, see Miller et al. (2012)). This voltage sensitive dye operate with photoinduced electron transfer (see Figure 12 A). Here, a voltage sensitive electron transfer occurs from an electron-rich donor (orange) via a membrane spanning anchor (black) to a fluorescence receptor (Miller et al., 2012). In the depolarizing state, the electrons migrate away from the extracellular side. The fluorescence receptor is excited by short-wave light and emits light, which is recorded by a CCD camera.

Both mechanosensory cells were either stimulated simultaneously or alternated with intracellular current injections. Meanwhile, the activities of all visible cells on the ventral side of the ganglion were monitored through a microscope (Zeiss Examiner D1, objective plan achromat 20x/1.0 DIC (UV)) and recorded with a CCD camera (Photometrics QuantEM:512SC). Imaging was performed with a temporal sampling frequency of 94Hz and a spatial resolution of 64 × 128 pixels. Prior to the recording, a snapshot was taken with the full spatial resolution of the camera, 512 × 512 pixels, based on which regions of interest (ROIs) representing individual cell bodies were selected manually (see Figure 12 B for an example and Fathiazar et al. (2018)). The sensory cells were electrically stimulated with short current pulses (2.5 nA T cell and 3 nA P cell) in a pattern that reproduces natural responses to tactile stimulation of 50mN in the ventral midline of the skin in a semi-intact preparation (after Kretzberg et al. (2016) and see Figure 10).

T cell spikes at half of the prominence has a shorter duration than P cell spikes. To be sure that only one spike is elicited, the duration of the pulses was 5ms for T cells and 10 ms for P cell.

Four different stimulus conditions were compared (Figure 12 C):

- In the PT-stimulated condition, both sensory cells were electrically stimulated.
- In the P stimulated only the P cell was stimulated, while the T cell remained unstimulated.
- In the T stimulated only the T cell was stimulated, while the P cell remained unstimulated.
- In control condition, both cells were not stimulated.

The recording software was VScope (developed by Daniel Wagenaar, University of Cincinnati, Cincinnati, OH, USA / California Institute of Technology, Pasadena, CA, USA). Stimulation was delivered via intracellular electrical currents by a current clamp.

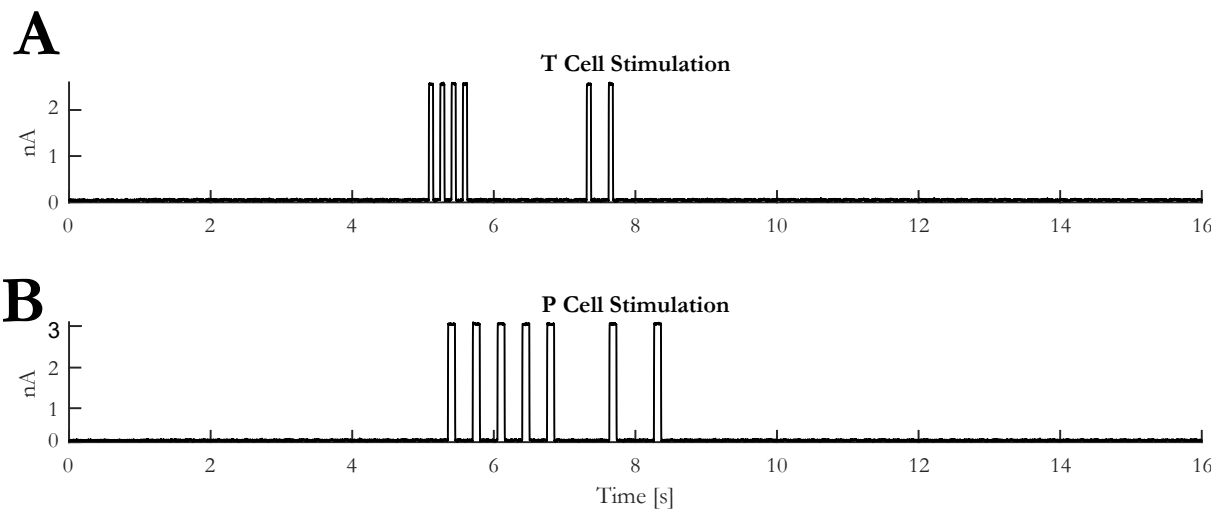

Figure 10 | Protocol Intracellular stimulation in VSD recordings. The sensory cells were electrically stimulated with short current pulses (2.5 nA for T cell and 3 nA for P cell) in a pattern that reproduces natural responses to tactile stimulation of 70m N in the ventral midline of the skin in a semi-intact preparation (after Kretzberg et al. (2016)). The duration of the pulses was 5 ms for T cells and 10 ms for P cell to make sure that exactly the same number of spikes are elicited in each trial. Time course for **(A)** T cell stimulation and **(B)** P cell stimulation.

2.4 Data Analysis

2.4.1 Electrophysiological Current Clamp Recordings

During the recordings, the electrode properties usually changed slightly, leading to an increase in electrode resistance and an electrode offset drift. Therefore, we excluded recordings from the analysis which change their electrode resistance by more than +10 MΩ due to clogging or the offset drifted by more than -9.5 mV.

In total 82 cells of 57 ganglia out of 36 preparations were selected for analysis (see chapter 2.4 for selecting criteria). The neuronal responses of these stimulated T cells and their synaptic partner neurons in the electrophysiological current clamp recordings were quantified by the following response features: spike count (SC), resting membrane potential (RMP), cell input resistance (IR), postsynaptic response (PR) and latency (LAT).

- **Spike count** [spike number] was defined as the total number of spikes elicited by the neuron and recorded in the soma between the stimulus onset and offset for current injection (see Figure 11 C) and during one tactile stimulus package of 20 sine waves (see Figure 11 B). Spike detection was performed using custom-developed MATLAB software. Spikes were defined by the following parameters: minimum threshold [mV], minimum duration [ms], and minimum spike amplitude [mV] (see Figure 11 A). A spike was detected when the membrane potential depolarized by the minimum spike threshold and the relative spike height, from rest to peak, was at least as high as the minimum spike amplitude. Additionally, a peak was only accepted as an action potential if the detected peak at half of the prominence had the required minimum duration (see Figure 11 A).

- **(Resting) membrane potential** [mV] (U_{rest}) was computed as the averaged membrane potential in the 2.5 s before the first current pulse in each trial starts for the pseudorandomized protocol. For the different baseline protocol membrane potential was computed as the averaged membrane potential in the 1.5 s before each current pulse in each trial. For the tactile protocol RMP was computed as the averaged membrane potential in the second before each tactile pulse starts.

  Furthermore, from March 2020 on all our recordings in all experimental set ups were superimposed by a massive electric drift. Therefore, the analysis and interpretation of RMP over trials was not done for the experimental sets: "pharmacology", "different baselines".

- **Input resistance** [MΩ] was calculated based on the average membrane potential (U_{stim}) in response to the 500 ms long hyperpolarizing current pulse of either I = -1 nA (pseudorandomized protocol and different baseline protocol) or -0.25 nA (protocol for the pharmacological blocking of Na^+/K^+ pump) to avoid the influence of active processes. IR in the tactile recordings were calculated based on the median membrane potential of the passive response of the +1 nA somatic current injection.

  IR was calculated with Ohm's law:

$$\boldsymbol{IR}\,[M\Omega] = \frac{\boldsymbol{Ustim}\,[mV] \times \boldsymbol{Urest}\,[mV]}{\boldsymbol{I}\,[nA]}$$

- **Postsynaptic response** [mV]: was calculated as average difference between the recorded membrane potential and the RMP of the postsynaptic (unstimulated) cell. The potential difference was averaged in the period from the start to 200 ms after the end of the presynaptic current stimulus, no matter if spikes were elicited postsynaptically or not. To reduce the noise caused by electric hum superimposed to the recorded postsynaptic signal, we used a notch filter which removed at least half the power of the frequency components in the range of 47–53 Hz.

- **Latency [ms]:** was calculated as the time difference between stimulus onset of each pulse in the tactile recordings and the peak of the first spike response (see chapter 3.2)

In the results sections 3.1, 3.2 and 3.3.1 response changes (ΔSC, ΔRMP, ΔIR, ΔPR) caused by repeated stimulation are displayed as differences in the measured response features (SC, RMP, IR, PR) between the N^{th} and the first trial or pulse repetition. The observed distributions of these response feature changes are reported as median and first (Q1) and third (Q3) quartiles in the figures. Linear fits were calculated for each cell individually to show the changes with repetitions. The obtained slopes were tested for differ significantly from 0 (t-test, a = 0.05). The average of the linear fits for all cells indicates if the response features changes with repetitions. In section 3.1.4 response changes (ΔSC, Δ(R)MP, ΔIR) are displayed as differences between the hyperpolarized and depolarized conditions to the resting state in the first trial. It was tested if the populations come from a distribution with zero median (signrank, a=0.05).

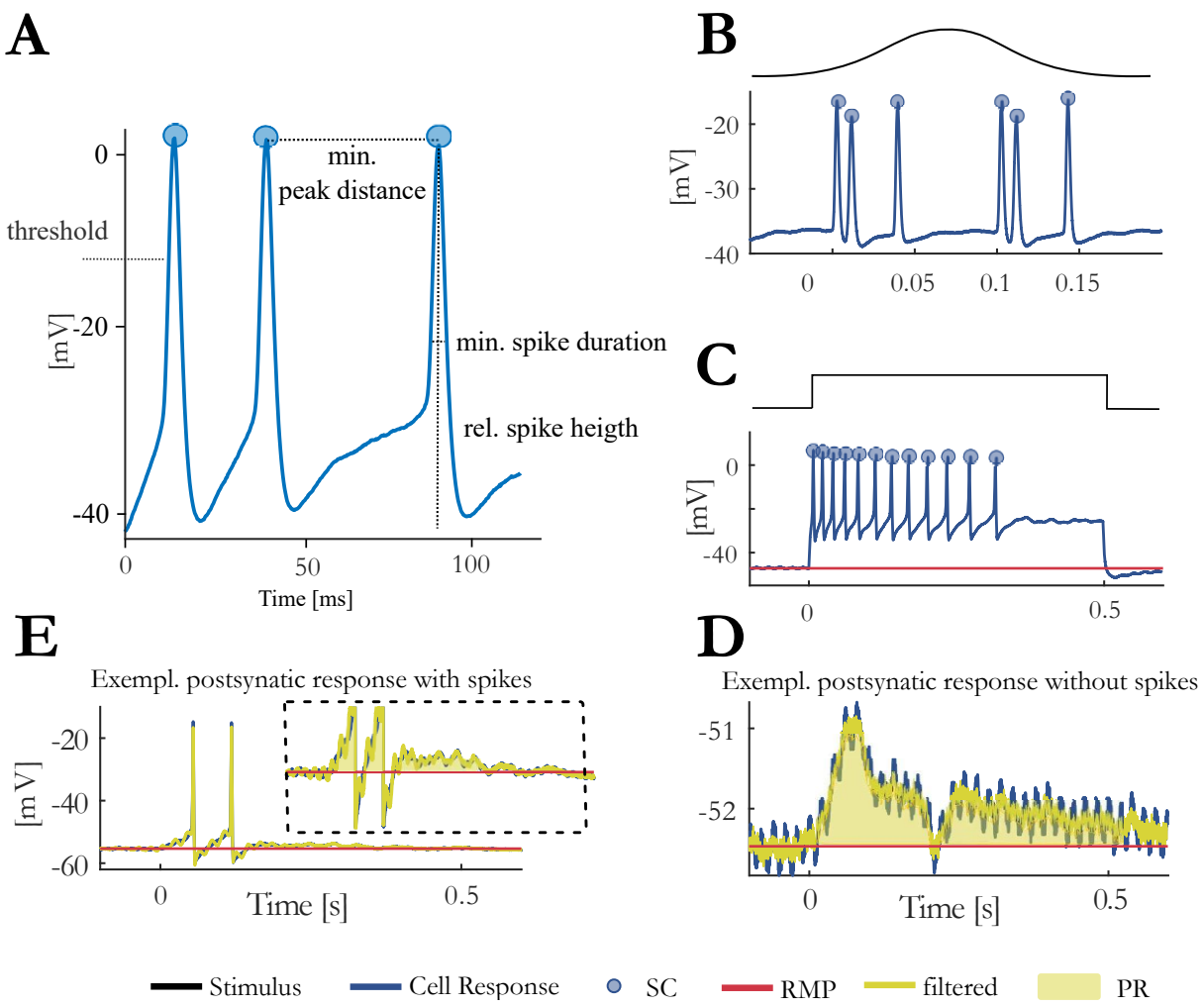

Figure 11 | Experimental design and data analysis. (A) Spikes were defined by the parameters: threshold [mV], minimum duration [ms], and minimum spike amplitude or relative spike height [mV] and min. peak distance. **(B,C)** Representative neuronal responses of a T cell to one sinusoidal up and down of the poker (B) and a somatic current injection of 1nA and 500 ms length (C) The neuronal responses were quantified by the following features: (presynaptic) Spike count (SC, blue dots indicate counted spikes): total number of spikes elicited by the neuron and recorded in the soma in a specific stimulus related time window**.** Resting membrane potential (RMP, red): averaged membrane potential prior the stimulus starts. **(D,E)** Postsynaptic response (PR): averaged difference between the filtered recorded membrane potential (yellow) and the RMP calculated from the start to 200 ms after the end of the presynaptic current stimulus (yellow transparent area). Synaptic potentials sometimes triggered spikes in the postsynaptic cell, but not in all. The calculation of PR included spikes if they were elicited. Subpanels D and E are modified from Meiser et al. 2019

2.4.2 Voltage Sensitive Dye Imaging

Data analysis was done as in Kretzberg et al. (2016) and Fathiazar et al. (2018). First, region of interests (ROIs) corresponding to all visible cell bodies were drawn over the first frame (Figure 12 B right subpanel) of the VSD recording. To localize the cell bodies of the neurons in the first frame with low resolution, the snapshot (Figure 12 B, left subpanel) with the higher resolution was used as orientation. For each stimulus condition (PT, T and P) the cell response traces were extracted from the sequence of images, by averaging and normalizing brightness of the pixels inside each cells' ROI (Figure 12 C, orange). Bleaching artifacts of the VSD signals were corrected as described in E. Fathiazar and J. Kretzberg (2015). Additionally, for each cell baseline was calculated from the VSD signals in the control condition in the same way as described before (Figure 12 C, blue). Baseline luminescence of all control trials was averaged for each cell and subtracted from all VSD signals obtained for all four stimulus conditions (exemplary calculation in Figure 12 D). To reduce the noise level, the difference signal was filtered with a moving average filter of three frames window size. The identification of stimulus-activated cells was performed by statistical analysis as described in Fathiazar et al. (2016). The histogram of the filtered VSD difference signals in control conditions was calculated for each cell (Figure 12 D). Applying a statistical significance level of $\alpha = 0.05$ on this histogram, defines the thresholds when activity differs significantly from baseline (black vertical lines in Figure 12 D, control), indicating very de-or hyperpolarization of the cell's membrane potential. These thresholds (quantiles 2.5 and 97.5% of control response distribution) were applied to the filtered VSD difference signals obtained for the three conditions of mechanoreceptor stimulation (Figure 12 D stimulation, red) to discriminate which individual cells were activated at each timeframe (Figure 12 E). The resulting numbers for each time frame and each cell were combined into an activity map. The lower inset of Figure 12 E shows the activity map for the sample cell in control and stimulated conditions, respectively, corresponding to one trial shown above each inset. In the results section the color of each pixel in the activity map indicates the number of significant deviations from the baseline.

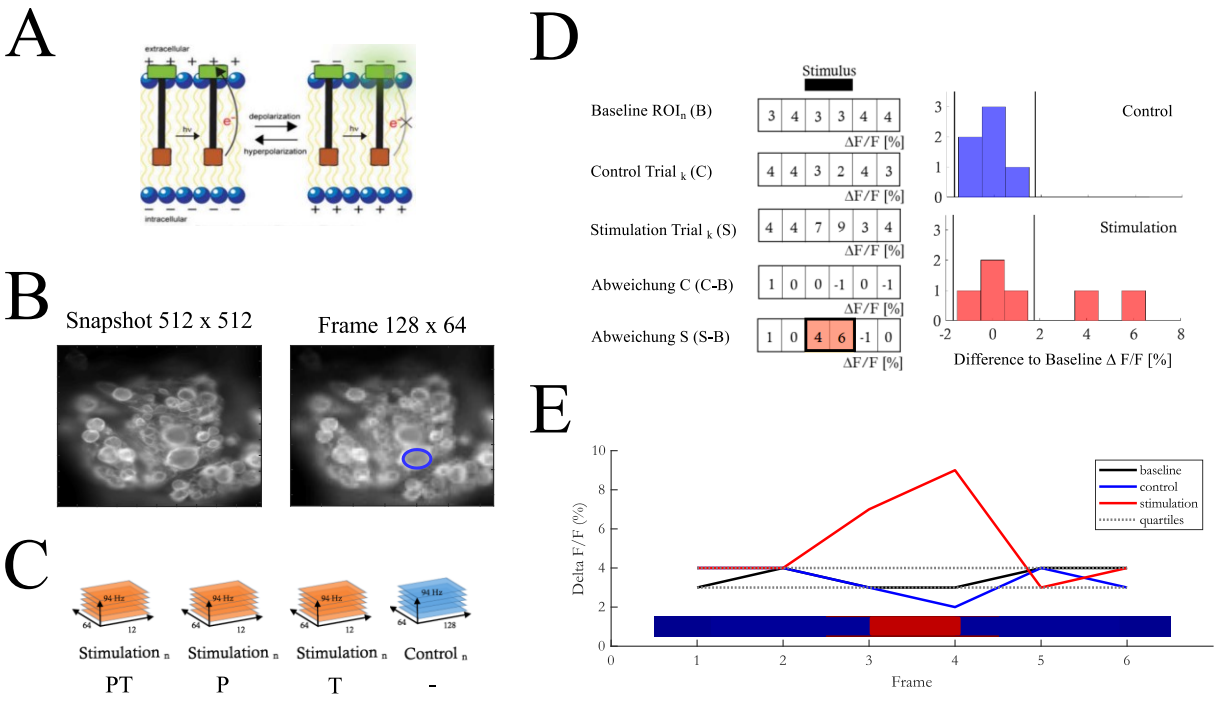

Figure 12| Voltage Sensitive Dye Imaging (A) Photoinduced electron transfer. Voltage sensitive electron transfer from an electron-rich donor (orange) via a membrane spanning anchor (black) to a fluorescence receptor. In the depolarizing state, the electrons migrate away from the extracellular side. The fluorescence receptor is excited by short-wave light and emits brightness which is recorded by a camera. Modified from Miller et al. 2012 **(B)** CCD camera recordings. (Left) High resolution VSD snapshot with 512x512 pixels. (Right) Low resolution VSD recording with 64x128 pixels and a schematic of a hand-drawn region of interest (ROI) as a blue circle. **(C)** Schematics of a VSD experiment trial. The fluorescence of the ganglion was recorded as a film at 94 frames per second (94, Hz, 1 frame = 1 frame) using a CCD camera through the microscope. In order to differentiate the self-fluorescence of the ganglion, mainly caused by the spontaneous activity of individual cells, from stimulus-induced fluorescence, time series (traces) with stimulation and without stimulation (control) were recorded alternately. Together these resulted in a trial. **(D)** Exemplary analysis of a trial of an ROI in the voltage-sensitive dye derivations. (left) The baseline of the ROI (cell) results from the averaging of the individual brightness values of all control trials. Based on a 95% confidence interval, a normal range of activity during the control condition was determined from the distribution of the deviation of all frames of the control. If the deviation of the activity of the VSD signal of a frame in this stimulated trial was outside the threshold values determined via the confidence interval, a stimulus-activated activity could be determined in this time segment. **(E)** Signal values (red (stimulus), blue (control), black (baseline)) above θ_1 and below θ_2 (dashed lines) indicate significantly different responses ($\alpha = 0.05$). Lower inset: Detail of the activity map of the exemplary cell responses in stimulated condition. The time frames between the onset of the intracellular stimulus (frame 3), and the offset of the stimulus (frame 4) are in the stimulated condition (red) above the 5% quartile and indicate an active cell. Subpanels C, D are modified from Sonja Meiser, 2016 (Master Thesis).

2.5 Neuron Modelling

A computational model of the leech T cell was built by Dr. Go Ashida, Post-Doc in the Computational Neuroscience division at the University of Oldenburg, Germany to investigate the physiological bases of the experimentally observed adaptive changes caused by repeated electrical somatic stimulation. We used a single-compartment Hodgkin-Huxley-type neuron model, modified with an additional Na^+/K^+-pump and a M-type slow potassium current (Table 1). The following two sections (2.5.1, 2.5.2) are published in Meiser et al. (2019).

2.5.1 Model Structure

Based on previous experimental recordings of leech neurons, we assumed a fast (transient) sodium channel with four activation and one inactivation gate, while the delayed rectifier potassium channel has two activation gates (Johansen, 1991). These channels are responsible for spike generation in response to positive current injections. The activity of the Na^+/K^+-pump was assumed to depend on the intracellular concentration of Na^+ ions. Increase of intracellular Na^+ due to repetitive spikes leads to the activation of the pump, which exchanges three intracellular Na^+ ions with two extracellular K^+ ions, resulting in the net negative current that hyperpolarizes the membrane potential (Forrest, 2014). The M-type K^+ conductance, whose kinetics are much slower than the spike-generating conductances, cause the cessation of spiking during current injection in a voltage dependent manner (W. Yamada et al., 1989; Benda and Herz, 2003). In order to focus on the fundamental biophysical mechanisms of spike-rate adaptation caused by repetitive current injections, we used this minimalistic description of ion channels and pumps, although the leech T cell may express a number of other ionic conductances (see chapter 4.1).

Table 2 | T cell model equations. The factor 3 for the intracellular Na^+ concentration change originates from the fact that three Na^+ ions are exchanged with two K^+ ions.

Variable	Equation
Membrane potential V	$c_{\mathrm{m}} \frac{dV}{dt} = I_{\mathrm{Na}} + I_{\mathrm{K}} + I_{\mathrm{M}} + I_{\mathrm{L}} + I_{\mathrm{pump}} + I_{\mathrm{inj}}$
Fast (transient) Na^+ current I_{Na}	$I_{\mathrm{Na}} = g_{\mathrm{Na}} \cdot m^4 \cdot h \cdot (E_{\mathrm{Na}} - V)$
Delayed rectifier K^+ current I_{K}	$I_{\mathrm{K}} = g_{\mathrm{K}} \cdot n^2 \cdot (E_{\mathrm{K}} - V)$
M-type K^+ current I_{M}	$I_{\mathrm{M}} = g_{\mathrm{M}} \cdot z^2 \cdot (E_{\mathrm{K}} - V)$
Leak current I_{L}	$I_{\mathrm{L}} = g_{\mathrm{L}} \cdot (E_{\mathrm{L}} - V)$
Kinetic equations for channel variables ($x = m$, h, n, or z)	$\frac{dx(t)}{dt} = \frac{x_\infty(V) - x}{\tau_x(V)}$
Steady state function for Na^+ activation	$m_\infty(V) = \frac{1}{1 + \exp(-(V + 20)/8)}$
Time constant for Na^+ activation (in ms)	$\tau_m(V) = 0.75 \cdot \left(\frac{2}{\exp(-(V + 20)/16) + \exp\big((V + 20)/16\big)} + 0.1 \right)$
Steady state function for fast Na^+ inactivation	$h_\infty(V) = \frac{1}{1 + \exp(+(V + 36)/5)}$
Time constant for fast Na^+ inactivation (in ms)	$\tau_h(V) = 7.5 \cdot \left(\frac{2}{\exp(-(V + 36)/10) + \exp\big((V + 36)/10\big)} + 0.1 \right)$
Steady state function for delayed rectifier K^+ activation	$n_\infty(V) = \frac{1}{1 + \exp(-(V + 20)/8)}$
Time constant for delayed rectifier K^+ activation (in ms)	$\tau_n(V) = 4.0 \cdot \left(\frac{2}{\exp(-(V + 20)/16) + \exp\big((V + 20)/16\big)} + 0.1 \right)$
Steady state function for M-type K^+ activation	$z_\infty(V) = \frac{1}{1 + \exp(-(V + 35)/3)}$
Time constant for M-type K^+ activation (in ms)	$\tau_z(V) = 450 \cdot \left(\frac{2}{\exp(-(V + 35)/6) + \exp\big((V + 35)/6\big)} + 1.0 \right)$
Na^+/K^+-pump current I_{pump}	$I_{\mathrm{pump}} = -I_{\mathrm{max}} \cdot p(c_{\mathrm{Na}})$
Na^+/K^+-pump activation function $p(c_{\mathrm{Na}})$	$p(c_{\mathrm{Na}}) = \left(\frac{1}{1 + \exp(-(c_{\mathrm{Na}} - 18)/18)} \right)^3$
Intracellular Na^+ concentration c_{Na} (measured from rest)	$\frac{dc_{\mathrm{Na}}}{dt} = \kappa_{\mathrm{chan}} \cdot I_{\mathrm{Na}} + 3\kappa_{\mathrm{pump}} \cdot I_{\mathrm{pump}}$

2.5.2 Model Fitting

Since the operating voltage range of leech T cells is considerably more depolarized than those of neurons in most other animals, we needed to adjust the model parameters (Table 3) to reproduce T cell response characteristics to repeated stimulation (shown in chapter 3.1.1). By using the standard membrane capacitance density of 1.0 μF/cm2, the effective size of the membrane and the leak conductance were determined. The membrane area we adopted is larger than what is expected solely from the size of the soma of a T cell, because the additional contribution of the dendritic processes near the cell body was considered.

There is no empirical data available for the ionic concentration in T cells at rest and at spiking. Therefore, we formulated the Na^+/K^+-pump model depending only on the change of Na^+ concentration (denoted as c_{Na}) from rest. In our simulations c_{Na} was assumed to be in a similar order as in Retzius cells, (Deitmer and Schlue, 1983), namely a few tens of mM. Time-dependent changes of the intracellular Na^+ concentration is caused by the Na^+ currents through Na^+ channels and Na^+/K^+-pumps. In order to separately account for the contribution of Na^+ channels and Na^+/K^+-pumps in c_{Na}, we adopted two conversion factors ($\varkappa_{chan}$ and $\varkappa_{pump}$ in Table 3). Theoretically, this conversion factor is the reciprocal of the product between the Faraday constant and the effective volume relevant to the diffusion of Na^+ ions (Barreto and Cressman, 2011). However, it is not simple to estimate these factors in a T cell, because of its complex neuronal morphology. If the diffusion of Na^+ ions, that affects the activity of Na^+/K^+-pump, is not uniform but restricted to the neighbor of the membrane, the effective volume becomes smaller, leading to a larger value of the conversion factor. Therefore, we varied $\varkappa_{chan}$ and $\varkappa_{pump}$ in the range between 0 and 1.20·10-6 mM/pA·ms, and selected values that led to a stable decrease of membrane potential with repeated stimulations.

Table 3 | T cell model parameters. Parameters were fitted to reproduce the experimentally measured T cell spike shape and to produce spike counts and resting potentials in the interquartile range of the experimental observations.

Parameter	Value
Membrane surface area S_m	15000 μm²
Membrane capacitance density C_m	1.0 μF/cm²
Membrane capacitance $c_m = C_m S_m$	150 pF
Fast (transient) Na^+ conductance density G_{Na}	160 mS/cm²
Delayed rectifier K^+ conductance density G_K	8.0 mS/cm²
M-type K^+ conductance density G_M	4.0 mS/cm²
Leak conductance density G_L	0.1 mS/cm²
Fast (transient) Na^+ conductance $g_{Na} = G_{Na} S_m$	24 μS
Delayed rectifier K^+ conductance $g_K = G_K S_m$	1.2 μS
M-type K^+ conductance $g_M = G_M S_m$	0.6 μS

Leak conductance $g_L = G_L S_m$	0.015 µS
Na^+ reversal potential E_{Na}	+30 mV
K^+ reversal potential E_K	-50 mV
Leak reversal potential E_L	-15 mV
Maximum pump current I_{max}	800 pA
Conversion factor from Na^+ channel current into Na^+ concentration $\varkappa_{chan}$	$0.60 \cdot 10^{-6}$ mM/pA·ms
Conversion factor from Na^+/K^+-pump current into Na^+ concentration $\varkappa_{pump}$	$0.12 \cdot 10^{-6}$ mM/pA·ms

2.6 Cell staining

For anatomical studies, T cells in isolated ganglia were filled with 2% Neurobiotin (NB, Vector Labs, Peterborough, UK) using sharp microelectrodes (~30 MΩ). Cells were ionophoretically injected either with positive current pulses (2.5 nA, 3 Hz) for 60 min. After injection, NB-samples rested for 75 min before further processing and fixed in PFA-Fix (0.1 M PB pH 7.4; 2 % CH_2O (Sigma, Munich, BY, Germany) for 1h. After 6x10 min washout in 0.1 M PBS (pH 7.6), the NB-samples were incubated in 1:500 Streptavidin conj. Cy3 (Vector Labs, Peterborough, UK) /PBS/0.3% Triton-X100 overnight at 4 °C. The next day, they were washed 6x10 min in 0.1 M PBS (pH 7.6) and embedded with Vectashield (Vector Laboratories, Burlingame, CA, USA) on a microscope slide for high resolution microscopy. The NB-samples were scanned with a Leica TCS SP 2 Confocal Microscope (Leica, Nussloch, BW, Germany) with an APO 40 x 1.25 Oil objective to obtain confocal stacks. Channel overlay and adjustment of contrast and brightness were performed with the software Fiji (Schindelin et al., 2012). The result of one intracellular staining is shown in the introduction in Figure 1 D.

3 Results

An animal's behavioral context strongly influences decision-making. For example intrinsic factors like attention, sleepiness, territorial status, reproductive situation and hunger all heavily modulate neural responses to auditory, olfactory, tactile or nociceptive inputs (Poulet and Hedwig, 2002; Fields, 2004; Murakami et al., 2005). This sensory gating allows animals to execute appropriate behaviors. Clearly, behavioral choice is inextricably linked to neuronal flexibility (Gaudry and Kristan, 2009), but the neural basis for this combination are not well understood.

It is known in the medicinal leech, that intrinsic and extrinsic factors like the neuromodulator concentration, the water depth and the position of the stimulation effect neuronal plasticity as well as behavioral choice (Gaudry and Kristan, 2009; Palmer et al., 2014). What is missing is a systematically investigation of how repeated skin stimulation can affect behavioral choice. Moreover, it is mostly unknown how the network reacts to repeated stimulation.

Previous studies indicate that one type of the mechanosensory cells (the T cell) might play a role in eliciting behaviors in leeches (Esch and Kristan, 2002; Frady et al., 2016; Brian D. Burrell, 2017; Fathiazar et al., 2018). This thesis investigates the biophysical properties, that underlie response flexibility in T cells and their postsynaptic targets after repeated stimulation. Burgin and Szczupak (2003) and Kretzberg et al. (2007) showed that T cells have at least two distinct spike initiation zones, one in the central ganglion and one in the peripheral branches. Therefore, we analyzed the effect of repeated stimulation on neuronal response flexibility separately in both spike initiation zones.

In the first part of this thesis the effect of repeated somatic T cell stimulation on neuronal response flexibility was investigated by combining experimental and theoretical approaches (see chapter 2.3.1 and 2.5). The second part contained the experimental analysis of repeated skin stimulation and the resulting effect on the intrinsic properties of the T cell. In the third and last part of this thesis the hypothesis that individual T cell spikes effects network activity could be further supported by experimentally analyzing the connection to postsynaptic partner cells. All three subprojects focus on the research question introduced in chapter 1.4

Which biophysical properties cause response flexibility in T cells and their postsynaptic targets?

The results presented here provide the basis and a detailed description of how cell intrinsic flexibility might influence the control of behavior (see chapter 4). The study of the cellular basis of non-synaptic plasticity is also given in a published manuscript (see appendix page I Publication). The content of the following chapters 3.1.1, 3.1.2, 3.3.1 is published in Meiser et al. 2019.

3.1 Repeated somatic current injection induces cell intrinsic plasticity in T cells due to increased Na^+/K^+ pump activity and a slow potassium current (K_M)

High frequency spiking in leech touch mechanoreceptors induces a long-term afterhyperpolarization (AHP), arising mainly from the increased activation of the Na^+/K^+-pump due to intracellular accumulation of Na^+ ions (Baylor and Nicholls, 1969a). Increased activity of Na^+/K^+-pumps provides a mechanism for intrinsic, activity dependent regulation of excitability (Gulledge et al., 2013; Duménieu et al., 2015). We assume that repeated stimulation can induce a form of non-synaptic plasticity in T cells based on changes in the opening probability of ion channels. In the first part of the study the focus lies on the central spike initiation zone of the T cell. By combining experimental, electrophysiological, and theoretical modelling approaches we investigated the effect of repeated somatic stimulation on the cell response parameter spike count (SC), resting membrane potential (RMP) and cell input resistance (IR).

3.1.1 Repeated somatic current injection increases SC and IR and hyperpolarizes RMP

By applying series of current pulses (500 ms duration, separated by 2500 ms break) into the T cell soma high frequency spiking was triggered (Figure 13). The cell response was analyzed for changes in the physiological properties SC, RMP, and cell IR. As can be seen in the representative intracellular response traces, repeated current injection caused an increase in SC and in IR, while the RMP hyperpolarized. These tendencies were seen in all recordings, even though the initial responses of individual T cells varied considerably in their SCs and the duration of their spiking activity (compare Figure 13 A / B for examples of a slowly and a rapidly adapting initial response, see Figure 14 H–J for the interquartile ranges of SC, RMP, and IR). The activity-dependent changes were found to be highly significant ($p < 0.001$) for all three physiological properties by testing if the slopes of linear regressions of individual cell responses differed from 0 (Figure 13 C/D/E). This approach is not meant to imply that the relationships are linear, but only that SC and IR increased, and RMP hyperpolarized consistently in all 20 cells. While Figure 13 shows the changes caused by repeated current injection, Figure 14 H–J indicate the interquartile ranges of the observed measurements of SC, RMP, and IR. For an input current of 1 nA, the SC gradually increased from a median value of 14.5 in trial 1 to 36 in trial 20. Meanwhile the median RMP gradually hyperpolarized from -37.5 to -48.8 mV and the median IR increased from 27.8 to 62.7 MΩ. The absolute changes of the physiological properties to a current injection of 1 nA, calculated as median and quartiles over cells, are shown in Table 4 (data for current injection of 0.5, 0.75, 1.25, and 1.5 nA are not shown, but followed the same trend).

Summarizing, the RMP of T cells hyperpolarizes in response to repeated somatic current injection, while the SC increases. Usually, one would expect that the probability for action potential generation is decreased at hyperpolarized RMP (Hogkin and Katz, 1949). However, the repetitive electrical stimulation also led to a substantial increase in cell IR, which cannot be explained by electrode clogging (see chapter 2.3). To investigate the reason of the experimentally observed increase in SC, we developed a Hodgkin–Huxley type neuron model, modified with an additional Na^+/K^+-pump and a M-type slow potassium current (see chapter 2.5 and Table 2).

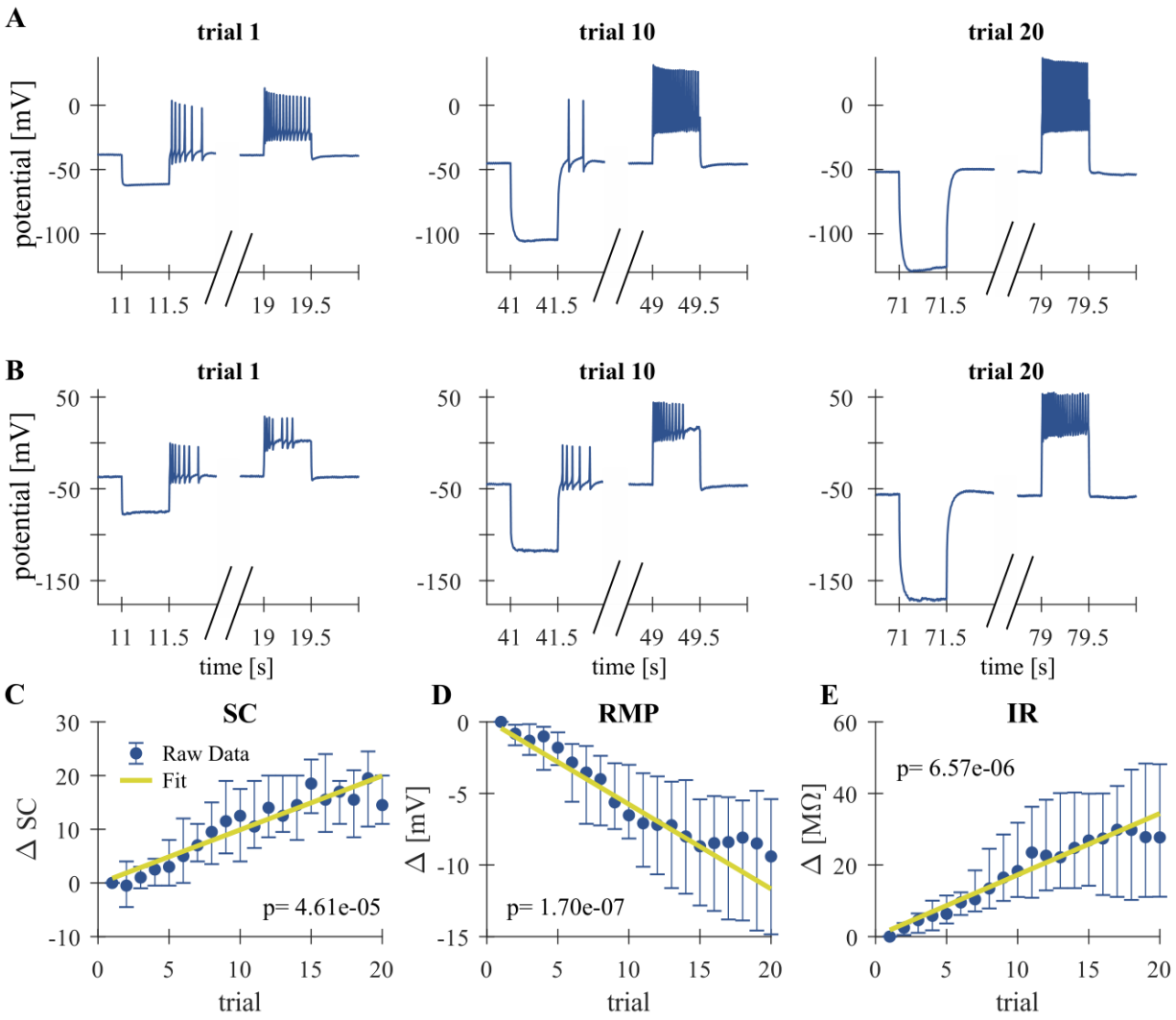

Figure 13 | Repeated somatic current injection effects physiological properties of T cells. (A,B) Representative responses of intracellularly recorded T cells to a 500 ms long somatic current pulse injection of –1 nA (seconds 11–11.5, 41–41.5, and 71–71.5), which was used for the calculation of the IR and often elicited rebound spikes, and +1 nA (seconds 19–19.5, 49–49.5, and 79–79.5) in Trial 1, 10, 20. **(A)** Example of a slowly adapting initial response, **(B)** Example of a rapidly adapting initial response. **(C–E)** Dependencies of changes in response parameters on trial repetitions shown as median and quartiles of all T cells (N = 20). Linear fits were calculated for each cell individually and the obtained slopes were tested to differ significantly from 0 (t-test, a = 0.05, p-values given in the panels). The yellow line indicates the average of the fits for all cells. **(C)** Spike count (SC) difference from first trial (absolute number). **(D)** Resting membrane potential (RMP) difference from first trial (mV). **(E)** Input resistance difference from first trial (MΩ). Figure from Meiser et. al, 2019.

3.1.2 Na^+/K^+ pump and a slow potassium current might induce cell intrinsic plasticity

Many previous studies already investigated how different forms of AHPs are affected by voltage- or calcium-dependent ionic conductances (reviewed in Vogalis et al. (2003) and Larsson (2013)(2003; Larsson). The time scales of intracellular calcium buffering (W. Yamada et al., 1989; Goldman et al., 2001) and the activation/inactivation of calcium dependent potassium currents (Vogalis et al., 2003), however, is on the order of 0.1–1 s, which is several orders of magnitude faster than the activity-dependent long-term decrease of the membrane potential we focus on (which is on the order of a few tens of seconds; Figure 13). In this slow potential change, the activity of the Na^+/K^+-pump is likely to be relevant (Barreto and Cressman, 2011; Forrest, 2014). Additionally, the involvement of Na^+/K^+ pump in the induction of a long term afterhyperpolarization due to high frequency spiking in leech touch mechanoreceptors was already examined (Nicholls and Baylor, 1968; Baylor and Nicholls, 1969a; Jansen and Nicholls, 1973; Scuri et al., 2002; Scuri et al., 2007). Hence, the involvement of the Na^+/K^+-pump on the changes in the physiological properties of T cells, namely the hyperpolarization of the RMP accompanied by the increase of SC and IR was investigated. To address this question, a minimalistic Hodgkin–Huxley-type neuron model of a T cell was constructed. It incorporates the fast Na^+, delayed rectifier K^+, leak, and slow M-type K^+ conductances as well as the Na^+/K^+-pump. Blue curves in Figure 14 show the responses of the default T cell model.

To simulate the spiking responses of the T cell, the same protocol as for the experimental recordings with somatic current injections was used (Figure 4). Parameters of the model were adjusted so that the simulated spike shape matched the time course of the original spike and the adaptive changes of the main features SC, RMP and IR stayed largely within the interquartile ranges of the original data (blue curves in Figure 14 H–J). The increase of the pump current (Figure 14 A, blue) was responsible for the decrease of the RMP from about -39 to -48 mV (Figure 14 I, blue), because in each pump cycle three intracellular sodium ions were exchanged with two extracellular potassium ions, leading to a net negative current. The SC of the standard model increased over trials (Figure 14 H), because of the voltage dependent deactivation of the M-type K^+ current (Figure 14 B,C), which in early trials activates during the current injection and hinders the repetitive spiking. Additionally, the decrease of the M-type K^+ conductance across trials also let to a decrease of the simulated IR from about 31–60 MΩ (which resembled the empirical observations (Figure 13 D,E), and also had a positive effect on SC.

Table 4 | Absolute values for non-synaptic plasticity effects in T cells. Responses to 500 ms current injection of 1 nA were obtained in 20 cells. Table from Meiser et. al, 2019.

	Trial 1			**Trial 20**		
Property	*Q1*	*median*	*Q3*	*Q1*	*median*	*Q3*
SC [spikes/0.5 s]	7.5	14.5	24	27.5	36	42
RMP [mV]	-32.9	-37.5	-40.6	-44.5	-48.8	-52.9
Resistance [MΩ]	19.4	27.8	38.7	46.4	62.7	74.1

In order to further investigate the roles of the Na^+/K^+- pump and the putative M-type K^+ conductance, these current were fixed and the resulting changes of the model neuron responses from the default condition examined (see chapter 4.1). When the pump current was fixed to the initial steady-state value, the stimulus-induced hyperpolarization as well as the increase of SC and IR vanished (Figure 13 E; compare the green and blue curves in Figure 14 H–J). This suggests that the experimentally observed stable hyperpolarization of the RMP is mainly due to the increase of Na^+/K^+-pump current and that this hyperpolarization is the basis for all observed changes.

When the M-type K^+ conductance was fixed to the initial steady-state, while the pump was allowed to change, the IR did not change, indicating that the observed increase in IR can be attributed to the changes in the slow KC current. In this model version, the SC decreased across trials (Figure 14 F and black curves in Figure 14 H,J), showing the intuitively expected effects of slow hyperpolarization (Figure 14 I, black). This SC decrease was diminished when the M-type K^+ conductance was kept unchanged only during the C1 nA stimulation (Figure 14 G), while it could change in an activity-dependent way at all other times. In this model, the closing of the modelled M-type K^+ channel still led to an increased IR (Figure 14 J, red) and counteracted the reduced excitability due to hyperpolarization (compare black and red curves in Figure 14 H). We also note, however, that the dynamic property of the M-type K^+ current, which activates on the time scale of a few 100 ms, turned out to be critical for determining the duration of repetitive spiking (compare Figure 14 D,G). Despite the realistic increase in IR, the number of spikes in the model version with partially fixed M-type KC current were very large (Figure 14 H, red), because spiking activity did not cease before the end of the stimulus (Figure 14 G). These results suggest that the experimentally observed repetitive spiking behavior (and its cessation) of leech T cells is associated with a K_M-like slow conductance, which affects the SCs more dynamically than the static increase of IR. In sum, our modelling results suggest that the inactivation of the slow KC current plays a role in increasing the SC in an activity-dependent manner (Figure 14 H). This inactivation is induced by the RMP hyperpolarization caused by the increased activity of Na^+/K^+-pumps (Figure 14 I).

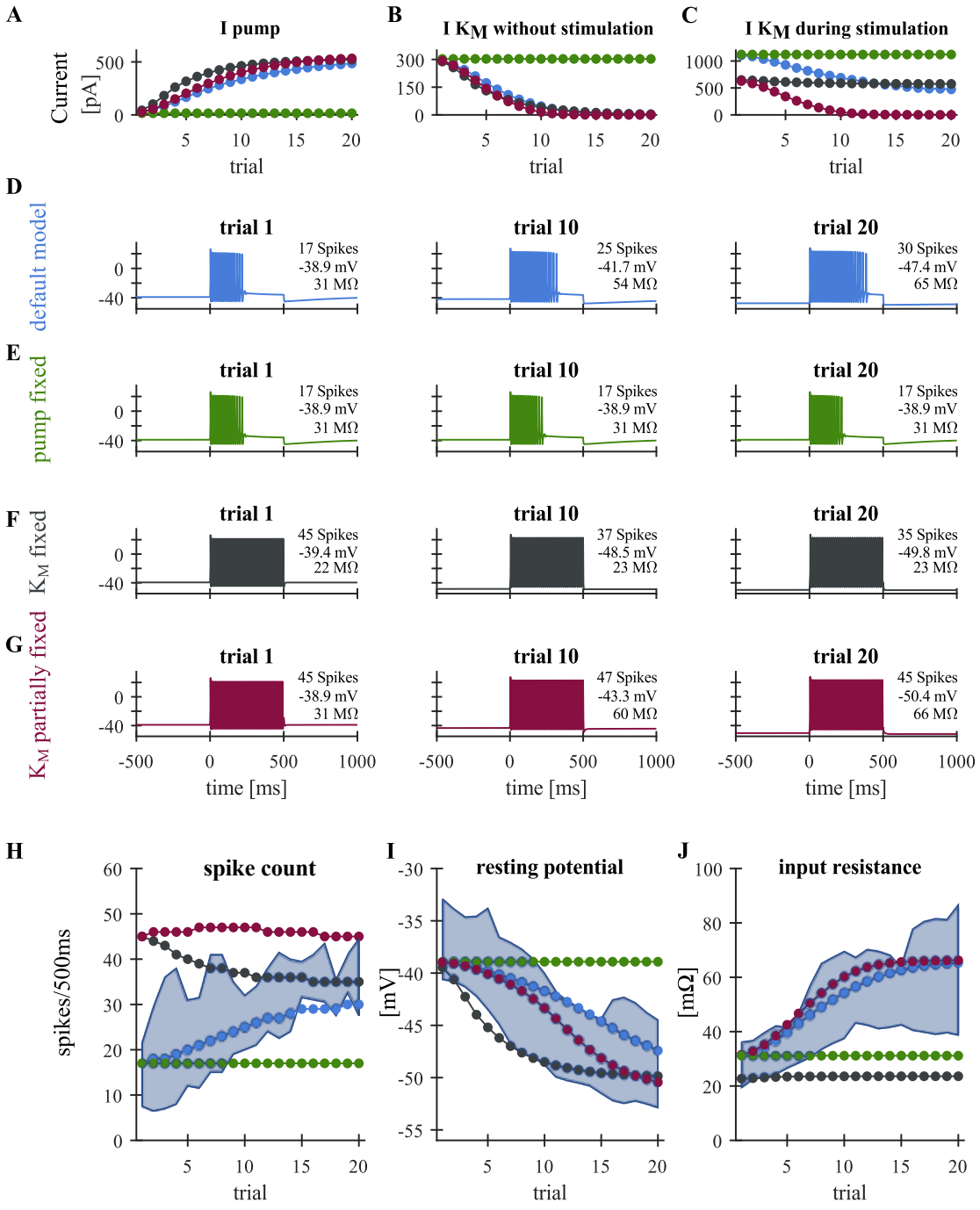

Figure 14: | Modeling T cell spike responses. (A) Average Na^+/K^+-pump current during +1 nA stimulation. **(B)** Average M-type K^+ current at 0–500 ms before the +1 nA stimulation. **(C)** Average M-type K^+ current during +1 nA stimulation. The K_M current is generally larger during stimulation (C) than without stimulation (B), because of the increased average driving voltage (EK–V) associated with spiking. (D–G) Responses of different T cell models to a current injection of +1 nA in Trials 1, 10 and 20. See Figure 5 for the stimulus protocol used. (D) Default model. (E) "Fixed pump model," in which the Na^+/K^+-pump current I_{pump} is fixed to the initial steady-state value. (F) "Fully fixed K_M model," in which the dynamics of the M-type K^+ conductance was fixed to the initial steady-state value. (G) "Partially fixed K_M model," in which the dynamics of the M-type K^+ conductance was fixed only during +1 nA current injection. (H–J) Simulated changes of the spike count (H), resting potential (I), and input resistance (J) across trials, plotted with the corresponding interquartile ranges observed experimentally (blue shading). Colors in panels (A–C) and (H–J) indicate the different model conditions: (blue) default model; (green) "fixed pump model"; (black) fully fixed K_M model; and (red) "partly fixed K_M model." Figure from Meiser et al. 2019.

3.1.3 Na^+/K^+ pump inhibition decreases SC in T cells after repeated stimulation

The experimental and modelling results in chapter 3.1 indicate that T cells modify their responses depending on their previous activity. Repeated somatic T cell stimulation enhances Na^+/K^+-pump activity, which gradually hyperpolarizes the RMP. This results in the suppression of a slow K^+ current, which leads to a higher IR and an increased SC. In this part of the thesis the hypothesis of the proposed non-synaptic plasticity mechanism is supported. We could show that after induction of non-synaptic plasticity a pharmacological block of the Na^+/K^+ pump with 10 nm Dihydrouabain (DHO) leads to a decrease in SC in nine selected T cell recordings. This tendency was seen in at least 15 recordings more, but they do not have the same stimulation sequence so that a compared analysis was not possible.

Before bath application of DHO non-synaptic plasticity was elicited by applying five trials of 20 current pulses each with an IPI of 2.5 s each (Figure 5). As can be seen in the representative intracellular response traces (Figure 15 A upper panels), repeated current injection caused an increase in SC as expected from the results in chapter 3.1.1. This tendency was seen in eight out of nine recordings, even though the initial responses of individual T cells varied considerably in their SCs and the length of their spiking activity (see Figure 15 and Table 5).

Median SC in this control condition increases from 4 spikes (Q1: 2 / Q3: 4) in pulse 1 to 7 spikes (Q1: 1.75 / Q3: 7) in pulse 100. The activity-dependent increase was found to be significant ($p = 0.006$), by testing if the slopes of linear regressions of the nine individual cell responses differed from 0. Such an approach does not mean to imply that the relationship is linear, but only that SC increased, consistently in all 8/9 cells. This can be seen in the individual fits of each cell in Figure 15 B (colored lines). However, when taking a closer look on the single slopes of the individual fits as well as the initial SC and final SC of each cell (Table 5 and Figure 15) the population can be split up into two groups. One group contains the cells, which seem to increase their activity in a significant way (slope above 0.01, magenta, green, red, cyan, orange). The other group seem not to increase their activity significantly (slope below 0.01, violet, yellow, blue and brown). However, for a valid statistic statement more recordings necessary.

Inhibition of Na^+/K^+ pump after spiking activity results in an increased amount of intracellular Na^+ (Bear et al., 2018). Usually this leads to a depolarized RMP, which should enhance the cell excitability because the distance to threshold for spiking is lower (Bear et al., 2018). Our experiments could not be interpreted regarding the RMP due to a high electric drift (see chapter 2.4.1 and 4.4.1).

However, as can be seen in the representative intracellular response traces (Figure 15 A middle panels), inhibition of Na^+/K^+ pump by DHO application leads to a delayed significant decrease in SC from a median SC of 5 (Q1: 1.75 / Q3: 7.75) in pulse 1 to 2 spikes (Q1: 0/ Q3: 5.5) spikes in pulse 100 by testing if the slopes of linear regressions of individual cell responses differed from 0 ($p=0.098$). This seems to be due to the fact, that DHO needs to diffuse through the glial membrane and the cell membrane before it can interact with the Na^+/K^+ pump. The decreasing effect seems to be due to a delayed opening of the putative K_M channels which changes spiking behavior of T cells from transient to sustained. When taking a closer look at the relative

tendencies (slopes) and the absolute SC of each individual cell (see Figure 15 C and Table 5), every single except of one (blue) showed a consistent decrease in SC over time.

Because the effect of DHO is reversible (Cox and Woods, 1987; Scuri et al., 2007), washout of the substance allows to study pump activity under control, experimental and after experimental conditions in the same tissue. Therefore, we would expect an increase in SC during washout condition as shown in (Scuri et al., 2007). However, we could not see an increase in SC in the washout condition. Instead the median SC decreased further from 1 spikes (Q1: 0/Q3: 4.25) in trial 1 to 0 spikes (Q1:0/ Q3: 4,35) in trial 50 to 0 spikes (Q1: 0/Q3: 1.7) in trial 100. This change was not found to be significant by testing if the slopes of linear regressions of individual cell responses differed from 0. This might be the case because the washout time was too short (see chapter 4).

Furthermore, the representative response of a T cell clearly shows that DHO application changes spike form (Figure 15 A right lower panel). The fast afterhyperpolarization after a single spike seems to be smaller than before and during DHO application.

Summarizing, these experiments show that blocking of Na^+/K^+ pumps decreases the previously increased SC of T cells due to repeated stimulation. This supports the hypothesis that the Na^+/K^+ pumps are involved in the proposed non-synaptic plasticity mechanism. Additionally, the results show that some T cells seem not to change their activity with repeated stimulation. This indicates that non-synaptic plasticity can only arise if the cell has the right intrinsic and extrinsic circumstances (see chapter 4.1 for a further discussion aspect).

Table 5 | Absolute SC on the first and the hundredth current pulse (length 500ms) of each condition for each cell (color code is the same as in Figure 15). Additionally, the slope of the linear regression fit of each cell is given. Linear regression was calculated from differences in SC between the Nth and the first pulse in the control condition. Example recording of Figure 15 A is not shown here.

Condition	**Control**			**Washin**			**Washout**		
Cell	Pulse 1	Pulse 100	Slope Fit	Pulse 1	Pulse 100	Slope Fit	Pulse 1	Pulse 100	Slope Fit
1	4	7	0.0324	13	7	-0.1422	5	4	-0.0161
2	0	1	0.0049	0	0	0.0001	0	0	0
3	2	1	-0.0024	1	0	-0.0016	1	0	-0.0012
4	9	12	0.0151	13	13	-0.0047	14	9	-0.0441
5	2	2	0.0061	2	2	0.0176	2	1	-0.0167
6	4	7	0.0157	5	0	-0.0525	0	0	-0.0000
7	4	3	0.0149	6	0	-0.0717	0	0	0.0005
8	4	7	0.0316	5	5	-0.0280	4	0	-0.0465
9	0	3	0.0090	3	3	0	3	0	0.0011

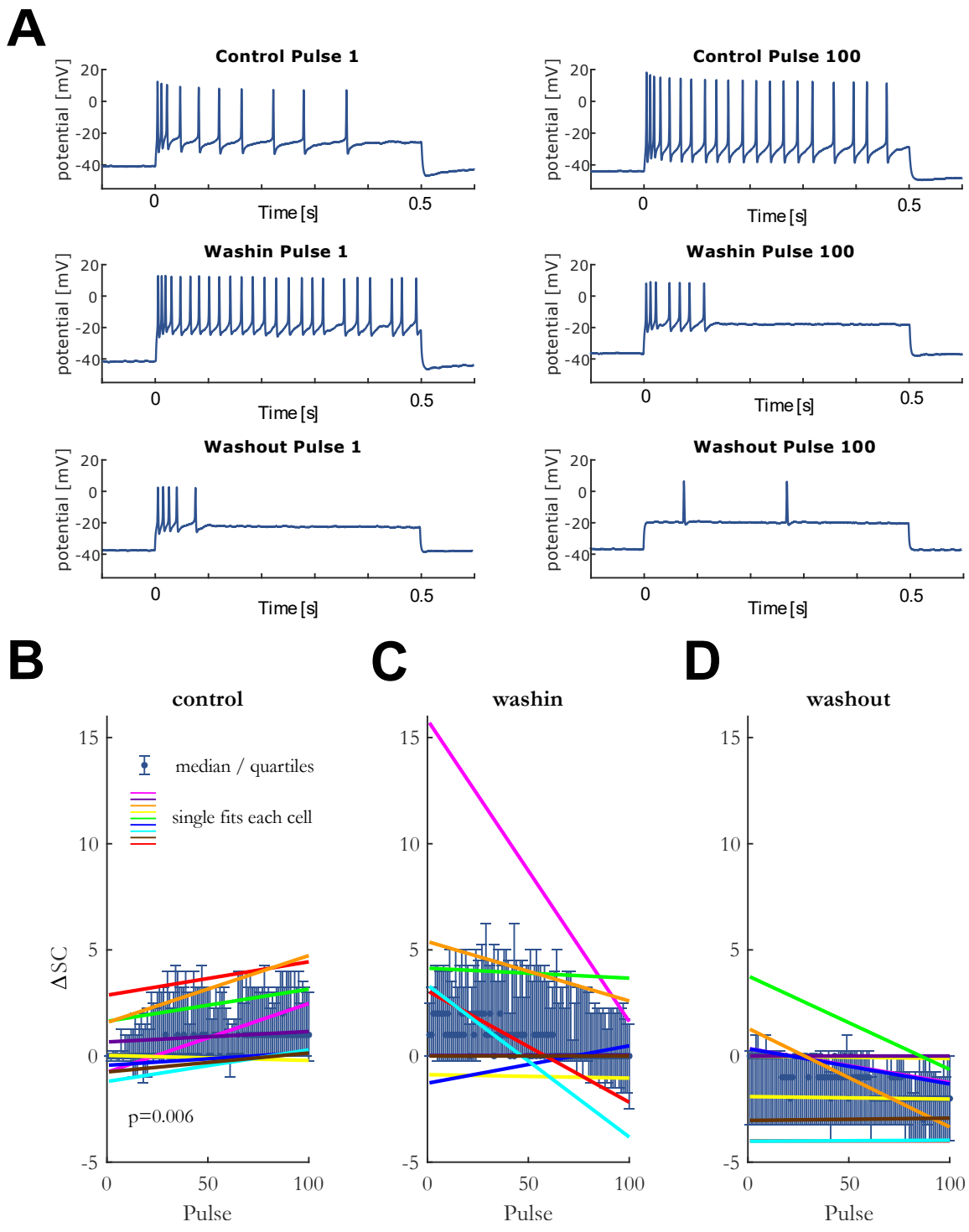

Figure 15 | Pharmacological Block of Na^+/K^+ pump changes somatic SC of T cells

(A) Representative responses of an intracellularly recorded T cell to a 500 ms long somatic current pulse injection of +1 nA. Pulses 1 and 100 of the control, the washin and the washout conditions are shown. **(B-D)** Dependencies of changes in spike count (SC) on pulse repetitions for each condition shown as median and quartiles of all T cells (N = 9 cells). It is shown the spike count (SC) difference from the first current pulse in the control condition (absolute number) for the **(B)** Control condition **(C)** Washin condition **(D)** Washout condition. The colored lines indicate the linear fits, which were calculated for each cell individually. The exemplary recording shown in A was not one of the nine selected recordings for the analysis.

3.1.4 Different holding potentials triggers different SC in T cells

The experimental and modeling results in chapter 3.1.1 and 3.1.2 indicate that a hyperpolarized membrane potential, due to increased Na^+/K^+ pump activity, might suppress a slow potassium current. Previous studies indicate, that this current flows through K_M-channels, whose opening probability increases with depolarization. This might cause spike responses to stop before the end of the stimulation. The electrophysiological recordings in chapter 3.1.1 and 3.1.2 show that the SC of a leech T cell depends on the RMP. If the membrane potential is hyperpolarized, then the cell generates more spikes. The modelling results (see chapter 3.1.2) support that K_M-channels might be candidates for regulating these cell intrinsic plasticity in T cells together with the sodium potassium pump.

To support this hypothesis, the membrane potential of a T cell was artificially set to different holding potentials by applying +0.5 nA or -0.5 nA current. From these baselines on current pulses of 0.5nA or 1nA (see chapter 2.3.1.2, Figure 6, Figure 16 A) were applied for 500 ms to analyze the physiological property SC depending on the holding potential for each current pulse in the first trial (see chapter 2.4.1). The data was not analyzed and could not interpreted over trials because the recordings were superimposed by an electric drift (see chapters 2.4.1 and 4.4).

In the first trial, the median membrane potential of all 16 measured T cells (Figure 16 C) was at -53.01 mV (Q1: -41.10 / Q3: -78.23) in the resting state, at -81.08 mV (Q1: -51.7/ Q3: -118.2) in the hyperpolarized state and at -37.52 mV (Q1: -25.36/ Q3: -57.41) in the depolarized state. This shows that an application of 0.5 nA leads to a positive change in the membrane potential of 15.5 mV, whereas an application of -0.5 nA leads to a negative change of -28.07 mV. Additionally, the artificial set membrane potentials (depol / hyperpol) were found to differ significantly from the resting state ($p<0.01$) by testing if the populations of the differences for each cell comes from a distribution with zero median.

As can be seen in the representative intracellular response trace (Figure 15 A), these significantly different holding potentials leads to different SC despite the same amount of amplitude of injected current. To be precise 1 nA current injection leads in the resting state to a SC of in median 23.5 (Q1: 9/ Q3: 30), in the hyperpolarized state to a SC of in median 26 (Q1: 13/ Q3: 31) and in the depolarized to a SC of in median 17.5 (4/24.5). A 0.5 nA current injection leads in the resting state to a SC of in median 14.5 (Q1: 1.5/ Q3: 19) and in the hyperpolarized state to a SC of in median 16 (Q1: 6/ Q3: 18).

The SC differences for each cell in the first trial for the 0.5 nA (cyan in Figure 16) and the 1 nA (magenta in Figure 16) current injections were also found to be significantly higher in the hyperpolarized state compared to the resting state $p<0.01$ by testing if the populations of the differences for each cell comes from a distribution with zero median. Additionally the SC for the 1 nA current injection (magenta in Figure 16) was found to be significantly lower in the depolarized state compared to the resting state ($p<0.01$) by testing if the populations of the differences for each cell comes from a distribution with zero median. This implies that a by -28 mV hyperpolarized membrane potential leads to a fewer SC change than a by +15.5 mV depolarized membrane potential.

Cell input resistance in the first trial was in median at 12.09 MΩ (Q1: 9.48 / Q3: 19.29). This was found to be significantly lower than the input resistance of the "pseudorandomized" experiments in the first trial (see Table 4) by testing if the populations come from continuous distributions with equal medians, against the alternative that they are not (p= 6.5173e-06).

To sum up, we could show that the SC, induced by somatic current injection, depends on the current membrane potential. This supports the hypothesis of K_M channel involvement in the previously proposed non-synaptic plasticity mechanism because the probability of open K_M channels increases with depolarization. This in turn could cause a cessation of spikes before stimulus presentation ends. Though, the effects seen in the presented results could also be occurred due to other voltage gated ion channels. Therefore, a pharmacological block of K_M channel would give further indications if K_M channels are present in leeches (see chapter 4).

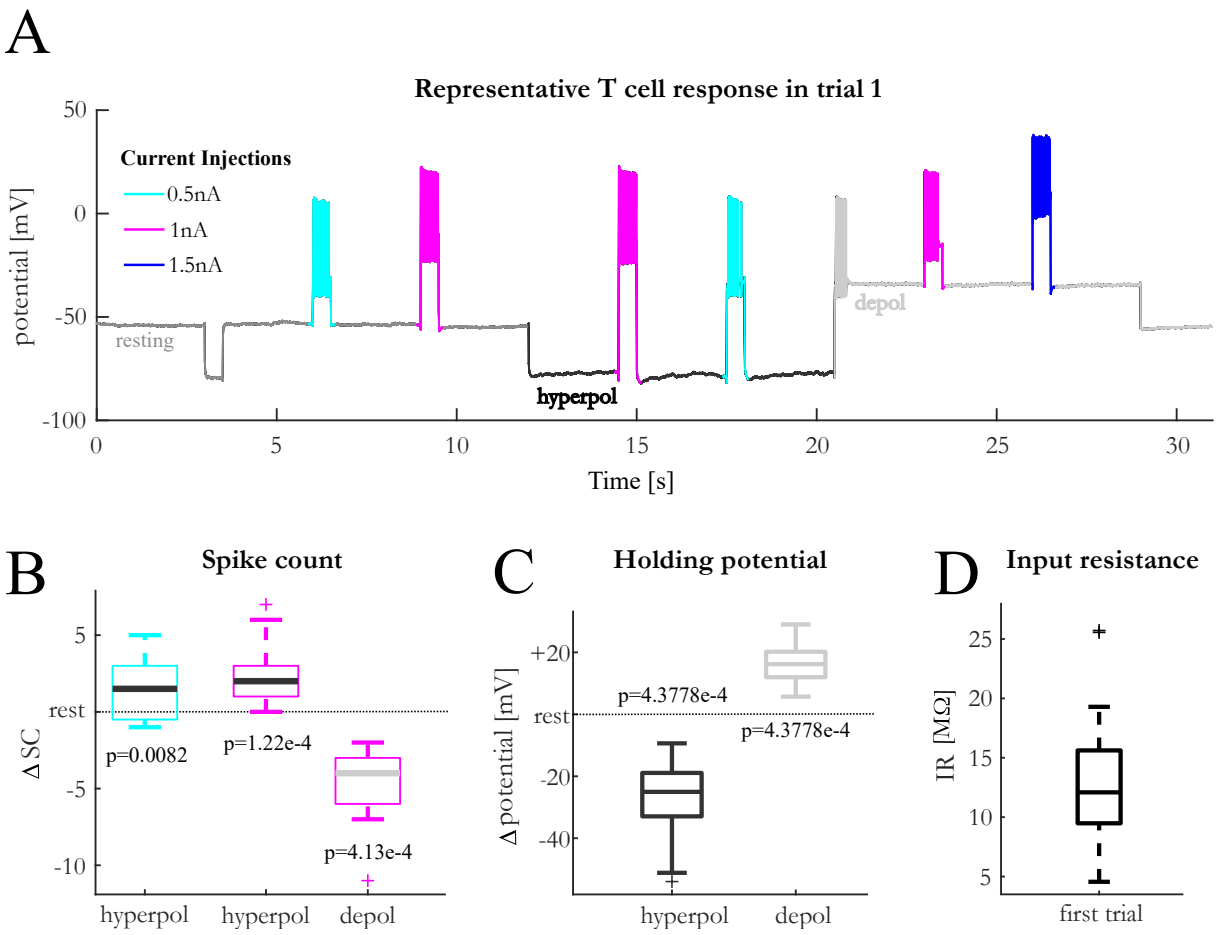

Figure 16 | The same amount of somatic current injection in T cells induce different SCs on different holding potentials. (A) Representative response trace of an intracellularly recorded T cell in trial 1 to the different baseline protocol (see Figure 6) **(B,C)** Difference of the response parameter SC and holding potential from the hyperpolarized (dark gray) and the depolarized (light gray) condition to the resting condition. The differences are shown as median and quartiles of all T cells (N=16). (B) SC (cyan 0.5 nA current injection, magenta 1 nA current injection) (C) Holding potential. (D) Input resistance for the first trial of all 16 T cells as boxplot. Calculation of the input resistance was done by using the hyperpolarized current step before any stimulation in the first trial.

3.2 Cell intrinsic plasticity occurring at multiple spike initiation zones (SIZs) interact

Previous studies suggested that, contrary to the classical view of neuronal information processing (Bear et al., 2018; Purves, 2019), leech T cells have at least two distinct spike-initiation zones (Burgin and Szczupak, 2003; Kretzberg et al., 2007). One is located in the periphery near to the skin to process touch stimuli and a second central one processes synaptic inputs within the ganglion (see Figure 1 E). The previous chapter 3.1 covered the investigation of the flexibility of the central spike initiation zone. In this chapter it is shown if and how repeated skin indentation influences peripherally initiated spikes, as well as the interaction of both spike initiation zones. It is technically not possible to record the membrane potential in the periphery, but spikes can travel from the periphery in the soma. Therefore, we recorded the somatic membrane potential of the T cell intracellularly in a body wall preparation, while stimulating the skin with sinusoidal up and down movements of a lever arm. Additionally, before and after tactile stimulation a somatic current injection activated central SIZ to test if both SIZs can influence each other.

As indicated in the representative intracellular response trace (Figure 17 A), repeated tactile stimulation causes spiking in a ventral T cell (red and blue traces in Fig 17 A). Furthermore, tactile induced spikes seem to lead to changes in somatic induced SC (dark and light green trace in Fig 17 A). More precisely, spikes, induced in the soma, increases from a median value of 9 spikes before the first tactile stimulation in trial 1 to a median value of 47 spikes after tactile pulse 60 in trial 3 (see Table 6 for absolute values and Fig 17 E for the dependency of the relative somatic SC on trials). This is an overall increase of 36 spikes in median. Additionally, it is interesting to mention, that the change in SC proceeds not linearly. To be more precise the somatic SC increases more in the time between two trials (no stimulation) than in the time within one trial (before and after tactile stimulation).

The representative intracellular response trace also indicates that the input resistance of the T cell before (IR_{before}) and after (IR_{after}) tactile stimulation changes in the same way as the somatic SC. Using the passive response of the somatic current injection for calculation shows that the T cell starts with a median IR_{before} of 9.95 MΩ and increases to 22.12 MΩ after the last tactile stimulation in the third trial (Fig 17 E). However, the 25 % and 75 % quartiles indicate a broad distribution of the 8 analyzed recordings/cells.

When taking a closer look at the tendencies of each individual cell, every single cell except one showed a decrease in SC, induced by tactile simulation, over time. Because T cells sometimes switch positions (Kretzberg et al., 2016), and we took into consideration that this cell might be not a ventral T cell, this data set were excluded from the following calculation. Now, the so-called *tactile SC* decreases over all trials from 47.5 to 29 spikes. However, between two trials (without stimulation) the cell seems to recover because SC in response to the first tactile pulse (red dot in Figure 17 D) in trial 2 / 3 was higher compared to the SC in response to the last tactile pulse of trial 1 / 2 (last blue dot of each trial in Figure 17 D)

The representative response trial indicates that RMP also decreases obviously over trials (Fig 17 D). However, this might be due to the strongly variable electrode drift that occurred during the experiments.

Furthermore, during repeated tactile stimulation, the first spike latency of each pulse increased in all recordings from a median of 4.30 ms to 4.7 ms. Though, as mentioned for the tactile SC this change is not linearly. The latency to the last tactile pulse of each trial was longer than to the latency of the first tactile pulse of the following trial.

To sum up, the T cell spike-initiation zone in the central ganglion showed obvious increases in SC and IR in response to repeated tactile stimulation. In contrast, the T cell spike-initiation zone in the periphery showed a decrease in SC and an increase in spike latency. The RMP, measure in the soma, hyperpolarizes slightly during the repeated stimulation. The absolute changes of the physiological properties, calculated as median and quartiles over cells, are shown in Table 6.

B.Sc. Maren Prelle, a Master Student from University of Cologne, who I supervised from January 2020 – March 2020, obtained the tactile recordings, and kindly provided them for my thesis.

Table 6 | Absolute values for non-synaptic plasticity effects in T cells induced by tactile skin stimulation. Responses to tactile pulses 1 and 20 as well as the 500 ms current injection of 1 nA before and after the repeated stimulation were obtained in 8 cells. Table from Meiser et. al, 2019.

	Pulse 1			**Pulse 20**			**Pulse 21**			**Pulse 40**			**Pulse 41**			**Pulse 60**		
Property	*Q1*	*med*	*Q3*	*Q1*	*med*	*Q3*	*Q1*	*med*	*Q3*	*Q1*	*med*	*Q3*	*Q1*	*med*	*Q3*	*Q1*	*med*	*Q3*
$SC_{tactile}$	39.5	**47.5**	57.5	26	**38.5**	42.5	43	47	53	26	**29**	42	39	42	43.5	24	**29**	39.5
RMP [mV]	-34.70	**-37.86**	-40.29	-40.15	**-40.83**	-42.74	-39.95	-41.63	-43.68	-41.17	**-43.24**	-49.20	-42.97	-45.24	-48.98	-42.75	**- 47.40**	-48.32
LAT [ms]	4.15	**4.30**	4.75	4.44	**4.59**	4.96	4.36	4.45	4,85	4.45	**4.58**	5.01	4.45	4.53	4.94	4.48	**4.57**	5.10
	Trial 1 before			**Trial 1** after			**Trial 2** before			**Trial 2** after			**Trial 3** before			**Trial 3** after		
IR [MΩ]	8.72	**9.96**	14.74	12.23	**17.75**	26.73	7.51	14.60	29.70	13.53	**19.83**	36.67	9.04	18.38	34.69	16.30	**22.12**	38.86
SC_{soma}	3.5	**9**	12	3.5	**8.5**	21	19.5	25.5	34	23.5	**36.5**	42.5	37.5	46.5	48.5	28.5	**47**	50

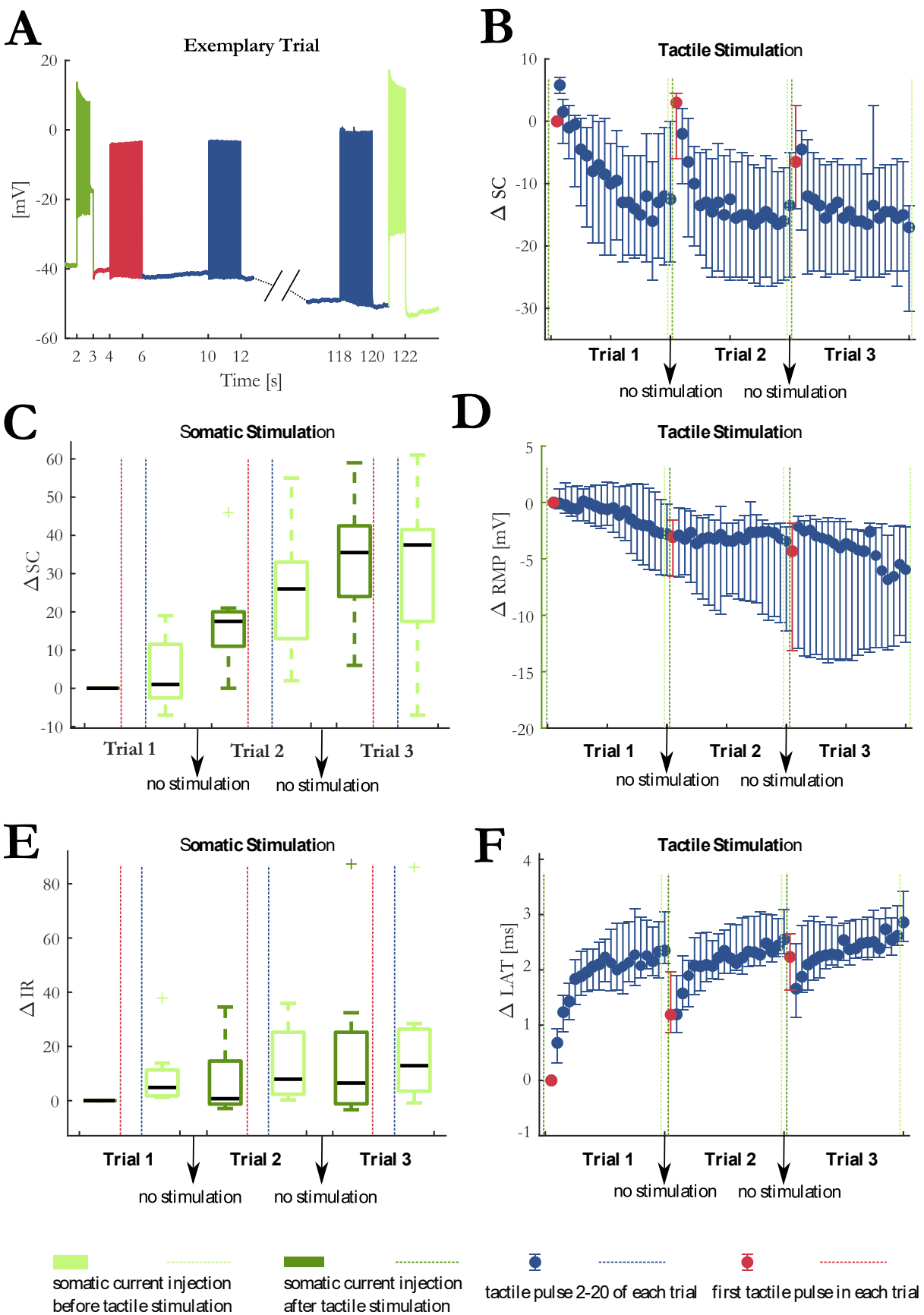
A
Exemplary Trial
[mV]
Time [s]
B
Tactile Stimulation
Δ SC
Trial 1
Trial 2
Trial 3
no stimulation
no stimulation
C
Somatic Stimulation
Δ SC
Trial 1
Trial 2
Trial 3
no stimulation
no stimulation
D
Tactile Stimulation
Δ RMP [mV]
Trial 1
Trial 2
Trial 3
no stimulation
no stimulation
E
Somatic Stimulation
Δ IR
Trial 1
Trial 2
Trial 3
no stimulation
no stimulation
F
Tactile Stimulation
Δ LAT [ms]
Trial 1
Trial 2
Trial 3
no stimulation
no stimulation
somatic current injection before tactile stimulation
somatic current injection after tactile stimulation
tactile pulse 2-20 of each trial
first tactile pulse in each trial

Figure 17 | Repeated tactile stimulation of the ventral midline effects physiological properties of T cells.

(A) Representative response of a somatic recorded T cell to two somatic current injections of 1 nA (dark and light green) and exemplarily three tactile pulse packages of 20 sine waves. Red color indicates the first package in the trial, Blue color indicated package two and 20. **(B, D, F)** Dependencies of changes in response parameters SC, RMP and LAT on tactile pulse repetition (20) for three trials shown as median and quartiles of all T cells (n=8). **(B)** Spike count (SC) difference from first pulse package (absolute number), **(D)** Resting membrane potential (RMP) difference from first pulse package repetition (mV), **(F)** First spike latency for each pulse (LAT) as difference for each pulse from first pulse package repetition (ms). **(C, E)** Boxplot of the changes in response parameters IR and SC on somatic current injections (n=8). **(C)** Spike count (SC) difference from first somatic current injection before any tactile stimulation per 500 ms. **(E)** Input resistance (IR) difference from first somatic current injection before any tactile stimulation (MOhm). Between each trial was a pause of 2 min without stimulation because of the storage time of the recording PC.

3.3 Timing and amount of T cell spikes effect network activity

Behavioral responses are based on muscle movements, which are controlled by a population of motor neurons. They receive synaptic inputs from a network of interneurons, which connect both the motor neurons and the sensor neurons. Soft touch at any position on the body surface causes the concerted firing of four sensor cells: two P cells and two T cells with overlapping receptive fields (Pirschel and Kretzberg, 2016; Kretzberg et al., 2016). Whereas some details were known about the interneurons (INs) involved in the local bend behavior and their connections to P cells (Lockery, SR and Kristan, 1990), only few experimental data existed about local bend INs and their connections to T cells so far. There are three bilateral pairs of T cells in one ganglion, which form both electrical and chemical synaptic connections with each other (Nicholls and Baylor, 1968; Baylor and Nicholls, 1969a; Burrell and Li, 2008). The aims of this part of the thesis were first to analyze the connections between two T cells, because they are electrically coupled via gap junctions. Secondly, it was investigated the effect of T cell spikes on specific interneurons and the network activity to support the hypothesis that they are involved in tactile processing.

3.3.1 Non-synaptic plasticity effects postsynaptic responses of other T cells

We first investigated the signal transmission between two ipsilateral T cells. Our goal was to see how the activity changes that were induced by non-synaptic plasticity in an electrically stimulated T cell (presynaptic) affected the responses in a non-stimulated T cell (postsynaptic). We analyzed how the PR, consisting of postsynaptic potentials and potentially elicited spikes, changed over repeated stimulation of the presynaptic cell (Figure 18).

As expected, the presynaptic SC increased with repeated current stimulation from a median of 6 spikes (Q1: 4.25/Q3: 20) in trial 1 to 20 spikes (Q1: 17.75/Q3: 21) in trial 15. Postsynaptically, we observed a tendency of increased PR size, but overall the slopes of the linear regressions of PR increases were not significantly different from 0 ($p > 0.05$, see Figure 18 B), because the PR increased only in 9 out of 11 cells over trials. However, the median of the averaged PR increased from 0.77 mV (Q1: 0.30/Q3: 1.23) in trial 1 to 0.96 mV (Q1: 0.44/Q3: 1.67) in trial 15. To clarify if the increase in PR observed in most of the T cell pairs was caused solely by the

increase of presynaptic SC that reflects the non-synaptic plasticity in the presynaptic (stimulated) T cell, or rather the synaptic plasticity also played a role, we elicited in the presynaptic cell a fixed number of single action potentials (Figure 8 C) and repeated the protocol over several trials. The PR size was found to depend highly significantly ($p < 0.001$) on the presynaptic SC Figure 18 D), because the linear regression yielded clearly positive slopes for all the cell pairs examined. The averaged PR increased from a median value of 0.34 mV in response to one spike (Q1: 0.31/Q3: 0.37) to 1.02 mV (Q1: 0.99/Q3: 1.10) in response to seven spikes. However, the PR size did not change significantly with stimulation repetitions in six out of seven conditions with fixed SC Figure 18 E, F), demonstrating that synaptic plasticity did not alter the PRs.

Summarizing, the increase in SC caused by non-synaptic plasticity in the repeatedly stimulated presynaptic cell in most T cell pairs was reflected by an increase in PR size in the postsynaptic cell. However, no indication for synaptic plasticity was found, because PR size stayed stable over trials, when the presynaptic SC did not change.

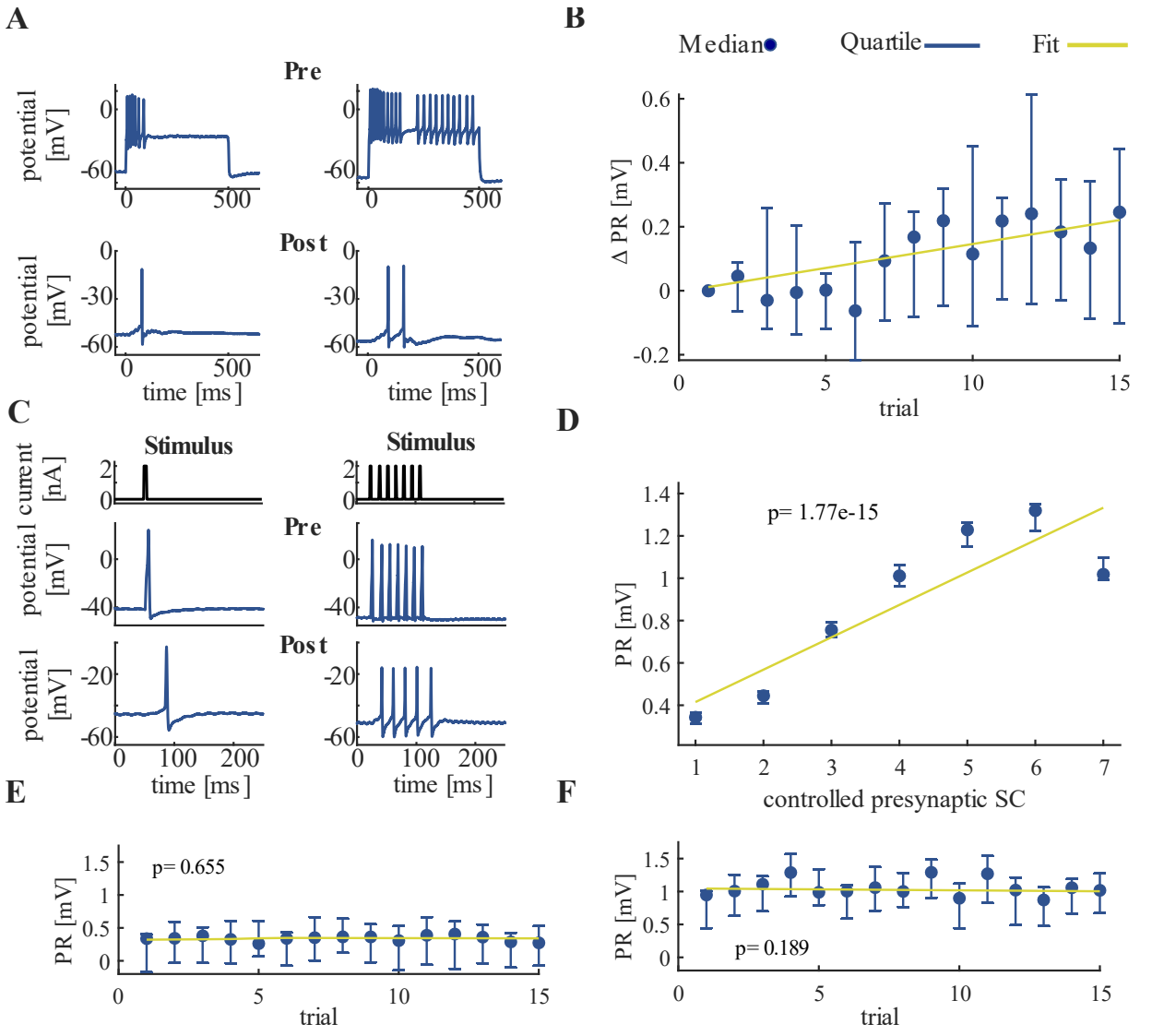

Figure 18 | Effect of repeated somatic current stimulation on the communication between two ipsilateral T cells. **(A)** Representative responses of an intracellularly recorded T cell pair to a 500 ms long somatic current injection of 1 nA in two different trial repetitions. **(B)** PR difference from first trial [mV] as median and quartiles of all T cells (N = 11) vs. trials. **(C)** Representative responses of an intracellularly recorded T cell pair to one and seven short current pulses. **(D)** Dependency of PR as median and quartiles of all T cells (N = 14) on controlled presynaptic SC. **(E,F)** Dependency of PR as median and quartiles of all T cells (N = 14) for one **(E)** and for seven **(F)** presynaptic spikes vs. trials. The slope of the PR vs. trial was not significant for six out of seven conditions (1 pulse, p = 0.655; 2 pulses, p = 0.032; 3 pulses, p = 0.092; 4 pulses, p = 0.051; 5 pulses, p = 0.772; 6 pulses, p = 0.512; 7 pulses, p = 0.190). Linear fits were calculated for each cell individually and the obtained slopes were tested to differ significantly from 0 (t-test, a = 0.05). Yellow line indicates the average of the fits for all cells. Figure from Meiser et al. 2019

3.3.2 Timing of T cell spikes effects response of postsynaptic interneurons

Repeated somatic stimulation effects intrinsic properties of stimulated T cells as well as the physiological response of postsynaptic T cells (see Figure 18). The three interneurons (INs) 157, 159, and 162 (see Figure 1 B for cell body positions in the ganglion) were previously identified as members of the local bend network according to the criteria that they responded to presynaptic P cell stimulation and influenced the activity of motor neuron 3 (Lockery, SR and Kristan, 1990).

To get a better idea about how T cell spikes could affect the network activity signal transmission between T and the local bend INs 212 and 157 were investigated by intracellular double recordings. A pulse package protocol was applied, that elicits a certain number of spikes with different ISI per trial (Figure 9). The postsynaptic response (PR), consisting of postsynaptic potentials and potentially elicited postsynaptic spikes, was analyzed by eye regarding changes depending on presynaptic SC and spike timing. Figure 19 C and D indicate that with increased ISI of the T cell the integral of the PR in IN 157 as well as in IN 212 increases. Furthermore, the interneurons seem to generate spikelets with increased presynaptic ISI, which indicated that every single spike is important in the formation of the postsynaptic response.

Summarizing, T cell on its own can elicit EPSPs and spikes, respectively spikelets, in postsynaptic interneurons. This supports the hypothesis of a strong involvement of T cells in tactile processing because they might activate a modulatory network with their very fast responses. However, more recordings with the same stimulation protocol are necessary to make significant statements about how the changes in PR depend on the presynaptic SC and spike timing.

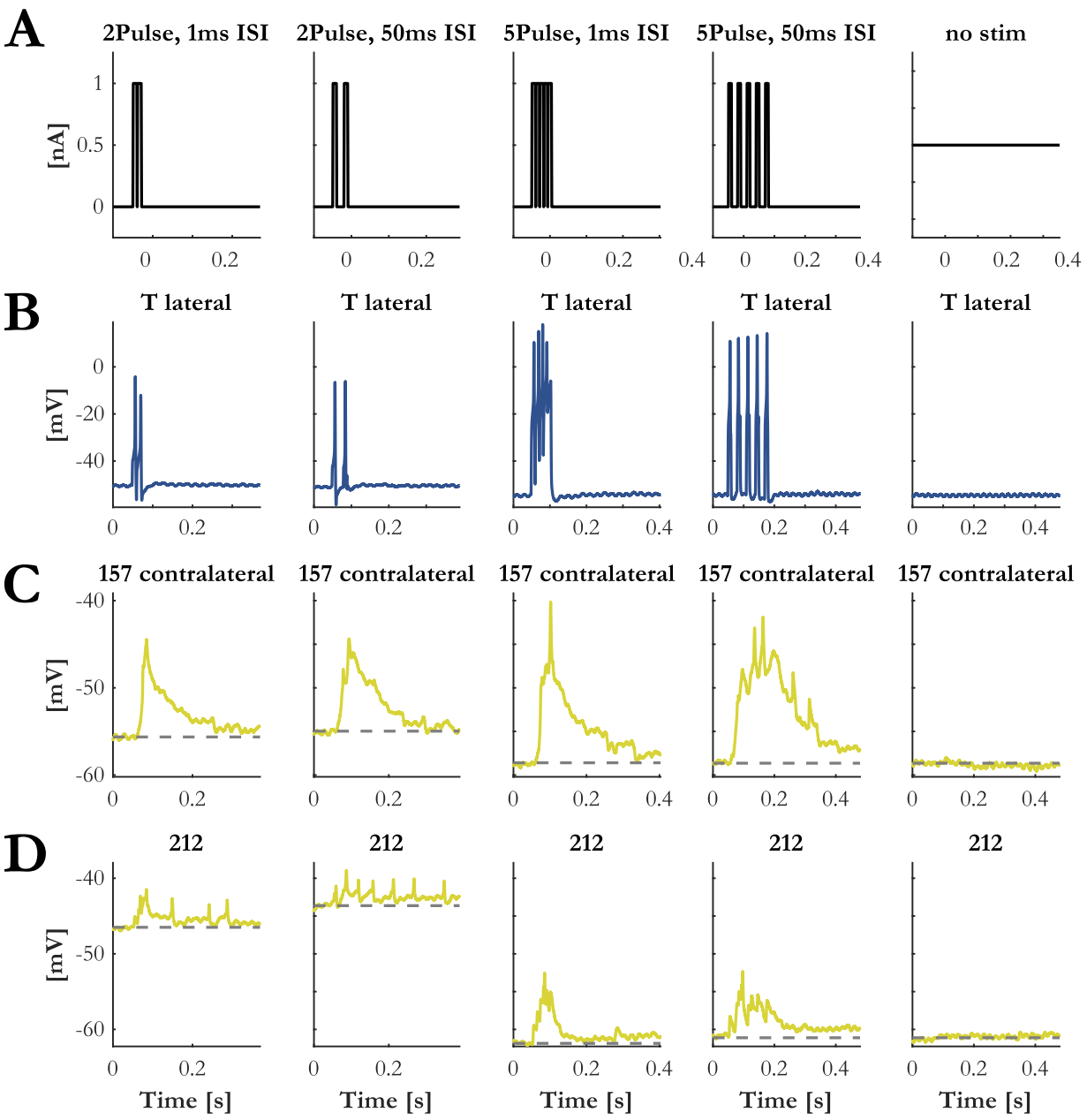

Figure 19 | Exemplary postsynaptic responses of the local bend INs 157 and 212 to different numbers of presynaptic T cell spikes with either 1 ms ISI or 50 ms ISI. (A) Detail of the electrical stimulus pattern that was applied to the presynaptic T cell (see Figure 9). **(B-D)** Neuronal response of the presynaptic T cell and the postsynaptic interneurons to the somatic current injection **(B)** T cell, **(C)** postsynaptic interneuron 157 **(D)** postsynaptic interneuron 212. The change in membrane potential in subpanel C and D is due to electric drift of the electrode. However spontaneous activity of 212 disappears with hyperpolarized RMP indicating a natural hyperpolarization and not an electric drift at least partially.

3.3.3 T cell spikes trigger network activity

The last step in the analyses how T cell spikes affect the underlying neuronal network, was to identify neurons involved in tactile processing using voltage sensitive dye (VSD) recordings. We performed replay experiments in which neuronal response patterns of T and P cells, evoked by tactile stimulation of 50 mN (Pirschel and Kretzberg, 2016), are reconstructed and applied as current injections (see chapter 2.3.3.2). Thereby, network responses to skin stimulation of a specific force, which activate both T and P cells, are comparable to the network responses to the T cell or P cell activity without the contribution of the other cell. However, in this recording we only compared P, T and PT activation. In the following experiments (Figure 20), intracellular double recordings of a T and a P cell were performed, while the activity of the ventral side of the ganglion was imaged. After VSD bath application, graded de- and hyperpolarization of all in the preparation visible neurons were estimated based on the emitted light of the corresponding pixels in the camera image (Miller et al., 2012). In the recording shown in Figure 20, 40 ROIs, representing individual cell bodies, were selected for analysis. Four different conditions of electrical stimulation were used during the recording (see chapter 2.4.2)

1. P-stimulated condition (Figure 20 C) with the same spike train elicited in the P cell as in the PT-stimulated condition, while the T cell remained unstimulated
2. T-stimulated condition (Figure 20 D) with the same spike train elicited in the T cell as in the PT-stimulated condition while the P cell remained unstimulated
3. PT-stimulated condition (Figure 20 E) with short current pulses injected into the cell bodies of the T cell and the P cell, which elicited spike trains reproducing typical mechanoreceptor responses to at touch stimulation of 50 mN (Pirschel and Kretzberg, 2016)
4. Control condition without stimulation (Figure 20 F), used to determine baseline spontaneous network activity.

In Figure 20 B cells were numbered according to the timing of their first activation (significant deviation from baseline in at least 8 of 10 stimulus presentation after stimulus onset in the PT – stimulated condition. Hence, cell numbers in Figure 20 differ from the cell identity numbers used in the standard ganglion map, e.g., in Figure 1 C. Comparison of different stimulation conditions revealed that electrical stimulation of T and P cells together (Figure 20 E) as well as activation of P cell alone (Figure 20 C) activated 10 of the 40 analyzed cells, while T cell stimulation (Figure 20 C) alone elicited significant activation only in 7 cells. However, populations of activated cells were not identical for PT-stimulated and P-stimulated conditions. Interestingly, cell 20 showed significant activity during P cell stimulation, but not in response to the combined PT-stimulated condition. This finding could indicate nonlinear interaction of inputs from different mechanoreceptors or inhibition by the T cell. According to the classification criterion, five cells responded with consistent significant activation to all three stimulated conditions (3, 4, 5, 6, 7). Some of them were easy to identify by soma positions and sizes and by their characteristic response patterns: Both Retzius cells (numbers 6 and 7 in Figure 20 B) and both AP cells (numbers 3 and 4 in Figure 20 B), which seems to be the fastest responding cells, unambiguously across different preparations. The cell labeled with number 5 could putatively be non-spiking IN 151 (compare ganglion map in Figure 1 C and Figure 20 A).

To conclude T cell on its own elicits network activity and seems to interact nonlinearly with the input from other mechanoreceptors types. Furthermore, T cells elicit interneuronal responses, before P cell spikes reach the ganglion, which was also previously shown (Kretzberg et al., 2016; Pirschel and Kretzberg, 2016; Pirschel et al., 2018; Fathiazar et al., 2018).

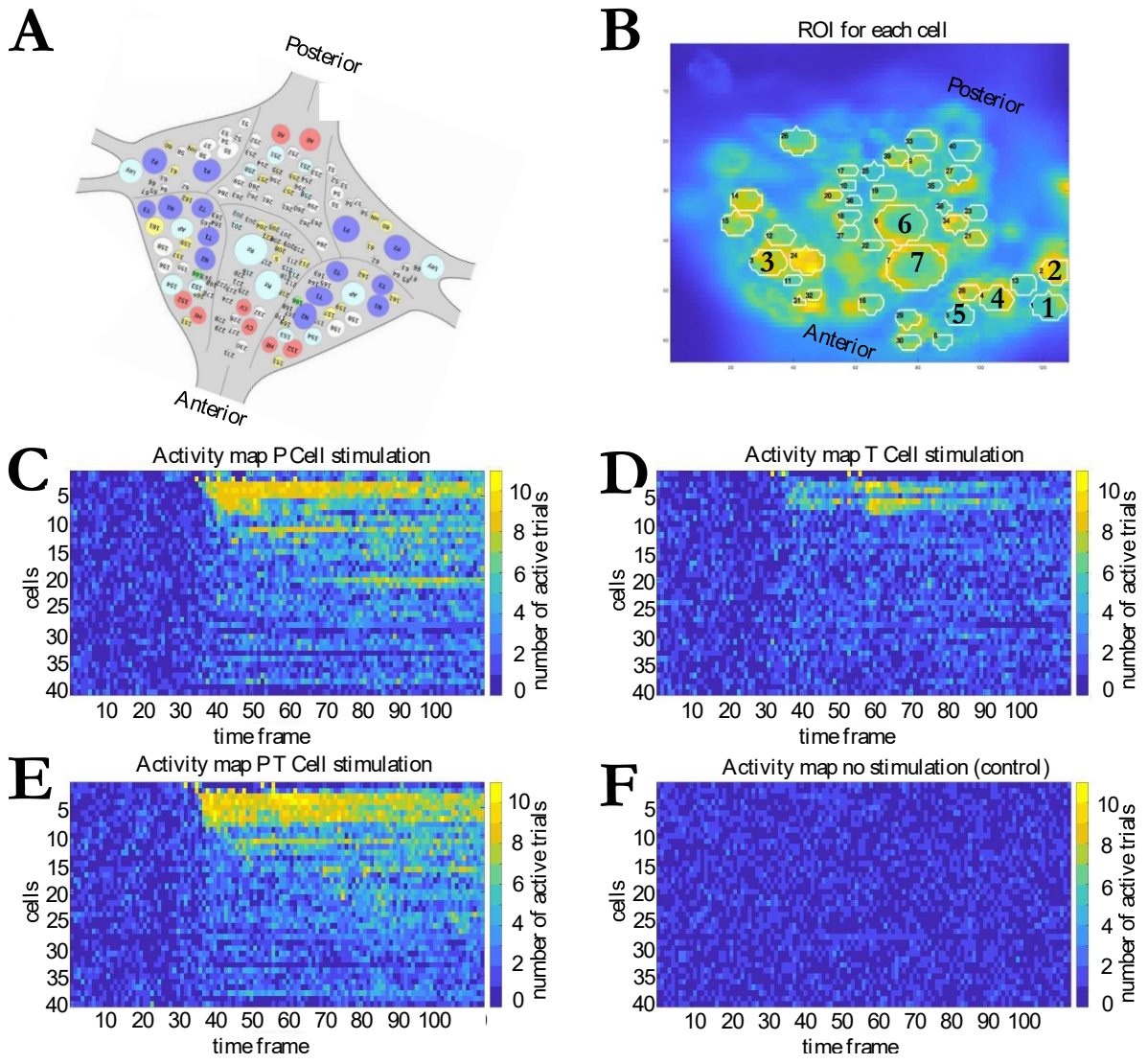

Figure 20 | Identification of Interneurons involved in the processing of tactile stimuli based on VSD recordings. (A) Ganglion map (B) Low resolution image of VSD labeled cells in the leech ganglion. For typical positions of the cell bodies located on the ventral surface of the ganglion, refer to subfigure A. (C-D) Activity maps of all 40 recorded cells in response to (C) P-Stimulation. (D) T-stimulation (E) PT- Stimulation and (F) control condition (no stimulation). The color of each pixel indicates in how many of the control trials the activity of a specific cell (row) at a specific recording frame (column) deviated significantly from baseline. The color varies between dark blue (0 trials) and yellow (10 trials). Cells were numbered according to the timing of their first activation (significant deviation from baseline in at least 8 / 10 stimulus presentation in the PT – stimulated condition). Data analysis and subfigure generation by B.Sc. Jimin Roh, a Master's student of the program Neuroscience at University of Oldenburg.

4 Discussion

The behavioral choice of a leech can be influenced by internal factors like the neuromodulator concentration or the feeding status and external factors like water depth or position of the stimulation (Esch and Kristan, 2002; Kristan et al., 2005; Gaudry and Kristan, 2009; Palmer et al., 2014). However, it is not clear if and how repeated skin stimulation influences behavioral choice. Previous studies were restricted to steady-state responses with stimuli separated by long recovery periods to prevent habituation or sensitization (Baca et al., 2005; Pirschel and Kretzberg, 2016). It was assumed that only P cell responses are relevant for eliciting a behavioral response to tactile stimulation (Lewis and Kristan, 1998; Thomson and Kristan, 2006; Baljon and Wagenaar, 2015). However, recent studies suggested that T cells also play a major role (Burgin and Szczupak, 2003; Kretzberg et al., 2007; Pirschel and Kretzberg, 2016; Meiser et al., 2019).

Clearly, behavioral choice is based on neuronal response flexibility (Gaudry and Kristan, 2009), but the neural basis for this combination is not well understood. However, neuronal response flexibility already starts with an individual spike (Mozzachiodi and Byrne, 2010). Therefore, this doctoral thesis investigated which biophysical properties cause response flexibility in T cells and their postsynaptic targets. Based on electrophysiological and modelling results (see chapter 3.1), the first part of this discussion shows how the Na^+/K^+-pump and a putative K_M current might be involved in activity-dependent non-synaptic plasticity in leech T cells. The second part of the discussion indicates that cell intrinsic flexibility, occurring at both SIZs in the T cell, seems to interact. This might cause a flexible shift in the relative impact of different computational tasks because one SIZ process synaptic input and the other tactile input. In the last part of the discussion the hypothesis is further supported that T cells might act as key players for behavioral responses. We could show that even a single T cell spike affects the response of the network. *Parts of the chapters 4.1, 4.3 and 4.5 are published in Meiser et al. (2019).*

4.1 Cellular basis of non-synaptic plasticity

The experimental and modelling results of chapter 3.1 indicate that T cells change their activity depending on previously generated spikes. As a consequence of continuous spiking, numerous types of neurons, as well as leech T cells (for an example see Figure 13 A, B; Figure 18 A), generate three types of an afterhyperpolarization (AHP). They can be described based on their temporal dynamics and the underlying current: fast AHPs lasting 2–5 ms, medium AHPs with durations ranging from 50–100 ms (mAHP), and slow AHPs lasting 0.1–2 s (sAHP) (Matthews et al., 2009). The fast AHP is carried by the calcium- and voltage-dependent BK channel (Storm, 1987). The medium AHP is carried by apamin-sensitive SK channels. However, the channel(s) that carry the slow AHP are still unknown for the most species (Disterhoft and Oh, 2006). In the leech the slow AHP is mainly based on Na^+/K^+-pump activity (Nicholls and Baylor, 1968; Baylor and Nicholls, 1969a; Jansen and Nicholls, 1973; Scuri et al., 2002; Scuri et al., 2007). This might provide a mechanism for intrinsic, activity dependent regulation of excitability, because intra and extracellular ion concentrations can change (Gulledge et al., 2013; Duménieu et al., 2015; Bear et al., 2018).

The theoretical results of this thesis indicate that enhanced repeated somatic stimulation of a leech T cell induce a non-synaptic plasticity mechanism based on changes in the opening probability of transmembrane proteins. Increased Na^+/K^+-pump activity leads to an increased efflux of Na^+. This in turn gradually hyperpolarizes the RMP, which might influence the activity of a specific voltage dependent ion channel, whose current affects spiking activity. The results presented in chapter 3.1 further indicate that the AHP, especially sAHP increase with SC due to repeated stimulation.

Tzingounis et al. (2007) showed that potassium channels of the KCNQ family, to which the voltage dependent K_M channel belongs to, contribute to the potassium currents during the sAHP in CA3 pyramidal cells. However, it is not clear if this is also the case for invertebrates, especially for leeches. The K_M-current is known to be involved in the regulation of excitability (Brown and Passmore, 2009; Passmore et al., 2012) and the production of burst-patterns in many neuronal systems by raising the threshold for firing an action potential (Benda and Herz, 2003). The changes in repetitive spiking behavior of the T cells could be explained by the dynamical ranges of the putative K_M current. M-channels activate at subthreshold potentials, but do not inactivate so generate a steady voltage-dependent outward current (Brown and Passmore, 2009). The probability of open K_M-channels is higher at rest than at a hyperpolarized membrane potential, causing spike responses to stop before the end of the stimulation (Brown, 1988). K_M-channels which are closed during hyperpolarization might lead to the higher IR and the more tonic firing response of the T cell. This could be observed experimentally in chapter 3.1.1 and is supported by our modelling results in chapter 3.1.2. Especially in early trials, many of the recorded T cells showed cessation of spikes well before the end of the current pulse period (Figure 13 A, B and Figure 14 A). While our model shows that the experimentally observed increase in IR could be one of the causes for the increase in SC, the cessation before the end of the stimulus only could be explained with the K_M channel (Figure 14).

However, leech sensory cells express several different ion channels (Johansen, 1991; Kleinhaus and Angstadt, 1995; Gerard et al., 2012), most of which we did not include in our model for the sake of simplicity. Sodium-dependent K^+ channels as they were found in leech pressure cells (Klees et al., 2005), for example, might also affect T cell spiking in an activity dependent manner. Additionally, we assumed that the kinetics of the slow K^+ channels were only voltage dependent. However, the activity of M-type K^+ channels was reported to be affected also by the intracellular concentration of ATP (Simmons and Schneider, 1998). Since ATP is consumed through Na^+/K^+-pump cycles (Morth et al., 2007), this additional mechanism could further modulate the spike rate adaptation. One important discrepancy between our model and the experimentally measured neuronal response was the difference in spike amplitudes. This difference might imply that the spike initiation site of the real T cell, responding to somatic stimulation, is not located exactly in the cell body. The recorded somatic spikes may only reflect the propagated action potentials that are generated elsewhere. Non-uniform distribution of ion channels in the T cell was found in previous studies: for example, T cells do have calcium-dependent channels (Kleinhaus and Angstadt, 1995) while their cell bodies largely lack voltage-dependent calcium channels (Valkanov and Boev, 1988; Johansen, 1991). To replicate the observed membrane potential changes, we had to adopt different factors (k_{chan} and k_{pump} in Table 2) that convert Na^+ channel currents and Na^+/K^+-pump currents into the intracellular Na^+ concentration; the difference between the two

conversion factors possibly implies that these current sources may exist in different locations. In addition, recorded spike heights did not decrease over trials (Figure 13 A). This is contrary to the naive expectation that the increased intracellular Na^+ concentration should lead to a decrease of the sodium reversal potential. Overall, these observations support the hypothesis that somatic spikes of the T cell may actually be generated not directly within the cell body, but somewhere nearby in the cell processes. Furthermore, leech neurons are packed in segmental ganglia, where the extracellular space is limited. Therefore, a model would need to consider both intracellular and extracellular ionic concentrations (Hübel and Dahlem, 2014) to better simulate the effect of limited resources. To theoretically investigate the possible roles of spatially distributed ion channels and pumps in neuronal information processing, multicompartment models would be required (Cataldo et al., 2005; Kretzberg et al., 2007). In the present thesis, however, we did not aim to create a multicompartment model for several reasons. First, the focus of our modelling was to investigate the activity-dependent long-term activity change of T cells induced by repetitive somatic current injection. Second there is almost no information available on the spatial distribution of ion channel over the T cell membrane that can be used for creating a multicompartment model. Third, we have no data recorded from the dendritic processes of T cells, which are essential for testing the simulated initiation and conduction of peripherally induced spikes. However, B.Sc. Kevin Sandbote is currently creating a two-compartment model of a leech T cell in his master's thesis to clarify this hypothesis. Preliminary results indicate that the spiking behavior (especially spike height) of T cells can be better reconstructed if the central SIZ is outsourced of the soma. Additionally, further experimental, and modelling studies, e.g., on the effects of varied intervals between stimulus applications, are needed to understand the biophysical mechanisms of non-synaptic plasticity in more detail.

To experimentally confirm the role of theoretically proposed involvement of Na^+/K^+-pumps and putative M-type K^+ channels in the change of IR and the spike rate adaptation of T cells, their pharmacological blockade was necessary. Such an experiment is not straightforward, because, in leech neurons, conventional blockers do not always suppress ionic currents as expected (Johansen and Kleinhaus, 1986).

The blocking of Na^+/K^+ pumps in leech by DHO was shown multiple times before (Catarsi et al., 1993; Scuri et al., 2007). However, it only was tested the effect on synaptic plasticity. We reported that application of DHO leads in the stimulated cell to a delayed decrease in SC (Figure 15). Usually we would expect an enhanced excitability of the T cell at a more depolarized RMP because inhibition of Na^+/K^+ pump increases the amount of intracellular Na^+ and reduce the distance to threshold for spiking (Morth et al., 2007; Bear et al., 2018). The delayed decrease in SC seems on the one hand to be due to the time the DHO needs to diffuse through the glial membrane and the cell membrane before it can interact at the Na^+/K^+ pumps. On the other hand, it might be due to the delayed depolarization-dependent opening of the putative K_M channels. When the probability of open channels increases then the spiking behavior of T cells changes from transient to sustained (Passmore et al., 2012). Probably, it is a combination of both. Because the effect of DHO is reversible (Cox and Woods, 1987), washout of the substance enables to study pump activity under control, experimental and after experimental conditions in the same tissue. The SC in the presented results decreases further during washout condition (Figure 15 D), which might be the case because the washout time was too short. Scuri et al. (2007), who also block Na^+/K^+ pump in leeches, could show that 20 min after DHO application the effect

was 50% reversible. Our washout condition only was 5 minutes long, because we were not able to record longer without losing the cell or clogging the recording electrode. Nevertheless, blocking of Na^+/K^+ pumps with DHO seems to open putative K_M channels, because the spiking behavior of the T cells changes decreases instead of the expected increase.

It was shown that XE-991 dihydrochloride blocks K_M channels in *drosophila melanogaster* and *Caenorhabditis elegans* (Wei et al., 2005; Cavaliere and Hodge, 2011), both well-known invertebrate model organisms. However, the existence of K_M- channels in leeches is not proved, we should clarify this assumption by blocking the putative channel with the blocker XE-991. If we would not see any effect, this does not mean that K_M is not present in leeches. Perhaps XE-991 does not interact with putative K_M channels in leeches. This could indicate that the genetic background of the channels is different in the systems. For example, Na^+ channels in vertebrates and invertebrates are definitely based on different genetics (Yu and Catterall, 2003). Therefore, we first simulate the assumed voltage dependency of K_M by an artificial setting of the membrane potential to different baselines. We could show that SC of the recorded T cells depends on the artificial membrane potential. At a hyperpolarized potential the SC is higher as at rest and at a depolarized potential the SC is lower than at rest. This supports the hypothesis of K_M channel involvement however a block is necessary and would give more obvious findings.

Furthermore, our results show that an application of -0.5 nA leads to a median hyperpolarization of the RMP by -28.07 mV, whereas injection of +0.5 nA depolarizes the RMP only by a median value of + 15.5 mV. This is due to the fact that at a hyperpolarized membrane potential more K_M channel are closed. This in turn increases RES and it is more difficult for the potassium ions to get into the cell. At a more depolarized membrane potential, RES is decreased due to open putative K_M channels, and the potassium ions can flow easier into the cell. This has the effect we can see in Figure 16: SC increase was higher than decrease.

Besides the discovered non-synaptic plasticity in leech T cells, the results of this thesis (especially chapter 3.1) show that the individual T cells varied considerably in their initial SCs and the duration of their spiking activity. Some cells start with few spikes in response to a 500 ms current pulse injection and do not really change their spiking activity see (Figure 15 and chapter 3.1.3). Other T cells increase their activity a lot after repeated somatic stimulation regardless if the initial spiking response was high or low. Surprisingly, it is not often clear from what the diversity in firing patterns of the same neurons in a network result (Sahasranamam et al., 2016). However, spike patterns are among the most common electrophysiological descriptors of neuron types (Marder and Taylor, 2011) and if they are different within one type than may be this type can be subdivided into two types. We assume, that either the recorded T cells are in different states before they were stimulated first or that the three different subtypes of T cells within one ganglion are more different than thought. Or may be a combination of both.

Each ganglion contains six T cells, which can be subdivided into three different types depending on the localization of their receptive field (Nicholls and Baylor, 1968; Baylor and Nicholls, 1969a; Brian D. Burrell, 2017). In most ganglia, cell bodies of the T_v cell (the cell with the ventral receptive field) were located most laterally (Kretzberg et al., 2016). We always try to record from the lateral T cell promising it is the T_v cell, but

the soma of the cells can switch positions (Kretzberg et al., 2016). Therefore, it can be the case that the more silent T cells are not ventral T cells but may be dorsal or lateral T cells. For the experiments with attached skin (see chapter 3.2 and Figure 17) we can clearly say, that we recorded from T_v cells, because the other T cell subtypes have their highest sensitivity in middle of the lateral and dorsal receptive field.

Furthermore, as previously suggested the low activity of some T cell may result from the case that the cell is in a different state before the stimulation starts. From a mathematical point of view a dynamical system contains functions which describe the time dependence of each point in a geometrical space (Ižikevič, 2010). An attractor is a set of numerical values describing a stable state toward which a system tends to evolve, for a wide variety of starting conditions of the system (Katok and Hasselblatt, 1996). May be a T cell seems to have at least to stable states: low activity and high activity. If a cell is in between these states than already a little influence (repeated stimulation) can transfer the cell into one of these stable states. If a cell is near an attractor or in a stable state than high influence is necessary to transfer it in a dynamical state. So, may be some of the silent T cells, which do not change their behavior with repeated stimulation, remain in a stable state or near an attractor and the repeated stimulation is too weak for transformation. This arises the following combined questions: Are there intrinsic and / or extrinsic factors which are responsible for holding a cell in a stable state and what is necessary that such cells change their response behavior respectively their dynamical state.

4.2 Non-synaptic plasticity might tune the relative impact of different computational tasks in T cells

In many vertebrate neurons, spikes are generated in the axon hillock, the part of the cell body that connects to the axon (Clarac and Cattaert, 1999). However, a lot of invertebrate neurons are unipolar, meaning that dendrites and the axon are not clearly separated, but form a continuum of processes (Rolls and Jegla, 2015). Leech T cells send several long-range touch-sensitive dendritic processes to their receptive fields in the skin several millimeters away (Nicholls and Baylor, 1968). Additionally, they arborize centrally to also reach the skin via both adjacent ganglia, leading to an even more extended receptive field (Yau, 1976). When the skin is touched lightly, T cells respond to the rate of skin indentation generating transient, rapidly adapting responses at stimulus onset and offset (Carlton and McVean, 1995; Kretzberg et al., 2016; Pirschel and Kretzberg, 2016; Pirschel et al., 2018). The action potentials are generated in the periphery and propagate through the ipsilateral nerve roots toward the soma. Moreover, spikes induced by central synaptic input can also travel in the opposite direction toward the periphery (Yau, 1976).

Burgin and Szczupak (2003) and Kretzberg et al. (2007) suggested that leech T neurons may have at least two spike initiation zones. Therewith, they could process different computational tasks of encoding touch stimuli in the periphery and processing synaptic inputs in the central ganglion. A similar anatomy was found in the LG motor neuron of the stomatogastric nervous system of the crab. It has a large soma with a nearby spike initiation zone and projects via dendritic processes to the periphery, where it also can initiate spikes up to 2 cm away from the soma (Meyrand et al., 1992).

We could show that somatic induced spikes increases the excitability of the central SIZ by a non-synaptic plasticity mechanism (see chapter 3.1 and 4.1). A further aspect of T cell response flexibility that was studied within this thesis was the interaction of both spike initiation zones. Synaptic inputs from the other mechanoreceptor types, P and N cells, were shown to influence spike responses to somatic current injection, but not the spikes generated in the skin during tactile input (Burgin and Szczupak, 2003). As shown by compartmental modeling studies (Cataldo et al., 2005; Kretzberg et al., 2007), these response features require at least two distinct spike initiation zones, one in the central ganglion and one in the peripheral branches of the T cell. When the leech skin is stimulated, T cell action potentials travel more than 1 cm from the skin to the T cell soma in only 10 ms (Pirschel and Kretzberg, 2016), which cannot be explained by passive, electrotonic spread. It was remained to be tested if the cell-intrinsic plasticity mechanism we discovered for spike initiation close to the soma also impacts spike generation in the skin and therefore sensory coding. Since the receptive field in the skin is more than a centimeter away from the recording electrode in the soma, only action potentials can cross this distance. Sub-threshold effects that could happen in the peripheral cell processes would not be visible in the soma. Therefore, it is possible to narrow down where cell-intrinsic plasticity could happen.

The presented results in chapter 3.2 and Figure 17 show that rapidly repeated skin stimulation leads to habituation of the T cell responses elicited in the skin. Furthermore, our results indicate that both SIZs are dependent from each other. Spikes elicited in the skin cause increased Na+/K+ ATPase activity in the central part of the T cell. This can be seen in an increased input resistance and more spikes, generated in response to the same repeated current pulse which was applied before the tactile stimulation (Figure 17 B, C).

If the spike initiation site in the skin would be the only place of cell-intrinsic plasticity, the only effect observed with somatic recordings should be changes in spike count and / or spike timing. However, our results indicate that central spike initiation is influenced. In addition to the changing spike count the input resistance increases and the membrane potential hyperpolarize (Figure 17 B, C,E). Though, the results regarding the membrane potential have to be handled with care due to electric drifts in our set ups.

These results mean that even spike responses that adapt to tactile stimulation are strong enough to induce an increase in excitability in the central part of the T cell. This in turn supports the hypothesis of tuning the relative impact of different computational tasks in T cell, because repeated stimulation leads to the adaptation rather than to the sensitization of T cell spikes triggered in the skin. If our hypothesis is correct, this multi-tasking ability and its activity-dependent tuning could make the T cell a key player in a fast-conducting preparatory network that regulates behaviors. In addition to the mutual T cell connections, the central part of the T cells receives polysynaptic inputs from the other mechanoreceptors, the P and N cells (Burgin and Szczupak, 2003). The postsynaptic potentials induced by these mechanoreceptor inputs can be excitatory, inhibitory, or a combination of both, indicating two interneuron pathways between the other mechanoreceptors and the T cells (Burgin and Szczupak, 2003). Hence, Na^+/K^+-pump activation in the context of non-synaptic plasticity probably shifts the membrane potential relative to the reversal potentials of these synapses, which could lead to an increase of the excitatory and a decrease of the inhibitory components of these postsynaptic potentials. In consequence, we propose that two complementary mechanisms following

repeated T cell stimulation increases the probability for centrally elicited spikes as a reactions to synaptic inputs from the other mechanoreceptors: The Na^+/K^+ pump dependent hyperpolarization might increase excitatory postsynaptic potential size and deactivate simultaneously a slow K^+-current, leading to an increase in SC due to IR increase and K+ conductance. The detected activity-dependent non-synaptic plasticity could serve the purpose of tuning the T cells – and maybe in consequence also postsynaptic cells in the preparatory network – in an activity-dependent way to the combination of two computational tasks.

Our results in chapter 3.2 and Figure 17 show a further interesting aspect. The changes in the measured properties proceed not linearly. To be more precise the somatic SC increases more in the time between two trials (no stimulation for 2 min) than in the time during the tactile stimulation (~2 min)). Contrary to the findings of repeated somatic current injection, the analysis revealed that spikes induced in the periphery led to a form of short-term depression within one trial of repeated tactile stimulation. However, the depression of the activity in the peripheral SIZ seems to recover during the time without stimulation.

This further indicates that the increase in SC in the soma is triggered by non-synaptic plasticity, because the kinetics of the Na^+/K^+ pump and the putative K_M channel are much slower than the ones of spike generation (W. Yamada et al., 1989; Benda and Herz, 2003). Furthermore, the recovery of the peripheral SIZ indicates a form of short-term-(non-synaptic) depression, because changes occur on timescales from milliseconds to minutes (Bear et al., 2018) . Since T cells are coupled with each other and receive input from the other mechanoreceptor types the depression maybe results from the changes in the synapses. However, this needs to be further investigated.

Finally, the higher sensitivity for processing synaptic inputs due to the change of intrinsic response properties could result in switching to an entirely different behavior, like crawling or swimming, that might help to avoid the aversive stimulus more effectively.

4.3 T cell as a key player for eliciting network activity

Leeches respond to tactile stimulation with multiple distinct reactions, which inspired the discussion of behavioral choice (Esch and Kristan, 2002; Kristan et al., 2005; Palmer et al., 2014; Baljon and Wagenaar, 2015). Behavioral responses are controlled by muscle movements, which are controlled by a population of motor neurons. The key to understand the control of behavioral responses is the analysis of the network activity from sensory input neurons over interneurons to motor output neurons. The cell bodies and dendrites of all these neurons are located in the central ganglion. Due to the small number of neurons, multifunctional cells play a role in shaping these patterns (Kristan et al., 2005; Briggman and Kristan, 2006; Frady et al., 2016). We assume that T cells are such multifunctional players in a network that controls the response to a light touch on the leech's skin. The activated segment produces shortening on the stimulated and lengthening on the opposite side of the body wall (Kristan, 1982; Kristan et al., 1982).

This local bend response is one of the fastest behaviors of the leech, with muscle movements starting only 200 ms after stimulus onset (Kristan et al., 2005). T cell respond very fast to tactile stimulation and give input to several local bend interneurons before P cell neuron spikes arrive at the central ganglion (Kretzberg et al.,

2016). Moreover, some of the postsynaptic interneurons integrate all mechanoreceptor inputs with a long time constant, while others responded more specifically to precisely timed inputs and the graded membrane potential in postsynaptic interneurons allow the estimation of tactile stimulus intensity and location (Pirschel et al., 2018). This hypothesis is supported by our results in chapter 3.3. We could show that each presynaptic T cell spike effects the amplitude of the postsynaptic response (PR) in local bend INs. Depending on the timing and amount of the presynaptic T cell spike the amplitude PR of the INs increases or decreases.

However, one T cell alone is not capable of eliciting a behavior on their own (Kristan, 1982; Fathiazar et al., 2018). We assume that they activate with their very fast responses a modulatory network that regulates the gain of behaviors (see chapter 1.3 chapter and chapter 3.3). Frady et al. (2016) have identified such a "preparatory network" of neurons that starts to react with a very short latency prior to the production of multiple behaviors, including local bending and whole-body shortening. After repeated stimulation causing non-synaptic plasticity, the enhanced activity might enable the T cell to transfer the animal into a state that prepares the muscles for a rapid start of a behavioral response by shifting the threshold for firing action potentials. T cell form synaptic connections with each other that have both an electrical and a chemical component (Nicholls and Baylor, 1968; Burrell and Li, 2008). Electrical synapses have shorter latencies compared to chemical synapses (Nicholls and Purves, 1970), and such fast-acting synaptic inputs could facilitate rapid transmission of sensory information to the preparatory network.

Our results in 3.3.1, revealed that the increase in SC by non-synaptic plasticity also increases the PR in other T cell, which may include postsynaptic spiking. These postsynaptic changes appear to be a mere reflection of the activity-dependent changes in the presynaptic T cell. This finding shows that each presynaptic T cell spike effect PR and might be an alternative interpretation to the conclusion of previous studies that the Na^+/K^+-pump is involved in activity dependent synaptic plasticity between two ipsilateral T neurons (Catarsi et al., 1993; Lombardo et al., 2004; Rossana Scuri et al., 2007; Scuri et al., 2007, 2007), which support the hypothesis that T cells play a major role in eliciting behavioral reactions. Additionally, T cell have a strong synaptic connection to the S cell, a prominent element of the preparatory network (Burrell and Sahley, 2004). Each ganglion contains a single unpaired S cell, which forms strong electrical connections to the S cells in adjacent ganglia (Sahley et al., 1994). This network is reminiscent of a fast-conducting system (Mistick, 1978), but its causal role in any behavior is unclear (Sahley et al., 1994).

To determine more neurons and their interactions involved in this preparatory network, VSD imaging with a double-sided-microscope is an appropriate method (Tomina and Wagenaar, 2017). It allows us to directly analyze functional relationships between neurons located on opposite surfaces and detect both action potentials and sub-threshold excitatory and inhibitory synaptic potentials (Miller et al., 2012). The results in indicate that T cells are able to elicit network activity on its own, although electrical stimulation of a single T cell triggers a response that would not occur in natural situations, because each patch of skin is innervated by a pair of T cells and a pair of P cells with overlapping receptive fields (Kretzberg et al., 2016). Interestingly we could show in the presented recording, that besides both AP and both RZ neurons the putative non-spiking interneuron 151 seems to react to single and combined mechanoreceptor stimulation. Before, it was only known that IN 151 process sensory information from P cells (Marín-Burgin and Szczupak, 2000). If this cell

is really IN 151, this would further support the hypothesis that T cells play a major role in sensory processing. Though, we need more experiments to verify this hypothesis and make meaningful statements about interneurons activated by single T cell stimulation. Additionally, the presented VSD experiment was done with a CCD camera with a time resolution of 98 frames per seconds. This is very slow to record spikes. Now, our lab has a faster sCMOS camera with a maximum frame rate of 192 frames per second. The fast dye and the temporal resolution of this camera would allow us to identify individual spikes. We expect that at least the start of the preparatory network activity is induced by T cell spikes and therefore should not differ between PT, P and T stimulated conditions. This would be a clear indication that T cells have the functional role of triggering the preparatory network (see chapter 4.6).

4.4 Reflection

Results always need to be interpreted within the context of other studies, but also in the light of methodological issues. Hence, this thesis shows several limitations, which can be separated into two major aspects: experimental and data analysis approaches.

4.4.1 Experimental limitations

One big experimental limitation was, that from January 2020 on, stable intracellular recordings were not possible. All of our recordings were superimposed by an electric drift in all of our three experimental set ups (see chapter 2.4.1). Therefore, the results in the chapters 3.1.3, 3.1.4 as well as 3.2, could not be interpreted regarding the RMP. By now we assume, that the pH value of the potassium acetate solution was not in the right scope. However, we still have problems, the recordings are clearly more stable since September 2020 on.

Furthermore, due to the corona pandemic I could not perform experiments for three months (03/2020 – 05/2020). Therefore, the direct involvement of K_M channels in the presented non-synaptic plasticity effects was not tested by using a pharmacological blocker. The most common blockers of K_M are XE-991 and Linopirdine. However, they were mainly used in vertebrates. Only a few studies are published about these blockers in invertebrates, like the fruit fly *drosophila melanogaster* or the nematode *Caenorhabditis elegans* (Wei et al., 2005; Cavaliere and Hodge, 2011). Though, our results indicate that K_M channels could be involved, because an artificially changed membrane potential influences SC and the opening probabilities of K_M depends on the current membrane potential. Nevertheless, there might be other voltage-dependent-channels which could generate similar effects. Hence, blocking of putative K_M would be the next step.

Regarding the pharmacological blocking of the Na^+/K^+ pump (see chapter 3.1.3), the experimental design needs to be optimized. We could not see any increase in SC during washout condition, as we would it expect if fewer pumps are blocked with DHO. Normally more active Na^+/K^+ pumps should hyperpolarize the RMP with repeated stimulation, which in turn closes putative K_M channels and change the spiking behavior from transient to sustained. However, we only could see a further shallowed decrease in SC during washout. Previous studies from Scuri et al. (2007) as well as our own results indicate that the time of the washin and washout condition needs to be longer. DHO is reversible (Cox and Woods, 1987) and it might take more time for the

substance to diffuse through glial membrane and cell membrane. Furthermore, the experimental set up for the pharmacology recordings (especially the switching of the tubes for the different solutions) needs to be improved because we usually lost the cell mostly between the conditions.

The use of voltage clamp recordings in a whole cell patch configuration for the T cell in combination of pharmacological blocking would be promising to verify the channel-kinetics for further modelling approaches. However, for patch clamps recordings, the glial sheath had to be removed. The glial sheath regulates the potassium concentration in the space between nerve cells and it could not be ruled out that its function influences the neuronal network activity (Baylor and Nicholls, 1969b; Costa and Neto, 2015). Furthermore, synaptic connections could be easily damaged by desheating the ganglion.

4.4.2 Data Analysis limitation

Besides experimental issues, compromises regarding the analysis of the neuronal responses had to be made. During the calculation of integrals for chapter 3.3.1 some compromises had to be made to keep the computations realizable. Due to a relatively high mains hum we decided to use a Notch-Filter for removing the sine wave of ~50 Hz from the data. The filtering was successful in eliminating the mains hum out of the signal (Figure 11). Nonetheless, the shape of the single spikes was not perfectly preserved. This was of distinct disadvantage for the further analysis. We need to pool the integrals of the sub-threshold T cell responses and spike responses. Fitted spike responses always lost their natural shape and therefore the calculated integral presumably deviates from the real integral. Additionally, the interval for integral calculation, was defined as time from the beginning of the stimulation of the presynaptic cell to a certain time after the end of the stimulation of the presynaptic cell. The time after end of the stimulation was held constant. However, the interval may not be optimal for every integral that were calculated, because the bigger the time window, the more likely it is to cover the whole postsynaptic effect, but also to deal with confounding noise and vice versa.

From a statistical point of view one can argue that a linear approximation might not be suitable to fit our data best. A steeper slope for lower x values in the "pseudorandomized data set" (see Figure 13 in chapter 3.1.1) as well as the double recordings between two T cells (see Figure 18 and chapter 3.3.1) than the slope for all x values indicates that a logarithmic function could provide a better fit. This could also be better explained by biological issues, because a neuron could not increase linearly its SC due to the refractory period of the Na^+ channels (Bear et al., 2018). Additionally, as mentioned before the N in the datasets for 3.1.3, 3.2 and 3.3.2 needs to be increased to make statistical valid statements regarding changes in the response properties. The current results only allow assumptions which could either be verified or retracted in prospective experiments.

Nevertheless, this thesis gave important insights into the biophysical basis of the response of a specific sensory neuron to repeated stimulation. It is assumed that general strategies for producing behaviors are expected to be found in all organisms with a central nervous system (Kristan et al., 2005). Therefore, the findings might constitute as an important basis for further studies regarding the behavioral aspect of non-synaptic plasticity in all animal species. This future study could be experimentally based on the following two questions, which will be further described in chapter 4.6: How can the same neuron serve multiple functions in a network? How can cell-intrinsic mechanisms impact behavior?

4.5 Conclusion

We could show that a specific cellular mechanism in one mechanoreceptor type (T cell) of the leech might be the basis for behavioral response flexibility triggered by repeated tactile stimulation. Two complementary mechanisms seem to increase the probability for centrally elicited spikes as reaction to synaptic inputs from the other mechanoreceptors. An activity dependent increase in Na^+/K^+ pump activity leads to a hyperpolarization of the RMP, which deactivate at the same time a slow K^+-current, leading to an increase in SC. This in turn increases excitatory postsynaptic potential size of coupled T cells and could affect the activity of the neuronal network (Meiser et al., 2019). Repeated tactile stimulation leads to an activity adaptation and therefore the relative impact of both spike initiation zones could shift to a higher sensitivity for processing synaptic inputs, but diminished responses to tactile stimulation. This effect of the presented non-synaptic plasticity mechanism could act on postsynaptic cells in the underlying network as well. Then a switching to an entirely different behavior, like crawling or swimming, that might help to avoid the aversive stimulus more effectively is possible. Depending on the previous activity, T cells could react more or less to the inputs from the other mechanoreceptors. They could combine these synaptic responses with the spikes that encode light skin stimulation, which are elicited by T cell processes in the periphery (Meiser et al., 2019).

On the network level this activity dependent tuning could make the T cell a key player in a fast-conducting preparatory network that regulates the triggering of behaviors. When the skin is touched repeatedly, the fast T cell spikes might first activate the preparatory network by giving input to interneurons. The first stimulus presentations could elicit local bending and later repetitions then a better stimulus avoidance behavior like crawling or swimming. Such an interaction of multiple computational tasks, which are processed by different spike-initiation sites, could be relevant for all types of vertebrate and invertebrate neurons featuring dendritic spiking as a basis for complex computations (Payeur et al., 2019).

4.6 Outlook

The results of this doctoral thesis describe fundamental computational principles of sensory information processing but raise two further questions.

- How can the same neuron serve multiple functions in a network?
- How can cell-intrinsic mechanisms impact behavior?

Such challenging questions can be studied rigorously in further experiments with the well accessible leech nervous system. Combining several necessary experimental approaches on the levels of individual cells, network activity, and behavioral responses might show, if repeated tactile stimulation leads to changes in the T cell response patterns, which in turn can change the underlying network and induce a shift in the behavioral level. Due to many similarities between the tactile systems of the leech and human (Burrell and Li, 2008; Pirschel and Kretzberg, 2016), they could inspire biomedical research, e.g., for optimizing tactile interfaces for hand prostheses (Downey et al., 2020).

4.6.1 Cellular basis of non-synaptic plasticity

First of all, it needs to be investigated if the discovered non-synaptic plasticity effect is really based on the Na^+/K^+ pump and the putative K_M channel. However, our results, especially chapter 3.1.3 indicate their involvement. The blocking of both transmembrane proteins should be done soon and systematically to make significant statements about the biophysical basis.

Our preliminary results of only eight experiments (see chapter 3.2 and Fig 17) suggest that repeated skin stimulation leads to habituation of the T cell responses elicited in the skin and measured in the soma. Additionally, the RMP hyperpolarizes, the IR increases, and more spikes are generated in response to the same current pulse which was applied before the tactile stimulation. This indicates on the one hand that the spikes, which are elicited in the skin and propagated to the central part of the T cell, trigger Na^+/K^+ ATPase activity everywhere in the cell membrane. On the other hand, this shows that both SIZs act dependent from each other. Otherwise we would expect all somatic current injections to lead to the same responses, no matter if they are applied before or after skin stimulation. This supports the idea of a shift in the relative impact of both spike initiation zones, which could lead to a higher sensitivity for processing synaptic inputs, but diminished responses to tactile stimulation. Finally, a higher number of successful recordings with the same stimulation protocol and an intact experimental setup, without electric drift, would lead to results that could be analyzed statistically.

Additionally, the opposite direction of interaction needs to be tested by first stimulating the skin, next somatically injecting a current that triggers cell-intrinsic plasticity in the central part of the neuron, and then again repeating the skin stimulation. Comparison of the responses to both touch stimuli will show if the increase in excitability in the soma also applies to the spike initiation zone in the skin. If more spikes are generated during the second skin stimulation, the conclusion would be that centrally generated spikes propagate back to the body wall and trigger increased Na^+/K^+ ATPase activity and closing of putative K_M channels also in the peripheral part of the cell. However, when the skin is touched at the ventral midline, both ventral T cells will react equally strongly (Kretzberg et al., 2016; Pirschel and Kretzberg, 2016) because of their overlapping receptive fields. Therefore, the same activity-dependent changes are expected in both T cells. However, if only one of the T cells is stimulated as described the responses of T cells to the subsequent tactile stimulation could deviate from each other. If the responses to the first and second tactile stimulation differ only for the cell that was stimulated somatically, this would exclude the possibility of a pure time effect and strengthen the hypothesis of spike propagation from the soma towards the skin.

Last, the importance of theoretical investigations should not be disregarded. A multicompartment model, which is currently created by Kevin Sandbote, would help us to understand how spatially distributed ion channels and pumps act in neuronal information processing.

4.6.2 T cells as key players for eliciting network activity

Avoidance behavior to tactile stimulation is in the leech triggered by mechanoreceptor responses (Kretzberg et al., 2016). Soft touch, below the threshold for nociceptors, at any position on the body surface causes the

concerted firing of four cells: two P cells and two T cells with overlapping receptive fields (Pirschel and Kretzberg, 2016; Kretzberg et al., 2016). T and P cells encode touch location and pressure intensity of tactile skin stimulation in a multiplexed way, combining spike count and temporal response features, as it was also suggested for primate mechanosensory afferents (Saal and Bensmaia, 2014). However, the behavioral effects of precisely timed spikes from a pair of T cells on the local bend response remain an open question (Brian D. Burrell, 2017). The key of understanding the control of behavioral responses is the analysis of the network activity following a sensory stimulation. Therewith, we could investigate the missing link if and how preparatory network activity is initiated by tactile skin stimulation. As pointed out by a recent review (Brian D. Burrell, 2017) several findings suggest that T cells trigger the activity of the preparatory network. We expect that at least the start of the preparatory network activity is induced by T cell spikes and therefore should not differ between PT, P and T stimulated conditions. For this question, it is essential that the 'standard' local bend network response and its variability (for example when touch location is varied) is characterized before as in (Fathiazar et al., 2018). The temporal resolution of 200 frames / ms provided by the new sCMOS camera would be sufficient for this task, because network activity develops over more than 100 ms (Kretzberg et al., 2016; Fathiazar et al., 2018). Then, it is possible to compare the standard activation sequence with the recordings of T, P and PT stimulation. It is expected that the initial phase of network activity (preparatory network) is independent while the later phase (control of local bending) may differ. If this hypothesis is confirmed, it would provide the answer to the question of which of the cells are members of only the preparatory network, or only the local bend network, and which are multifunctional. The plan for further studies would be to perform experiments, in which tactile stimulation is alternated with an intracellular electrical stimulation that triggers the same T cell spike trains as were recorded in response to the previous touch. This is called a replay experiment. The first approach to quantify the behavior is video analysis in semi-intact body wall preparations because the pattern of the muscle movement in the local bend is already known. Comparing the muscle movements elicited in both conditions performs the ultimately test if the concerted activity of a T cell pair can elicit local bending. By systematically varying the relative spike counts and timing of both T cells, the impact of these spike features on the local bend movement profile can be analyzed. Video analysis of the moving body wall preparation would be the perfect way to clarify if the concerted activity of a T cell pair can elicit a local bend response. However, the body wall video analysis cannot be combined with VSD recordings in the same preparation. Therefore, the second approach is extracellular nerve recordings from the roots, the four nerves that connect the ganglion with the body wall (see Figure 1 B, C). The goal is to infer behavior from the temporal discharge pattern of different motoneurons, which can be measured in the roots (Kristan et al., 2005; Alonso et al., 2020). These experiments could confirm the possibility of correlating the spike activity in the nerve with the local bend movements and of predicting the movement from the spikes, the extracellular root recordings could be used as a proxy for behavioral muscle movements.

A future step would be the creation of a small artificial neuronal network model of the T cell and some important interneurons of the preparatory network. The neuronal networks could be trained on experimentally derived input / output patterns and finally could be used to predict and analyze the response of the real biological neural circuit (Lockery et al., 1990).

5 References

Abraira VE, Ginty DD (2013) The sensory neurons of touch. Neuron 79:618–639.

Akemann W, Lundby A, Mutoh H, Knöpfel T (2009) Effect of voltage sensitive fluorescent proteins on neuronal excitability. Biophys J 96:3959–3976.

Alonso I, Sanchez Merlinsky A, Szczupak L (2020) Phase-Specific Motor Efference during a Rhythmic Motor Pattern. J. Neurosci. 40:1888–1896.

Baca SM, Thomson EE, Kristan WB (2005) Location and intensity discrimination in the leech local bend response quantified using optic flow and principal components analysis. J Neurophysiol 93:3560–3572.

Baljon PL, Wagenaar DA (2015) Responses to conflicting stimuli in a simple stimulus-response pathway. J. Neurosci. 35:2398–2406.

Baltzley MJ, Gaudry Q, Kristan WB (2010) Species-specific behavioral patterns correlate with differences in synaptic connections between homologous mechanosensory neurons. J Comp Physiol A 196:181–197.

Barreto E, Cressman JR (2011) Ion concentration dynamics as a mechanism for neuronal bursting. J Biol Phys 37:361–373.

Baylor DA, Nicholls JG (1969a) After-effects of nerve impulses on signalling in the central nervous system of the leech. The Journal of Physiology 203:571–589.

Baylor DA, Nicholls JG (1969b) Chemical and electrical synaptic connexions between cutaneous mechanoreceptor neurones in the central nervous system of the leech. The Journal of Physiology 203:591–609.

Bear MF, Connors BW, Paradiso MA (2018) Neurowissenschaften. Ein grundlegendes Lehrbuch für Biologie, Medizin und Psychologie. Berlin, Heidelberg: Springer Berlin Heidelberg.

Bear MF, Linden (2001) The mechanisms and meaning of long-term synaptic depression in the mammalian brain.

Benda J, Herz AV (2003) A universal model for spike-frequency adaptation. Neural Computation 15.

Benjamin PR, Kemenes G, Kemenes I (2008) Non-synaptic neuronal mechanisms of learning and memory in gastropod molluscs. Front Biosci 13:4051–4057.

Blackshaw SE (1981) Morphology and distribution of touch cell terminals in the skin of the leech. The Journal of Physiology 320:219–228.

Blackshaw SE, Nicholls JG, Parnas I (1982) Physiological responses, receptive fields and terminal arborizations of nociceptive cells in the leech. The Journal of Physiology 326:251–260.

Bordas C, Kovacs A, Pal B (2015) The M-current contributes to high threshold membrane potential oscillations in a cell type-specific way in the pedunculopontine nucleus of mice. Front Cell Neurosci 9:121.

Brian D. Burrell (2017) Leech Mechanosensation. In: Oxford Research Encyclopedia of Neuroscience.

Briggman KL, Kristan WB (2006) Imaging dedicated and multifunctional neural circuits generating distinct behaviors. J. Neurosci. 26:10925–10933.

Brown DA, Adams PR (1980) Muscarinic suppression of a novel voltage-sensitive K+ current in a vertebrate neurone. Nature 283:673–676.

Brown DA, Passmore GM (2009) Neural KCNQ (Kv7) channels. Br J Pharmacol 156:1185–1195.

Burgin AM, Szczupak L (2003) Network interactions among sensory neurons in the leech. J Comp Physiol A Neuroethol Sens Neural Behav Physiol 189:59–67.

Burrell BD, Li Q (2008) Co-induction of long-term potentiation and long-term depression at a central synapse in the leech. Neurobiol Learn Mem 90:275–279.

Burrell BD, Sahley CL (2004) Multiple forms of long-term potentiation and long-term depression converge on a single interneuron in the leech CNS. J. Neurosci. 24:4011–4019.

Cacciatore TW, Brodfuehrer PD, Gonzalez JE, Jiang T, Adams SR, Tsien RY, Kristan WB, Kleinfeld D (1999) Identification of Neural Circuits by Imaging Coherent Electrical Activity with FRET-Based Dyes. Neuron 23:449–459.

Calabrese RL (1980) Control of multiple impulse-initiation sites in a leech interneuron. J Neurophysiol 44:878–896.

Carlton T, McVean A (1995) The role of touch, pressure and nociceptive mechanoreceptors of the leech in unrestrained behaviour. J Comp Physiol A 177:781–791.

Cataldo E, Brunelli M, Byrne JH, Av-Ron E, Cai Y, Baxter DA (2005) Computational model of touch sensory cells (T Cells) of the leech: role of the afterhyperpolarization (AHP) in activity-dependent conduction failure. Journal of Computational Neuroscience 18:5–24.

Catarsi S, Brunelli M (1991) Serotonin depresses the after-hyperpolarization through the inhibition of the Na+/K+ electrogenic pump in T sensory neurones of the leech. Journal of Experimental Biology 155:261–273.

Catarsi S, Scuri R, Brunelli M (1993) Cyclic AMP mediates inhibition of the Na(+)-K+ electrogenic pump by serotonin in tactile sensory neurones of the leech. The Journal of Physiology 462:229–242.

Cavaliere S, Hodge JJL (2011) Drosophila KCNQ channel displays evolutionarily conserved electrophysiology and pharmacology with mammalian KCNQ channels. PLoS ONE 6:e23898.

Clarac F, Cattaert D (1999) Functional multimodality of axonal tree in invertebrate neurons. Journal of Physiology-Paris 93:319–327.

Costa FAL, Neto FLM (2015) Satellite glial cells in sensory ganglia: its role in pain. Brazilian Journal of Anesthesiology (English Edition) 65:73–81.

Cox TC, Woods RE (1987) Dihydroouabain, a reversible inhibitor of the sodium pump in frog skin. Pflugers Arch 409:323–327.

Deitmer JW, Schlue WR (1983) Intracellular Na+ and Ca2+ in leech Retzius neurones during inhibition of the Na+-K+ pump. Pflugers Arch 397:195–201.

Disterhoft JF, Oh MM (2006) Learning, aging and intrinsic neuronal plasticity. Trends in Neurosciences 29:587–599.

Downey JE, Jack Brooks, Sliman J. Bensmaia (2020) Artificial sensory feedback for bionic hands. In: Intelligent biomechatronics in neurorehabilitation (Hu X, ed), pp 131–145. London: Academic Press, an imprint of Elsevier.

Duménieu M, Fourcaud-Trocmé N, Garcia S, Kuczewski N (2015) Afterhyperpolarization (AHP) regulates the frequency and timing of action potentials in the mitral cells of the olfactory bulb: role of olfactory experience. Physiol Rep 3.

E. Fathiazar, J. Kretzberg (2015) Estimation of neuronal activity based on voltage-sensitive dye imaging in a moving preparation. In: 2015 37th Annual International Conference of the IEEE Engineering in Medicine and Biology Society (EMBC), pp 6285–6288.

Eaton DC (1985) Ionic channels of excitable membranes. Bertil Hille. Sunderland, Ma: Sinauer Associates, 1984. J. Neurosci. Res. 13:599–600.

Esch T, Kristan WB (2002) Decision-making in the leech nervous system. Integr Comp Biol 42:716–724.

Fathiazar E, Anemuller J, Kretzberg J (2016) Statistical identification of stimulus-activated network nodes in multi-neuron voltage-sensitive dye optical recordings. Annual International Conference of the IEEE Engineering in Medicine and Biology Society. IEEE Engineering in Medicine and Biology Society. Annual International Conference 2016:3899–3903.

Fathiazar E, Hilgen G, Kretzberg J (2013) Removing bleaching artifacts from voltage sensitive dye recordings with ICA. CNS 2013 14.

Fathiazar E, Hilgen G, Kretzberg J (2018) Higher Network Activity Induced by Tactile Compared to Electrical Stimulation of Leech Mechanoreceptors. Front Physiol 9:173.

Fields H (2004) State-dependent opioid control of pain. Nat Rev Neurosci 5:565–575.

Forrest MD (2014) The sodium-potassium pump is an information processing element in brain computation. Front. Physiol. 5:472.

Frady EP, Kapoor A, Horvitz E, Kristan WB (2016) Scalable Semisupervised Functional Neurocartography Reveals Canonical Neurons in Behavioral Networks. Neural Computation 28:1453–1497.

Fuchs E, Flügge G (2014) Adult neuroplasticity: more than 40 years of research. Neural Plast 2014:541870.

Ganguly K, Poo M-M (2013) Activity-dependent neural plasticity from bench to bedside. Neuron 80:729–741.

Gaudry Q, Kristan WB (2009) Behavioral choice by presynaptic inhibition of tactile sensory terminals. Nature neuroscience 12:1450–1457.

Geddes JW, Wilson MC, Miller FD, Cotman CW (1990) Molecular Markers of Reactive Plasticity. In: Excitatory Amino Acids and Neuronal Plasticity (Ben-Ari Y, ed), pp 425–432. Boston, MA: Springer US.

Gerard E, Hochstrate P, Dierkes P-W, Coulon P (2012) Functional properties and cell type specific distribution of I(h) channels in leech neurons. J Exp Biol 215:227–238.

Goldman MS, Golowasch J, Marder E, Abbott LF (2001) Global Structure, Robustness, and Modulation of Neuronal Models. J. Neurosci. 21:5229–5238.

González JE, Tsien RY (1995) Voltage sensing by fluorescence resonance energy transfer in single cells. Biophys J 69:1272–1280.

Greene DL, Kang S, Hoshi N (2017) XE991 and Linopirdine Are State-Dependent Inhibitors for Kv7/KCNQ Channels that Favor Activated Single Subunits. J Pharmacol Exp Ther 362:177–185.

Gulledge AT, Dasari S, Onoue K, Stephens EK, Hasse JM, Avesar D (2013) A sodium-pump-mediated afterhyperpolarization in pyramidal neurons. J. Neurosci. 33:13025–13041.

Hakizimana P, Brownell WE, Jacob S, Fridberger A (2012) Sound-induced length changes in outer hair cell stereocilia. Nat Commun 3:1094.

Harley CM, Cienfuegos J, Wagenaar DA (2011) Developmentally regulated multisensory integration for prey localization in the medicinal leech. J Exp Biol 214:3801–3807.

Hermey G (2011) Der Experimentator: Neurowissenschaften. Heidelberg: Spektrum Akademischer Verlag.

Hogkin AL, Huxley AF (1952) A quantitative description of membrane current and its application to conduction and excitation in nerve. The Journal of Physiology 117:500–544.

Hogkin AL, Katz B (1949) The effect of sodium ions on the electrical activity of giant axon of the squid. The Journal of Physiology 108:37–77.

Hübel N, Dahlem MA (2014) Dynamics from seconds to hours in Hodgkin-Huxley model with time-dependent ion concentrations and buffer reservoirs. PLOS Computational Biology 10:e1003941.

Ižikevič EM (2010) Dynamical systems in neuroscience: the geometry of excitability and bursting. Cambridge, Mass.: MIT Press.

Jacob R, Lieberman M, Murphy E, Piwnica-Worms D (1987) Effects of sodium-potassium pump inhibition and low sodium on membrane potential in cultured embryonic chick heart cells. The Journal of Physiology 387:549–566.

Jansen JKS, Nicholls JG (1973) Conductance changes, an electrogenic pump and the hyperpolarization of leech neurones following impulses. The Journal of Physiology 229:635–655.

Johansen J (1991) Ion conductances in identified leech neurons. Comparative Biochemistry and Physiology Part A: Physiology 100:33–40.

Johansen J, Kleinhaus AL (1986) Differential sensitivity of tetrodotoxin of nociceptive neurons in 4 species of leeches. J. Neurosci. 6:3499–3504.

Johnson K (2001) The roles and functions of cutaneous mechanoreceptors. Current Opinion in Neurobiology 11:455–461.

Kandel ER, Tauc L (1965a) Heterosynaptic facilitation in neurones of the abdominal ganglion of Aplysia depilans. The Journal of Physiology 181:1–27.

Kandel ER, Tauc L (1965b) Mechanism of heterosynaptic facilitation in the giant cell of the abdominal ganglion of Aplysia depilans. The Journal of Physiology 181:28–47.

Katok A, Hasselblatt B (1996) Introduction to the modern theory of dynamical systems. Cambridge: Cambridge Univ. Press.

Klees G, Hochstrate P, Dierkes PW (2005) Sodium-dependent potassium channels in leech P neurons. J Membrane Biol 208:27–38.

Kleinhaus AL, Angstadt JD (1995) Diversity and modulation of ionic conductances in leech neurons. Journal of Neurobiology 27:419–433.

Kretzberg J, Kretschmer F, Marin-Burgin A (2007) Effects of multiple spike-initiation zones in touch sensory cells of the leech. Neurocomputing 70:1645–1651.

Kretzberg J, Pirschel F, Fathiazar E, Hilgen G (2016) Encoding of Tactile Stimuli by Mechanoreceptors and Interneurons of the Medicinal Leech. Front Physiol 7:506.

Kristan WB (1982) Sensory and Motor Neurones Responsible for the Local Bending Response in Leeches. Journal of Experimental Biology 96:161–180.

Kristan WB, Calabrese RL, Friesen WO (2005) Neuronal control of leech behavior. Prog Neurobiol 76:279–327.

Kristan WB, McGirr SJ, Simpson GV (1982) Behavioural and Mechanosensory Neurone Responses to Skin Stimulation in Leeches. Journal of Experimental Biology 96:143–160.

Larsson HP (2013) What determines the kinetics of the slow afterhyperpolarization (sAHP) in neurons? Biophys J 104:281–283.

Lee CH, Ruben PC (2008) Interaction between voltage-gated sodium channels and the neurotoxin, tetrodotoxin. Channels (Austin) 2:407–412.

Lewis JE, Kristan WB (1998) Quantitative Analysis of a Directed Behavior in the Medicinal Leech: Implications for Organizing Motor Output. J. Neurosci. 18:1571–1582.

Li Q, Burrell BD (2009) Two forms of long-term depression in a polysynaptic pathway in the leech CNS: one NMDA receptor-dependent and the other cannabinoid-dependent. J Comp Physiol A 195:831–841.

Li Q, Burrell BD (2010) Properties of cannabinoid-dependent long-term depression in the leech. J Comp Physiol A 196:841–851.

Lin JW, Ju W, Foster K, Lee SH, Ahmadian G, Wyszynski M, Wang YT, Sheng M (2000) Distinct molecular mechanisms and divergent endocytotic pathways of AMPA receptor internalization. Nat Neurosci 3:1282–1290.

Lockery SR, Fang Y, Sejnowski TJ (1990) A dynamical neural network model of sensorimotor transformations in the leech. In: 1990 IJCNN International Joint Conference on Neural Networks. IEEE.

Lockery, SR, Kristan WB (1990) Distributed processing of sensory information in the leech. II. Identification of interneurons contributing to the local bending reflex. J. Neurosci. 10:1816–1829.

Lombardo P, Scuri R, Cataldo E, Calvani M, Nicolai R, Mosconi L, Brunelli M (2004) Acetyl-L-carnitine induces a sustained potentiation of the afterhyperpolarization. Neuroscience 128:293–303.

Madison DV, Nicoll RA (1984) Control of the repetitive discharge of rat CA 1 pyramidal neurones in vitro. The Journal of Physiology 354:319–331.

Marder E, Taylor AL (2011) Multiple models to capture the variability in biological neurons and networks. Nat Neurosci 14:133–138.

Marín-Burgin A, Szczupak L (2000) Processing of sensory signals by a non-spiking neuron in the leech. J Comp Physiol A 186:989–997.

Matthews EA, Linardakis JM, Disterhoft JF (2009) The fast and slow afterhyperpolarizations are differentially modulated in hippocampal neurons by aging and learning. J. Neurosci. 29:4750–4755.

Meiser S, Ashida G, Kretzberg J (2019) Non-synaptic Plasticity in Leech Touch Cells. Front Physiol 10:1444.

Meyrand P, Weimann JM, Marder E (1992) Multiple axonal spike initiation zones in a motor neuron: serotonin activation. J. Neurosci. 12:2803–2812.

Miller EW, Lin JY, Frady EP, Steinbach PA, Kristan WB, Tsien RY (2012) Optically monitoring voltage in neurons by photo-induced electron transfer through molecular wires. PNAS 109:2114–2119.

Mistick DC (1978) Neurones in the leech that facilitate an avoidance behaviour following nearfield water disturbances. Journal of Experimental Biology 75:1–23.

Molecular Devices (2020) What is an action potential? https://www.moleculardevices.com/applications/patch-clamp-electrophysiology/what-action-potential#gref. Accessed Oct 1, 2020.

Morth JP, Pedersen BP, Toustrup-Jensen MS, Sørensen TL-M, Petersen J, Andersen JP, Vilsen B, Nissen P (2007) Crystal structure of the sodium-potassium pump. Nature 450:1043–1049.

Mozzachiodi R, Byrne JH (2010) More than synaptic plasticity: role of nonsynaptic plasticity in learning and memory. Trends in Neurosciences 33:17–26.

Mozzachiodi R, Lorenzetti FD, Baxter DA, Byrne JH (2008) Changes in neuronal excitability serve as a mechanism of long-term memory for operant conditioning. Nature neuroscience 11:1146–1148.

Muller KJ, Scott SA (1981) Transmission at a 'direct' electrical connexion mediated by an interneurone in the leech. The Journal of Physiology 311:565–583.

Müller WA, Frings S, Möhrlen F (2015) Tier- und Humanphysiologie. Eine Einführung. Berlin: Springer Spektrum.

Murakami M, Kashiwadani H, Kirino Y, Mori K (2005) State-dependent sensory gating in olfactory cortex. Neuron 46:285–296.

Nicholls JG, Baylor DA (1968) Specific modalities and receptive fields of sensory neurons in CNS of the leech. J Neurophysiol 31:740–756.

Nicholls JG, Purves D (1970) Monosynaptic chemical and electrical connexions between sensory and motor cells in the central nervous system of the leech. The Journal of Physiology 209:647–667.

O'Dell TJ, Kandel ER (1994) Low-frequency stimulation erases LTP through an NMDA receptor-mediated activation of protein phosphatases. Learn. Mem. 1:129–139.

Palmer CR, Barnett MN, Copado S, Gardezy F, Kristan WB (2014) Multiplexed modulation of behavioral choice. J Exp Biol 217:2963–2973.

Passmore GM, Reilly JM, Thakur M, Keasberry VN, Marsh SJ, Dickenson AH, Brown DA (2012) Functional significance of M-type potassium channels in nociceptive cutaneous sensory endings. Front. Mol. Neurosci. 5:63.

Payeur A, Béïque J-C, Naud R (2019) Classes of dendritic information processing. Current Opinion in Neurobiology 58:78–85.

Peng AW, Salles FT, Pan B, Ricci AJ (2011) Integrating the biophysical and molecular mechanisms of auditory hair cell mechanotransduction. Nat Commun 2:523.

Peterka DS, Takahashi H, Yuste R (2011) Imaging voltage in neurons. Neuron 69:9–21.

Peterson EL (1984) Photoreceptors and visual interneurons in the medicinal leech. Journal of Neurobiology 15:413–428.

Pirschel F, Hilgen G, Kretzberg J (2018) Effects of Touch Location and Intensity on Interneurons of the Leech Local Bend Network. Sci Rep 8:3046.

Pirschel F, Kretzberg J (2016) Multiplexed Population Coding of Stimulus Properties by Leech Mechanosensory Cells. J Neurosci 36:3636–3647.

Poulet JFA, Hedwig B (2002) A corollary discharge maintains auditory sensitivity during sound production. Nature 418:872–876.

Purves D (2019) Neuroscience. New York, Oxford: Oxford University Press Sinauer Associates is an imprint of Oxford University Press.

Rolls MM, Jegla TJ (2015) Neuronal polarity: an evolutionary perspective. J Exp Biol 218:572–580.

Rossana Scuri, Paola Lombardo, Enrico Cataldo, Chiara Ristori, Marcello Brunelli (2007) Inhibition of Na+/K+ ATPase potentiates synaptic transmission in tactile sensory neurons of the leech. European Journal of Neuroscience 25:159–167.

Russell JT (2011) Imaging calcium signals in vivo: a powerful tool in physiology and pharmacology. Br J Pharmacol 163:1605–1625.

Saal HP, Bensmaia SJ (2014) Touch is a team effort: interplay of submodalities in cutaneous sensibility. Trends in Neurosciences 37:689–697.

Sahasranamam A, Vlachos I, Aertsen A, Kumar A (2016) Dynamical state of the network determines the efficacy of single neuron properties in shaping the network activity. Sci Rep 6:26029.

Sahley CL, Modney BK, Boulis NM, Muller KJ (1994) The S cell: an interneuron essential for sensitization and full dishabituation of leech shortening. J. Neurosci. 14:6715–6721.

Schindelin J, Arganda-Carreras I, Frise E, Kaynig V, Longair M, Pietzsch T, Preibisch S, Rueden C, Saalfeld S, Schmid B, Tinevez J-Y, White DJ, Hartenstein V, Eliceiri K, Tomancak P, Cardona A (2012) Fiji: an open-source platform for biological-image analysis. Nature methods 9:676–682.

Scuri R, Lombardo P, Cataldo E, Ristori C, Brunelli M (2007) Inhibition of Na+/K+ ATPase potentiates synaptic transmission in tactile sensory neurons of the leech. Eur J Neurosci 25:159–167.

Scuri R, Mozzachiodi R, Brunelli M (2002) Activity-dependent increase of the AHP amplitude in T sensory neurons of the leech. J Neurophysiol 88:2490–2500.

Simidu U, Kita-Tsukamoto K, Yasumoto T, Yotsu M (1990) Taxonomy of four marine bacterial strains that produce tetrodotoxin. International journal of systematic bacteriology 40:331–336.

Simmons MA, Schneider CR (1998) Regulation of M-Type Potassium Current by Intracellular Nucleotide Phosphates. J. Neurosci. 18:6254–6260.

Smith ESJ, Lewin GR (2009) Nociceptors: a phylogenetic view. Journal of Comparative Physiology A 195:1089–1106.

Storm JF (1987) Action potential repolarization and a fast after-hyperpolarization in rat hippocampal pyramidal cells. The Journal of Physiology 385:733–759.

Tada M, Takeuchi A, Hashizume M, Kitamura K, Kano M (2014) A highly sensitive fluorescent indicator dye for calcium imaging of neural activity in vitro and in vivo. European Journal of Neuroscience 39:1720–1728.

Terracciano CM (2001) Rapid inhibition of the Na+-K+ pump affects Na+-Ca2+ exchanger-mediated relaxation in rabbit ventricular myocytes. The Journal of Physiology 533:165–173.

Thomson EE, Kristan WB (2006) Encoding and decoding touch location in the leech CNS. J. Neurosci. 26:8009–8016.

Tomina Y, Wagenaar DA (2017) A double-sided microscope to realize whole-ganglion imaging of membrane potential in the medicinal leech. Elife 6.

Tzingounis AV, Kobayashi M, Takamatsu K, Nicoll RA (2007) Hippocalcin gates the calcium activation of the slow afterhyperpolarization in hippocampal pyramidal cells. Neuron 53:487–493.

Valkanov M, Boev K (1988) Ionic currents in the somatic membrane of identified T-mechanosensory neurons isolated from segmental ganglia of the medicinal leech. General physiology and biophysics 7:643–649.

Vallbo AB, Johansson RS (1984) Properties of cutaneous mechanoreceptors in the human hand related to touch sensation. Hum Neurobiol 3:3–14.

Vogalis F, Storm JF, Lancaster B (2003) SK channels and the varieties of slow after-hyperpolarizations in neurons. Eur J Neurosci 18:3155–3166.

W. Yamada, C. Koch, P. Adams (1989) Multiple channels and calcium dynamics. UR - https://www.semanticscholar.org/paper/Multiple-channels-and-calcium-dynamics-Yamada-Koch/f5a47289cca7e1d9696d58d6d05f48afd1f8b3b9.

Wagenaar DA (2015) A classic model animal in the 21st century: recent lessons from the leech nervous system. J Exp Biol 218:3353–3359.

Wei AD, Butler A, Salkoff L (2005) KCNQ-like potassium channels in Caenorhabditis elegans. Conserved properties and modulation. Journal of Biological Chemistry 280:21337–21345.

Yau KW (1976) Receptive fields, geometry and conduction block of sensory neurones in the central nervous system of the leech. The Journal of Physiology 263:513–538.

Yu FH, Catterall WA (2003) Overview of the voltage-gated sodium channel family. Genome Biol 4:207.

APPENDIX

Publication

Non-synaptic plasticity in leech touch neurons

Sonja Meiser[1*], Go Ashida[1,2] and Jutta Kretzberg[1,2]

[1] Computational Neuroscience, Department of Neuroscience, Faculty VI, Carl von Ossietzky University of Oldenburg, Oldenburg, Germany

[2] Cluster of Excellence Hearing4all, Department of Neuroscience, Faculty VI, Carl von Ossietzky, University of Oldenburg, Oldenburg, Germany

The role of Na^+/K^+-pumps in activity-dependent synaptic plasticity has been described in both vertebrates and invertebrates. Here, we provide evidence that the Na^+/K^+-pump is also involved in activity-dependent non-synaptic cellular plasticity in leech sensory neurons. We show that the resting membrane potential (RMP) of T cells hyperpolarizes in response to repeated somatic current injection, while at the same time their spike count (SC) and the input resistance (IR) increase. Our Hodgkin–Huxley-type neuron model, adjusted to physiological T cell properties, suggests that repetitive action potential discharges lead to increased Na^+/K^+-pump activity, which then hyperpolarizes the RMP. In consequence, a slow, non-inactivating current decreases, which is presumably mediated by voltage-dependent, low-threshold potassium channels. Closing of these putative M-type channels due to hyperpolarization of the resting potential increases the IR of the cell, leading to a larger number of spikes. By this mechanism, the response behavior switches from rapidly to slowly adapting spiking. These changes in spiking behavior also effect other T cells on the same side of the ganglion, which are connected via a combination of electrical and chemical synapses. An increased SC in the presynaptic T cell results in larger postsynaptic responses (PRs) in the other T cells. However, when the number of elicited presynaptic spikes is kept constant, the PR does not change. These results suggest that T cells change their responses in an activity-dependent manner through non-synaptic rather than synaptic plasticity. These changes might act as a gain-control mechanism. Depending on the previous activity, this gain could scale the relative impacts of synaptic inputs from other mechanoreceptors, versus the spike responses to tactile skin stimulation. This multi-tasking ability, and its flexible adaptation to previous activity, might make the T cell a key player in a preparatory network, enabling the leech to perform fast behavioral reactions to skin stimulation.

Original Research ARTICLE

Front. Physiol., 27 November 2019 | https://doi.org/10.3389/fphys.2019.01444

frontiers in Physiology

ORIGINAL RESEARCH
published: 27 November 2019
doi: 10.3389/fphys.2019.01444

Non-synaptic Plasticity in Leech Touch Cells

Sonja Meiser[1]*, *Go Ashida*[1,2] and *Jutta Kretzberg*[1,2]

[1] Computational Neuroscience, Department of Neuroscience, Faculty VI, Carl von Ossietzky University of Oldenburg, Oldenburg, Germany, [2] Cluster of Excellence Hearing4all, Department of Neuroscience, Faculty VI, Carl von Ossietzky University of Oldenburg, Oldenburg, Germany

The role of Na^+/K^+-pumps in activity-dependent synaptic plasticity has been described in both vertebrates and invertebrates. Here, we provide evidence that the Na^+/K^+-pump is also involved in activity-dependent non-synaptic cellular plasticity in leech sensory neurons. We show that the resting membrane potential (RMP) of T cells hyperpolarizes in response to repeated somatic current injection, while at the same time their spike count (SC) and the input resistance (IR) increase. Our Hodgkin–Huxley-type neuron model, adjusted to physiological T cell properties, suggests that repetitive action potential discharges lead to increased Na^+/K^+-pump activity, which then hyperpolarizes the RMP. In consequence, a slow, non-inactivating current decreases, which is presumably mediated by voltage-dependent, low-threshold potassium channels. Closing of these putative M-type channels due to hyperpolarization of the resting potential increases the IR of the cell, leading to a larger number of spikes. By this mechanism, the response behavior switches from rapidly to slowly adapting spiking. These changes in spiking behavior also effect other T cells on the same side of the ganglion, which are connected via a combination of electrical and chemical synapses. An increased SC in the presynaptic T cell results in larger postsynaptic responses (PRs) in the other T cells. However, when the number of elicited presynaptic spikes is kept constant, the PR does not change. These results suggest that T cells change their responses in an activity-dependent manner through non-synaptic rather than synaptic plasticity. These changes might act as a gain-control mechanism. Depending on the previous activity, this gain could scale the relative impacts of synaptic inputs from other mechanoreceptors, versus the spike responses to tactile skin stimulation. This multi-tasking ability, and its flexible adaptation to previous activity, might make the T cell a key player in a preparatory network, enabling the leech to perform fast behavioral reactions to skin stimulation.

Keywords: invertebrate, mechanoreceptor, sodium–potassium pump, Hodgkin–Huxley neuron model, M-type K^+ current, spike count, resting potential, input resistance

OPEN ACCESS

Edited by:
Sylvia Anton,
Institut National de la Recherche Agronomique (INRA), France

Reviewed by:
Brian Burrell,
University of South Dakota, United States
Daniel A. Wagenaar,
California Institute of Technology, United States

***Correspondence:**
Sonja Meiser
sonja.meiser@uni-oldenburg.de

Specialty section:
This article was submitted to Invertebrate Physiology, a section of the journal Frontiers in Physiology

Received: *31 May 2019*
Accepted: *08 November 2019*
Published: *27 November 2019*

Citation:
Meiser S, Ashida G and Kretzberg J (2019) Non-synaptic Plasticity in Leech Touch Cells. Front. Physiol. 10:1444. doi: 10.3389/fphys.2019.01444

INTRODUCTION

Understanding the mechanisms of how sensory information elicits behavioral reactions is a major goal in neuroscience. The experimentally easily amenable nervous system of the medicinal leech makes this animal a useful model organism to investigate the neuronal basis of sensory processing (Kristan et al., 2005; Wagenaar, 2015). Touching a leech's skin triggers a behavioral response with

a surprisingly high accuracy – the local bend (Kristan et al., 1982). The animal can distinguish between two touch locations just as precisely as the human fingertip (Johnson, 2001; Baca et al., 2005; Thomson and Kristan, 2006; Pirschel and Kretzberg, 2016). The leech central nervous system (CNS) contains a highly repetitive ventral nerve cord with one ganglion per segment. Each ganglion contains an ensemble of around 400 mostly paired neurons serving as the basis of diverse sensory-input motor-output networks (Kristan et al., 2005). The sensory input layer consists of three different types of leech mechanosensory cells [touch (T), pressure (P), and nociceptive (N) cells], which share several fundamental properties with the human tactile receptors (Baca et al., 2005; Smith and Lewin, 2009; Pirschel and Kretzberg, 2016). Early studies focused mostly on P cells, because stimulation of a single P cell is sufficient to elicit muscle movements for several behavioral responses, like swimming or local bending (Kristan, 1982; Kristan et al., 1982). Since T and N cells showed only minor contributions to these movements, they were not further investigated. However, Pirschel and Kretzberg (2016) suggested that T cells might play a substantial role in the local bend response, making in-depth investigations on these sensory neurons necessary.

The current study focuses on these T cells, which are low threshold, rapidly adapting sensory neurons. They primarily encode the temporal qualities, especially velocity, of applied mechanosensory stimuli during the onset and offset phases of the stimulation (Nicholls and Baylor, 1968b; Carlton and McVean, 1995). There are three bilateral pairs of T cells in one ganglion which form both electrical and chemical synaptic connections with each other (Nicholls and Baylor, 1968b; Baylor and Nicholls, 1969b; Li and Burrell, 2008). Moreover T cells receive polysynaptic input from the other mechanoreceptor type (P cells) and nociceptors (N cells), leading to a combination of excitatory and inhibitory potentials (Burgin and Szczupak, 2003). Several long-range dendritic processes of T cells run through the ipsilateral nerve roots in the body wall to branch extensively in the base of the layer of epithelial cells and end at a few micrometers from the skin surface (Blackshaw, 1981). The rapidly adapting human Meissner corpuscles show similar response properties, elicited by encapsulated unmyelinated nerve endings with stretch-sensitive ion channels in the tip. Potentially, the nerve endings of T cells may also contain these mechanosensitive channels, which may change opening probability after repeated stimulation, like in human hair cells during stimulation with a high sound pressure level (Hakizimana et al., 2012). Because the entire extent of arborization of one T cell spans three segmental ganglia, each cell responds to touch of the skin at its own and the adjacent anterior and posterior segments (Yau, 1976). The receptive fields of each T cell cover either the dorsal, lateral, or ventral skin area on one side (Nicholls and Baylor, 1968b). Like other invertebrate neurons, T cells are unipolar, meaning that dendrites and axon are not clearly separated, but form a continuum of processes (Rolls and Jegla, 2015). Moreover, like several invertebrate neurons (Calabrese, 1980; Meyrand et al., 1992), leech T cells were found to have at least two distinct spike-initiation zones. A peripheral spike initiation zone near the skin conveys information about touch stimuli, and a central one close to the soma processes synaptic inputs within the ganglion (Burgin and Szczupak, 2003; Kretzberg et al., 2007).

High frequency spiking in touch mechanoreceptors triggered by somatic electrical stimulation or peripheral skin stimulation (Baylor and Nicholls, 1969a) induces a long-term afterhyperpolarization (AHP), arising from the activation of the Na^+/K^+-pump (also called the Na^+/K^+-ATPase) and a Ca^{2+}-dependent K^+ current (Nicholls and Baylor, 1968a; Baylor and Nicholls, 1969a; Jansen and Nicholls, 1973; Scuri et al., 2002, 2007). Previous studies pointed out that modulation of the Na^+/K^+-pump activity is involved in activity-dependent synaptic plasticity between two ipsilateral T neurons (Catarsi and Brunelli, 1991; Catarsi et al., 1993; Scuri et al., 2002, 2007; Lombardo et al., 2004). Additionally, high-frequency stimulation of a T cell elicits long-term depression in the activated pathway and potentiation in the non-activated T cell synapses (Burrell and Sahley, 2004). Furthermore, low-frequency stimulation of T cells can depress synapses through an endocannabinoid-dependent mechanism, which has also been observed in the mammalian spinal cord (Li and Burrell, 2009, 2010).

Here, we show that T cell activity is also influenced by non-synaptic plasticity. Based on our electrophysiological experiments and modeling approaches, we demonstrate that repeated somatic T cell stimulation enhances Na^+/K^+-pump activity, which gradually hyperpolarizes the resting membrane potential (RMP). In consequence, a slow, non-inactivating (putative M-type K^+) current decreases, resulting in a higher input resistance (IR) and a larger number of tonic spikes. Furthermore, our T cell double recordings show that the Na^+/K^+-pump is also involved in activity-dependent non-synaptic cellular plasticity among leech sensory neurons. Our recording results indicate that the increase in presynaptic spike count (SC) due to non-synaptic plasticity also affects the PR in another ipsilateral T cell. However, this effect is not specific to stimulus history, indicating non-synaptic rather than synaptic plasticity.

MATERIALS AND METHODS

Animals and Preparation

The experiments were performed on adult hermaphrodite medicinal leeches (*Hirudo verbana*) obtained from the Biebertaler Leech Breeding Farm (Biebertal, HE, Germany). According to German regulations, no approval of an ethics committee was required for the work on these invertebrates. The animals were kept at room temperature in tanks with ocean sea-salt diluted with purified water (1:1000). All experiments were performed at room temperature. The leeches were anesthetized with ice-cold saline (mM: 115 NaCl, 4 KCl, 1.8 $CaCl_2$, 10 Glucose, 4.6 Tris–maleate, 5.4 Tris base and buffered at pH 7.4 with NaOH, modified after Muller and Scott, 1981) before and during dissection. We used isolated ganglia, dissected from segments 9–13 and pinned them, ventral side up, to a plastic petri dish, coated with the silicone elastomer *Sylgard* (Dow Corning Corporation, Midland, MI, United States) (**Figure 1A**).

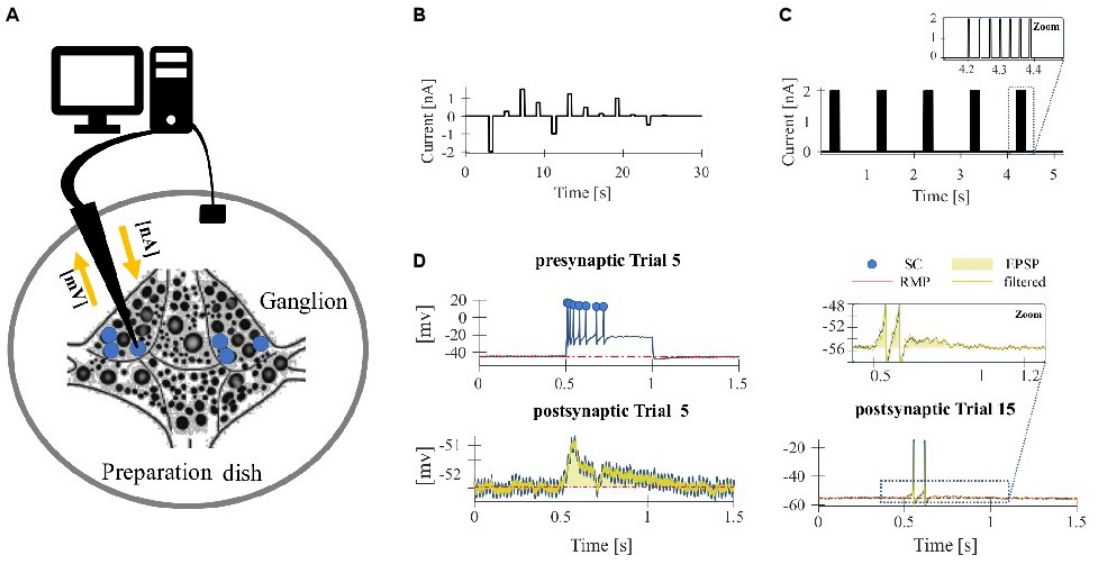

FIGURE 1 | Experimental design. **(A)** Sketch of the isolated ganglia preparation and the principle of the current-clamp recording. The membrane potential of one of the T cells (blue) was recorded with an intracellular electrode (black arrow). **(B,C)** Stimulus protocol for repeated electrical soma stimulation. Each experiment consisted of 15–20 identical trial repetitions. **(B)** For the experiments presented in **Figures 2**, **4A,B**, 12 electrical pulses of different current amplitudes were injected into the T cell soma. **(C)** For studying synaptic interaction of T cells (**Figures 4C–F**), five pulse packages were injected into the soma if one T cell. Each package contained a fixed number (1–7) of pulses that elicits the same number of single action potentials. The zoom inset shows a package with 7 pulses. **(D)** The neuronal responses were quantified by the following features: (presynaptic) spike count (SC, blue dots indicate counted spikes): total number of spikes elicited by the neuron and recorded in the soma between the stimulus onset (0.5 s) and offset (1 s); resting membrane potential (RMP, red): averaged membrane potential in the 2.5 s prior to the first current pulse; postsynaptic response (PR): averaged difference between the filtered recorded membrane potential and the RMP calculated from the start to 200 ms after the end of the presynaptic current stimulus (yellow transparent area). Synaptic potentials sometimes triggered spikes in the postsynaptic cell (see Trial 15 for an example), but not in all (see Trial 5 for an example). The calculation of PR included spikes if they were elicited.

Electrophysiological Technique

The experimental rig consisted of two mechanical micromanipulators type MX-1 (TR 1, Narishige, Tokyo, Japan) and two amplifiers (SEC-05X, NPI Electronic, Tamm, Germany) (Kretzberg et al., 2016). Neuronal responses were recorded (sample rate 100 kHz) and analyzed using custom-written MATLAB software (MATLAB 9.1-9.5, MathWorks, Natick, MA, United States). We performed intracellular single and double recordings from mechanosensory touch cells, while injecting current into one T cell soma. For these current clamp recordings, the cell soma was impaled with borosilicate microelectrodes (TW100F-4, World Precision Instruments Inc., Sarasota, FL, United States) pulled with the micropipette puller P97 Flaming Brown (Sutter Instruments Company, Novato, CA, United States). The glass electrodes were filled with 3 M potassium acetate and had resistances of 15–30 MΩ. The neurons were identified by the size and the location of their cell bodies with a binocular microscope (Olympus szx7, Olympus, Tokyo, Japan) as well as by their firing pattern (Nicholls and Baylor, 1968b).

Experimental Design

To investigate the effect of repeated mechanoreceptor stimulation on the physiological properties of T cells and their synaptic partners we used somatic current injection. Intracellular single recordings of T cells in isolated ganglia were performed by stimulating the neuron in each trial with a series of 12 current pulses in a pseudo-randomized order (**Figure 1B**). The amplitude of the pulses varied between −2 and +1.5 nA. The duration of each pulse was 500 ms and the inter-pulse-interval was 2.5 s long. The inter-trial-interval was 5 s long. Each experiment consisted of 15–20 identical trial repetitions. While injecting current into the T cell soma with the intracellular electrode, we recorded the membrane potential of the stimulated T cell with the same electrode.

To analyze the synaptic connections between T cells, we performed ipsilateral double recordings and recorded from two of the three T cells in all combinations. While injecting current into one T cell soma (presynaptic) with one electrode, we recorded the membrane potential of the unstimulated T cell (postsynaptic) with a second electrode. In addition to the protocol shown in **Figure 1B**, a pulse-package protocol (**Figure 1C**) was applied. One pulse-package comprised a fixed number (1–7) of short current pulses (2 nA, 5 ms), which were injected into the T cell soma to trigger one action potential each. In consequence, the pulse-package protocol elicited the same number and timing of presynaptic action potentials in each trial. Each trial consisted of five pulse packages and each

sub-experiment was composed of 25 trial repetitions. The pause between the single pulses in a package was 30 ms and the starting times of the packages were always separated by 1 s (independent of the number of pulses in the package).

In total, we analyzed 20 single and 23 double recordings (9 with 500 ms current pulse injections, 14 with single current pulse injections) of T cells. During the recordings, the electrode properties usually changed slightly, leading to an average increase in electrode resistance by +7 MΩ, and an average electrode offset drift by −4 mV. Five additional single recordings were excluded from the analysis, because the electrode resistance changed by more then10 MΩ due to clogging, or because the electrode offset drifted by more than −6.25 mV.

Data Analysis

The neuronal responses of the stimulated T cells and their synaptic partner neurons were quantified by the following response features (**Figure 1D**): SC, RMP, cell IR, and postsynaptic response (PR).

- **SC** [spike number] was defined as the total number of spikes elicited by the neuron and recorded in the soma during the 500 ms between the stimulus onset and offset. Spike detection was accomplished using custom-developed MATLAB software. Spikes were defined by the following parameters: minimum threshold [mV], minimum duration [ms], and minimum spike amplitude [mV]. A spike was detected when the membrane potential depolarized by the minimum spike threshold and the relative spike height, from rest to peak, was at least as high as the minimum spike amplitude. Additionally, a peak was only accepted as an action potential if the detected peak at half of the prominence had the required minimum duration.
- **RMP** [mV] of each trial (U_{rest}) was computed as the averaged membrane potential in the 2.5 s before the first current pulse starts.
- **IR** [MΩ] was calculated based on the average membrane potential (U_{stim}) in response to a 500 ms long hyperpolarizing current pulse of $I = -1$ nA to avoid the influence of active processes. It was calculated with Ohm's law: R [MΩ] = (U_{stim} [mV] − U_{rest} [mV])/I [nA].
- **PR** [mV] was calculated as average difference between the recorded membrane potential and the RMP of the postsynaptic (unstimulated) cell. The potential difference was averaged in the period from the start to 200 ms after the end of the presynaptic current stimulus, no matter if spikes were elicited postsynaptically or not. To reduce the noise caused by electric hum superimposed to the recorded postsynaptic signal, we used a notch filter which removed at least half the power of the frequency components in the range of 47–53 Hz.

In the results section, response changes (ΔSC, ΔRMP, ΔIR, ΔPR) caused by repeated stimulation are displayed as differences in the measured response features (SC, RMP, IR, PR) between the N_{th} and the first trial repetition. The observed distributions of these response feature changes are reported as median, and first (Q1) and third (Q3) quartiles in the figures. To show the increase (ΔSC, ΔIR, ΔPR) or decrease (ΔRMP) over trial repetitions, linear fits were calculated for each cell individually. The obtained slopes were tested to differ significantly from 0 (t-test, $\alpha = 0.05$). In **Figures 2**, **4**, the average of the linear fits for all cells indicates if the response features increased or decreased with trial repetitions.

Biological Neuron Model

We built a computational model of the leech T cell to investigate the physiological bases of the experimentally observed adaptive changes caused by repeated electrical stimulation. We used a single-compartment Hodgkin–Huxley-type neuron model modified with an additional Na^+/K^+-pump and a M-type slow potassium current (**Table 1**). We did not aim to create a more complex multi-compartment model, because we focus on the activity of T cells induced by somatic current injection and because the information on ion channel distribution over the T cell membrane is fundamentally lacking. This and other limitations of our modeling approach are addressed in section "Discussion."

Model Structure

Based on previous experimental recordings of leech neurons, we assumed a fast (transient) sodium channel with four activation and one inactivation gate, while the delayed rectifier potassium channel has two activation gates (Johansen, 1991). These channels are responsible for spike generation in response to positive current injections. The activity of the Na^+/K^+-pump was assumed to depend on the intracellular concentration of Na^+ ions. Increase of intracellular Na^+ due to repetitive spikes leads to the activation of the pump, which exchanges three intracellular Na^+ ions with two extracellular K^+ ions, resulting in the net negative current that hyperpolarizes the membrane potential (Forrest, 2014). The M-type K^+ conductance, whose kinetics are much slower than the spike-generating conductances, cause the cessation of spiking during current injection in a voltage dependent manner (Yamada et al., 1998; Benda and Herz, 2003). In order to focus on the fundamental biophysical mechanisms of spike-rate adaptation caused by repetitive current injections, we used this minimalistic description of ion channels and pumps, although the leech T cell may express a number of other ionic conductances (see section "Discussion").

Model Fitting

Since the operating voltage range of leech T cells is considerably more depolarized than those of neurons in most other animals, we needed to adjust the model functions (**Table 1**) and parameters (**Table 2**) to reproduce known T cell response characteristics (shown in sections "Results" and "Repeated Somatic Current Injection Induces Non-synaptic Plasticity"). Starting from previous measurements in leeches (reviewed, e.g., in Johansen, 1991), the ion channel kinetics were determined to fit our T cell data, including the RMP, spike threshold, single spike duration, and SCs. By using the standard membrane capacitance density of 1.0 μF/cm^2, the effective size of the membrane and the leak conductance were determined. The membrane area we adopted is larger than what is expected solely from the size of the soma of a T cell, because the additional contribution of the dendritic processes near the cell body was considered.

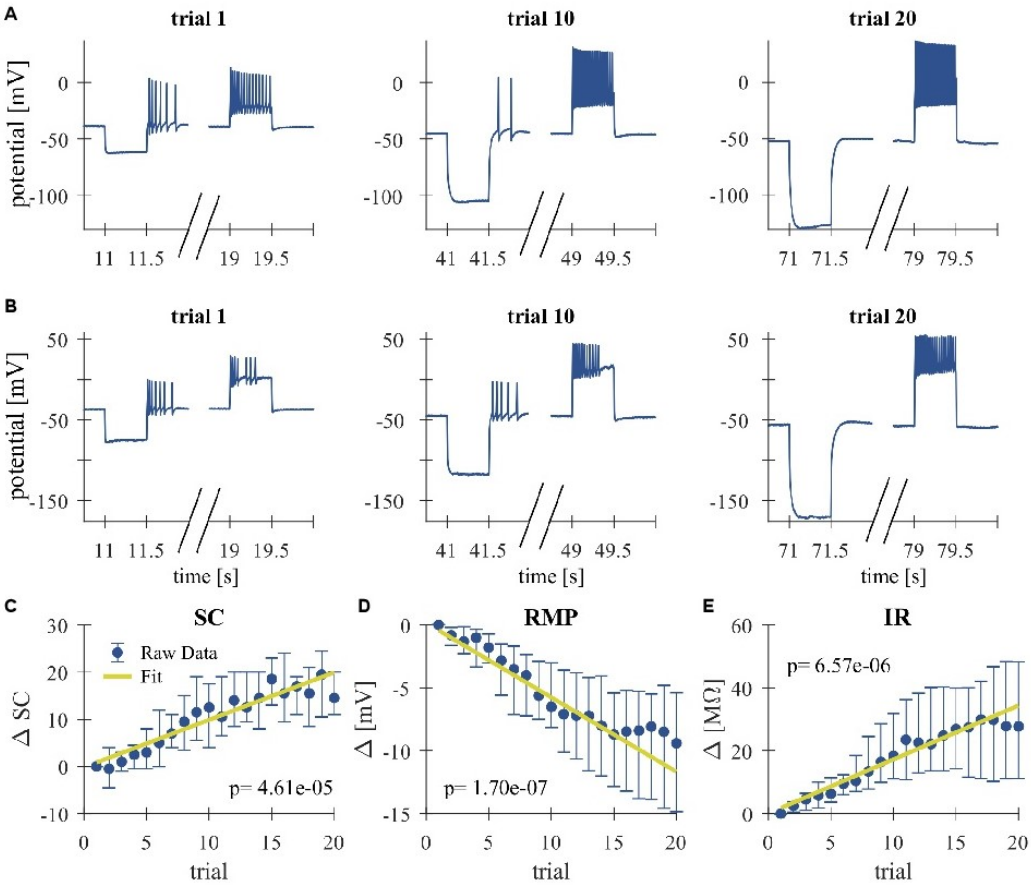

FIGURE 2 | Repeated somatic current injection effects physiological properties of T cells. **(A,B)** Representative responses of intracellularly recorded T cells to a 500 ms long somatic current pulse injection of −1 nA (seconds 11–11.5, 41–41.5, and 71–71.5), which was used for the calculation of the IR and often elicited rebound spikes, and +1 nA (seconds 19–19.5, 49–49.5, and 79–79.5) in Trial 1, 10, 20. **(A)** Example of a slowly adapting initial response, **(B)** Example of a rapidly adapting initial response. **(C–E)** Dependencies of changes in response parameters on trial repetitions shown as median and quartiles of all T cells ($N = 20$). Linear fits were calculated for each cell individually and the obtained slopes were tested to differ significantly from 0 (*t*-test, $\alpha = 0.05$, *p*-values given in the panels). The yellow line indicates the average of the fits for all cells. **(C)** Spike count (SC) difference from first trial (absolute number). **(D)** Resting membrane potential (RMP) difference from first trial (mV). **(E)** Input resistance difference from first trial (MΩ).

There is no empirical data available for the ionic concentration in T cells at rest and at spiking. Therefore, we formulated the Na^+/K^+-pump model depending only on the change of Na^+ concentration (denoted as c_{Na}) from rest. In our simulations c_{Na} was assumed to be in a similar order as in Retzius cells (Deitmer and Schlue, 1983), namely a few tens of mM. Time-dependent changes of the intracellular Na^+ concentration is caused by the Na^+ currents through Na^+ channels and Na^+/K^+-pumps. In order to separately simulate the contribution of Na^+ channels and Na^+/K^+-pumps in c_{Na}, we adopted two conversion factors (κ_{chan} and κ_{pump} in **Table 2**). Theoretically, this conversion factor is the reciprocal of the product between the Faraday constant and the effective volume relevant to the diffusion of Na^+ ions (Barreto and Cressman, 2011). However, it is not simple to estimate these factors in a T cell, because of its complex neuronal morphology. If the diffusion of Na^+ ions, which affects the activity of Na^+/K^+-pump, is not uniform but restricted to the vicinity of the membrane, the effective volume becomes smaller, leading to a larger value of the conversion factor. Therefore, we varied κ_{chan} and κ_{pump} in the range between 0 and $1.20 \cdot 10^{-6}$ mM/pA · ms, and selected values that led to a stable decrease of membrane potential with repeated stimulations.

TABLE 1 | T cell model equations.

Variable	Equation
Membrane potential V	$c_m \frac{dV}{dt} = I_{\mathrm{Na}} + I_K + I_M + I_L + I_{\mathrm{pump}} + I_{\mathrm{inj}}$
Fast (transient) Na^+ current I_{Na}	$I_{\mathrm{Na}} = g_{\mathrm{Na}} \cdot m^4 \cdot h \cdot (E_{\mathrm{Na}} - V)$
Delayed rectifier K^+ current I_K	$I_K = g_K \cdot n^2 \cdot (E_K - V)$
M-type K^+ current I_M	$I_M = g_M \cdot z^2 \cdot (E_K - V)$
Leak current I_L	$I_L = g_L \cdot (E_L - V)$
Kinetic equations for channel variables ($x = m, h, n,$ or z)	$\frac{dx(t)}{dt} = \frac{x_\infty(V) - x}{\tau_x(V)}$
Steady state function for Na^+ activation	$m_\infty(V) = \frac{1}{1 + \exp(-(V+20)/8)}$
Time constant for Na^+ activation (in ms)	$\tau_m(V) = 0.75 \cdot \left(\frac{2}{\exp(-(V+20)/16) + \exp((V+20)/16)} + 0.1 \right)$
Steady state function for fast Na^+ inactivation	$h_\infty(V) = \frac{1}{1 + \exp(+(V+36)/5)}$
Time constant for fast Na^+ inactivation (in ms)	$\tau_h(V) = 7.5 \cdot \left(\frac{2}{\exp(-(V+36)/10) + \exp((V+36)/10)} + 0.1 \right)$
Steady state function for delayed rectifier K^+ activation	$n_\infty(V) = \frac{1}{1 + \exp(-(V+20)/8)}$
Time constant for delayed rectifier K^+ activation (in ms)	$\tau_n(V) = 4.0 \cdot \left(\frac{2}{\exp(-(V+20)/16) + \exp((V+20)/16)} + 0.1 \right)$
Steady state function for M-type K^+ activation	$z_\infty(V) = \frac{1}{1 + \exp(-(V+35)/3)}$
Time constant for M-type K^+ activation (in ms)	$\tau_z(V) = 450 \cdot \left(\frac{2}{\exp(-(V+35)/6) + \exp((V+35)/6)} + 1.0 \right)$
Na^+/K^+-pump current I_{pump}	$I_{\mathrm{pump}} = -I_{\mathrm{max}} \cdot p(c_{\mathrm{Na}})$
Na^+/K^+-pump activation function $p(c_{Na})$	$p(c_{\mathrm{Na}}) = \left(\frac{1}{1 + \exp(-(c_{\mathrm{Na}} - 18)/18)} \right)^3$
Intracellular Na^+ concentration c_{Na} (measured from rest)	$\frac{dc_{\mathrm{Na}}}{dt} = \kappa_{\mathrm{chan}} \cdot I_{\mathrm{Na}} + 3\kappa_{\mathrm{pump}} \cdot I_{\mathrm{pump}}$

The factor 3 for the intracellular Na^+ concentration change originates from the fact that three Na^+ ions are exchanged with two K^+ ions. The membrane potential V is in mV and the intracellular Na^+ concentration c_{Na} is in mM. I_{inj} denotes injected current.

Comparison of Model Conditions

In order to investigate the effects of the Na^+/K^+-pump and putative M-type K^+ (K_M) conductance on the long-term change of repetitive spiking, we compared the following four conditions in the T cell model: (1) the "default model" introduced above with the functions and parameters fitted to our T cell data; (2) the "fixed pump" model in which the Na^+/K^+-pump current is fixed to the value at the initial steady-state obtained without any current injection; (3) the "fully fixed K_M" model in which the M-type K conductance is fixed to the value at the initial steady-state obtained without any current injection; and (4) the "partially fixed K_M" model in which the M-type K conductance is not allowed to change only during the +1 nA current stimulation in each trial. However, the K_M conductance may change normally as in the default model when there is no input, or during injected current of any other size than +1 nA (see **Figure 1B** for the stimulus protocol of each trial). The comparison of the default model and the partially fixed K_M model is expected to reveal how the dynamic property of the M-type K conductance may play a role during the specific current stimulation of +1 nA (500-ms long per trial).

TABLE 2 | T cell model parameters.

Parameter	Value
Membrane surface area S_m	15,000 μm^2
Membrane capacitance density C_m	1.0 $\mu F/cm^2$
Membrane capacitance $c_m = C_m S_m$	150 pF
Fast (transient) Na^+ conductance density G_{Na}	160 mS/cm^2
Delayed rectifier K^+ conductance density G_K	8.0 mS/cm^2
M-type K^+ conductance density G_M	4.0 mS/cm^2
Leak conductance density G_L	0.1 mS/cm^2
Fast (transient) Na^+ conductance $g_{Na} = G_{Na} S_m$	24 μS
Delayed rectifier K^+ conductance $g_K = G_K S_m$	1.2 μS
M-type K^+ conductance $g_M = G_M S_m$	0.6 μS
Leak conductance $g_L = G_L S_m$	0.015 μS
Na^+ reversal potential E_{Na}	+30 mV
K^+reversal potential E_K	−50 mV
Leak reversal potential E_L	−15 mV
Maximum pump current I_{max}	800 pA
Conversion factor from Na^+ channel current into Na^+ concentration κ_{chan}	$0.60 \cdot 10^{-6}$ mM/pA · ms
Conversion factor from Na^+/K^+-pump current into Na^+ concentration κ_{pump}	$0.12 \cdot 10^{-6}$ mM/pA · ms

Parameters were fitted to reproduce the experimentally measured T cell spike shape and to produce spike counts, resting potentials and input resistances in the interquartile range of the experimental observations of the 1st and 20th trial.

RESULTS

Repeated Somatic Current Injection Induces Non-synaptic Plasticity

High-frequency spike discharge leads to an intracellular accumulation of Na^+ ions which activate Na^+/K^+-pumps and thereby provide a mechanism for intrinsic, activity-dependent regulation of excitability (Gulledge et al., 2013;

Duménieu et al., 2015). We investigated the effect of high frequency spiking due to repeated stimulation with series of current pulse injections (500 ms duration, separated by 2500 ms break) into the T cell soma (**Figure 1**). Responses were analyzed for changes in the physiological properties SC, RMP, and cell IR. As can be seen in the representative intracellular response traces (**Figures 2A,B**), repeated current injection caused an increase in SC and in IR, while the RMP hyperpolarized.

These tendencies were seen in all recordings, even though the initial responses of individual T cells varied considerably in their SCs and the duration of their spiking activity (compare **Figures 2A,B** for examples of a slowly and a rapidly adapting initial response, see **Figures 3H–J** for the interquartile ranges of SC, RMP, and IR). The activity-dependent changes were found to be highly significant ($p < 0.001$) for all three physiological properties by testing if the slopes of linear regressions of individual cell responses differed from 0 (**Figures 2C–E**). This approach is not meant to imply that the relationships are linear, but only that SC and IR increased, and RMP hyperpolarized consistently in all 20 cells.

While **Figure 2** shows the changes caused by repeated current injection, **Figures 3H–J** indicate the interquartile ranges of the observed measurements of SC, RMP, and IR. For an input current of 1 nA, the SC gradually increased from a median value of 14.5 in trial 1 to 36 in trial 20. Meanwhile the median RMP gradually hyperpolarized from −37.5 to −48.8 mV and the median T cell IR increased from 27.8 to 62.7 MΩ. The absolute changes of the physiological properties to a current injection of 1 nA, calculated as median and quartiles over cells, are shown in **Table 3** (data for current injection of 0.5, 0.75, 1.25, and 1.5 nA are not shown, but followed the same trend).

Summarizing, the RMP of T cells hyperpolarizes in response to repeated somatic current injection, while the SC increases. Usually, one would expect that the probability for action potential generation is decreased at hyperpolarized RMP (Hodgkin and Katz, 1949). However, the repetitive electrical stimulation also led to a substantial increase in cell IR, which cannot be explained by electrode clogging (see section "Experimental Design"). To investigate the reason of the experimentally observed increase in SC, we developed a Hodgkin–Huxley type neuron model, modified with an additional Na^+/K^+-pump and a M-type slow potassium current (**Table 1**).

Sodium Pump and Slow Potassium Current Can Induce Non-synaptic Plasticity

A large number of previous studies already investigated how different forms of AHPs are affected by voltage- or calcium-dependent ionic conductances (reviewed in Vogalis et al., 2003; Larsson, 2013). The time scales of intracellular calcium buffering (Yamada et al., 1998; Goldman et al., 2001) and the activation/inactivation of calcium dependent potassium currents (Vogalis et al., 2003), however, is on the order of 0.1–1 s, which is several orders of magnitude faster than the activity-dependent long-term decrease of the membrane potential we focus on (which is on the order of a few tens of seconds; **Figure 2A**). In this slow potential change, the activity of the Na^+/K^+-pump is likely to be relevant (Barreto and Cressman, 2011; Forrest, 2014). Hence, we investigated the involvement of the Na^+/K^+-pump on the changes in the physiological properties of T cells, namely the hyperpolarization of the RMP accompanied by the increase of SC and IR. To address this question, we constructed a minimalistic Hodgkin–Huxley-type neuron model of a T cell incorporating the fast Na^+, delayed rectifier K^+, leak, and slow M-type K^+ conductances as well as the Na^+/K^+-pump. Blue curves in **Figure 3** show the responses of the default T cell model. To simulate the spiking responses of the T cell, we used the same protocol as for our experimental recordings with somatic current injections (**Figure 1B**). Parameters of the model were adjusted so that the simulated spike shape matched the time course of the original spike and the adaptive changes of the main features SC, RMP and IR stayed largely within the interquartile ranges of the original data (blue curves in **Figures 3H–J**). The increase of the pump current (**Figure 3A**, blue) was responsible for the decrease of the RMP from about −39 to −48 mV (**Figure 3I**, blue), because in each pump cycle three intracellular sodium ions were exchanged with two extracellular potassium ions, leading to a net negative current. The SC of the standard model increased over trials (**Figure 3H**), because of the voltage-dependent deactivation of the M-type K^+ current (**Figures 3B,C**), which in early trials activates during the current injection and hinders the repetitive spiking. Additionally, the decrease of the M-type K^+ conductance across trials also let to a decrease of the simulated IR from about 31–60 MΩ (**Figure 3J**), which resembled the empirical observations (**Figures 2D,E**), and also had a positive effect on SC.

In order to further investigate the roles of the Na^+/K^+-pump and the putative M-type K^+ conductance, we fixed these current and examined the resulting changes of the model neuron responses from the default condition (see section "Comparison of Model Conditions" for more detail of the conditions compared). When the pump current was fixed to the initial steady-state value, the stimulus-induced hyperpolarization as well as the increase of SC and IR vanished (**Figure 3E**; compare the green and blue curves in **Figures 3H–J**). This suggests that the experimentally observed stable hyperpolarization of the RMP is mainly due to the increase of Na^+/K^+-pump current and that this hyperpolarization is the basis for all observed changes. When the M-type K^+ conductance was fixed to the initial steady-state, while the pump was allowed to change, the IR did not change, indicating that the observed increase in IR can be attributed to the changes in the slow K^+ current. In this model version, the SC decreased across trials (**Figure 3F** and black curves in **Figures 3H,J**), showing the intuitively expected effects of slow hyperpolarization (**Figure 3I**, black). This SC decrease was diminished when the M-type K^+ conductance was kept unchanged only during the +1 nA stimulation (**Figure 3G**), while it could change in an activity-dependent way at all other times. In this model, the closing of the modeled M-type K^+ channel still led to an increased IR (**Figure 3J**, red) and counteracted the reduced excitability due to hyperpolarization (compare black and red curves in **Figure 3H**). We also note, however, that the dynamic property of the M-type K^+ current, which activates on the time

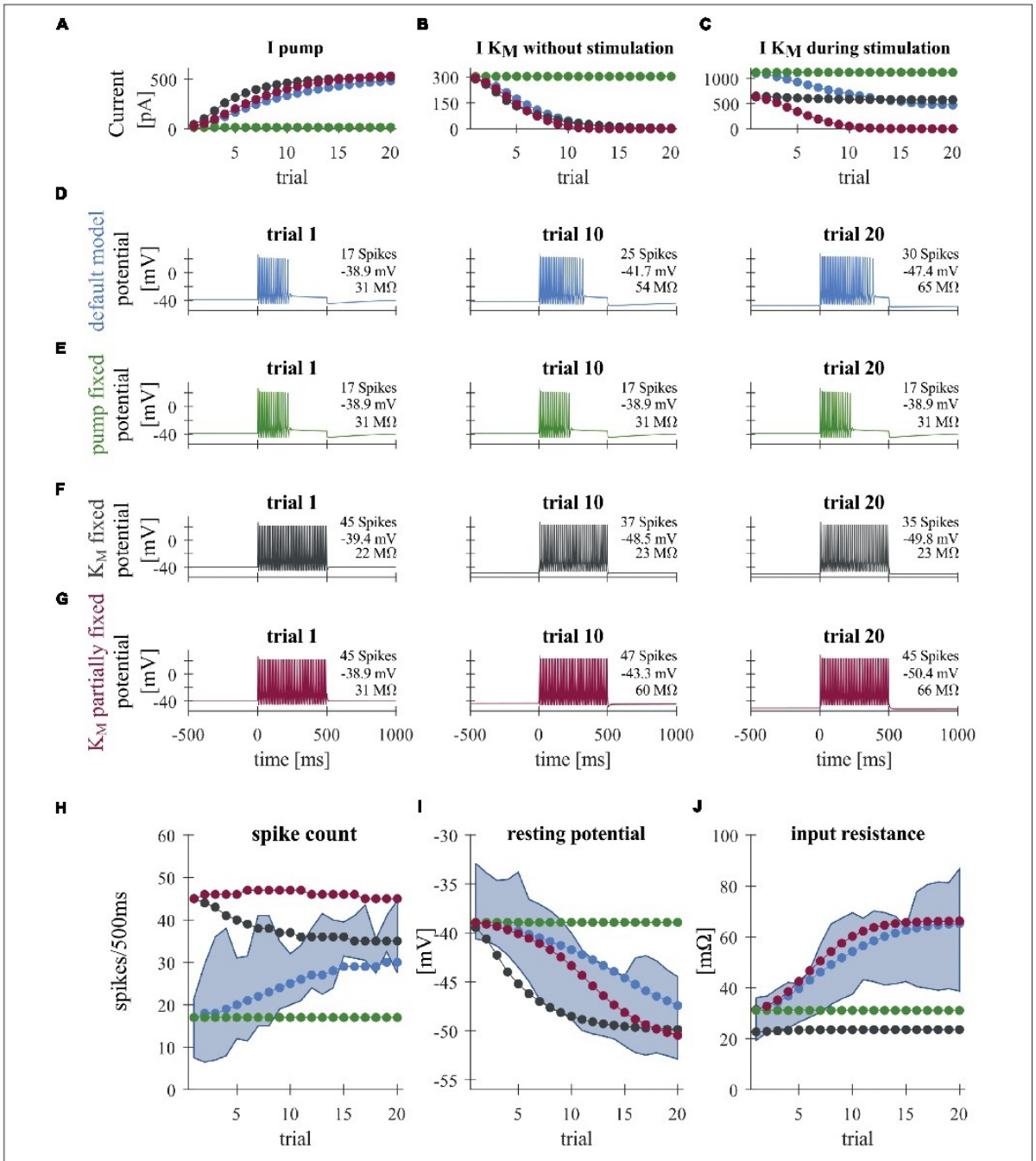

FIGURE 3 | Modeling T cell spike responses. **(A)** Average Na^+/K^+-pump current during +1 nA stimulation. **(B)** Average M-type K^+ current at 0–500 ms before the +1 nA stimulation. **(C)** Average M-type K^+ current during +1 nA stimulation. The K_M current is generally larger during stimulation **(C)** than without stimulation **(B)**, because of the increased average driving voltage (E_K–V) associated with spiking. **(D–G)** Responses of different T cell models to a current injection of +1 nA in Trials 1, 10 and 20. See **Figure 1B** for the stimulus protocol used. **(D)** Default model. **(E)** "Fixed pump model," in which the Na^+/K^+-pump current I_{pump} is fixed to the initial steady-state value. **(F)** "Fully fixed K_M model," in which the dynamics of the M-type K^+ conductance was fixed to the initial steady-state value. **(G)** "Partially fixed K_M model," in which the dynamics of the M-type K^+ conductance was fixed only during +1 nA current injection. **(H–J)** Simulated changes of the spike count **(H)**, resting potential **(I)**, and input resistance **(J)** across trials, plotted with the corresponding interquartile ranges observed experimentally (blue shading). Colors in panels **(A–C)** and **(H–J)** indicate the different model conditions: (blue) default model; (green) "fixed pump model"; (black) fully fixed K_M model; and (red) "partly fixed K_M model."

TABLE 3 | Absolute values for non-synaptic plasticity effects in T cells.

	Trial 1			Trial 20		
Property	**Q1**	**Median**	**Q3**	**Q1**	**Median**	**Q3**
SC [spikes/0.5 s]	7.5	14.5	24	27.5	36	42
RMP [mV]	−32.9	−37.5	−40.6	−44.5	−48.8	−52.9
Resistance [MΩ]	19.4	27.8	38.7	46.4	62.7	74.1

Responses to 500 ms current injection of 1 nA were obtained in 20 cells.

scale of a few 100 ms, turned out to be critical for determining the duration of repetitive spiking (compare **Figures 3D,G**). Despite the realistic increase in IR, the number of spikes in the model version with partially fixed M-type K^+ current were very large (**Figure 3H**, red), because spiking activity did not cease before the end of the stimulus (**Figure 3G**). These results suggest that the experimentally observed repetitive spiking behavior (and its cessation) of leech T cells is associated with a K_M-like slow conductance, which affects the SCs more dynamically than the static increase of IR. In sum, our modeling results suggest that the inactivation of the slow K^+ current plays a role in increasing the SC in an activity-dependent manner (**Figure 3H**). This inactivation is induced by the RMP hyperpolarization caused by the increased activity of Na^+/K^+-pumps (**Figure 3I**).

Non-synaptic Plasticity Effects Postsynaptic Responses of Other T Cells

We investigated the signal transmission between two ipsilateral T cells. Our goal was to see how the activity changes that were induced by non-synaptic plasticity in an electrically stimulated T cell (presynaptic) affected the responses in a non-stimulated T cell (postsynaptic). We analyzed how the PR, consisting of postsynaptic potentials and potentially elicited spikes, changed over repeated stimulation of the presynaptic cell (**Figure 4**). As expected, the presynaptic SC increased with repeated current stimulation from a median of 6 spikes (Q1: 4.25/Q3: 20) in trial 1 to 20 spikes (Q1: 17.75/Q3: 21) in trial 15. Postsynaptically, we observed a tendency of increased PR size, but overall the slopes of the linear regressions of PR increases were not significantly different from 0 ($p > 0.05$, cf. **Figure 4B**), because the PR increased only in 9 out of 11 cells over trials. However, the median of the averaged PR increased from 0.77 mV (Q1: 0.30/Q3: 1.23) in trial 1 to 0.96 mV (Q1: 0.44/Q3: 1.67) in trial 15.

To clarify if the increase in PR observed in most of the T cell pairs was caused solely by the increase of presynaptic SC that reflects the non-synaptic plasticity in the presynaptic (stimulated) T cell, or rather the synaptic plasticity also played a role, we elicited in the presynaptic cell a fixed number of single action potentials (**Figure 4C**) and repeated the protocol over several trials. The PR size was found to depend highly significantly ($p < 0.001$) on the presynaptic SC (**Figure 4D**), because the linear regression yielded clearly positive slopes for all the cell pairs examined. The averaged PR increased from a median value of 0.34 mV in response to one spike (Q_1: 0.31/Q_3: 0.37) to 1.02 mV (Q_1: 0.99/Q_3: 1.10) in response to seven spikes. However, the PR size did not change significantly with stimulation repetitions in six out of seven conditions with fixed SC (**Figures 4E,F**), demonstrating that synaptic plasticity did not alter the PRs.

Summarizing, the increase in SC caused by non-synaptic plasticity in the repeatedly stimulated presynaptic cell in most T cell pairs was reflected by an increase in PR size in the postsynaptic cell. However, no indication for synaptic plasticity was found, because PR size stayed stable over trials, when the presynaptic SC did not change.

DISCUSSION

Many studies have reported the involvement of the Na^+/K^+-pump in activity-dependent synaptic plasticity in both vertebrates (Wyse et al., 2004) and invertebrates (Pinsker and Kandel, 1969; Scuri et al., 2007). Based on electrophysiological and modeling results, the present study showed that the Na^+/K^+-pump might also be involved in activity-dependent non-synaptic plasticity in leech sensory neurons. Repeated somatic T cell stimulation enhances Na^+/K^+-pump activity which gradually hyperpolarizes the RMP while the SC and IR increase (**Figures 2**, **3**). Furthermore, we showed that this non-synaptic plasticity, rather than synaptic plasticity, leads to increased PRs in a second T cell on the same side of a segmental ganglion (**Figure 4**).

Biophysical Mechanisms Underlying Activity-Dependent Non-synaptic Plasticity

Our experimental and modeling results indicate that T cells modify their responses depending on their previous activity. Repeated somatic T cell stimulation enhances Na^+/K^+-pump activity which gradually hyperpolarizes the RMP. This might result in the suppression of a slow K^+ current, which leads to a higher IR and an increased SC. This putative K_M-current is involved in producing burst-patterns in many neuronal systems by raising the threshold for firing an action potential (Benda and Herz, 2003). Some of the K_M-channels are open at rest and they are even more likely to be open during depolarization, causing spike responses to stop before the end of the stimulation. But when the cell hyperpolarizes, this slow K^+ channel closes and the neuron fires in a more tonic manner. Especially in early trials, many of the recorded T cells showed cessation of spikes well before the end of the current pulse period. While the experimentally observed increase in IR could be one of the causes for the increase in SC, it did not lead to the cessation before the end of the stimulus. The changes in repetitive spiking behavior could be explained by the dynamical changes of the putative K_M current. Further experimental and modeling studies, e.g., on the effects of varied intervals between stimulus applications, are needed to understand the biophysical mechanisms of non-synaptic plasticity in more detail.

Leech sensory cells express several different ion channels (Johansen, 1991; Kleinhaus and Angstadt, 1995; Gerard et al., 2012), most of which we did not include in our model for the sake of simplicity. Sodium-dependent K^+ channels as they were found in leech pressure cells (Klees et al., 2005), for example,

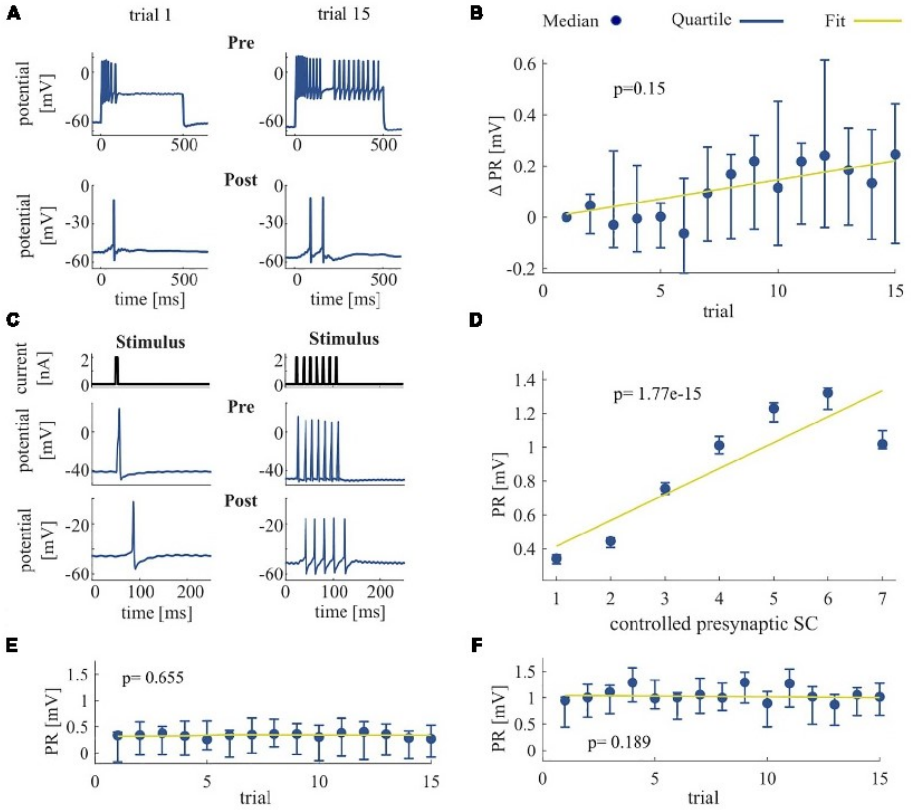

FIGURE 4 | Effect of repeated somatic current stimulation on the communication between two ipsilateral T cells. **(A)** Representative responses of an intracellularly recorded T cell pair to a 500 ms long somatic current injection of 1 nA in two different trial repetitions. **(B)** PR difference from first trial [mV] as median and quartiles of all T cells (N = 11) vs. trials. **(C)** Representative responses of an intracellularly recorded T cell pair to one and seven short current pulses. **(D)** Dependency of PR as median and quartiles of all T cells (N = 14) on controlled presynaptic SC. **(E,F)** Dependency of PR as median and quartiles of all T cells (N = 14) for one **(E)** and for seven **(F)** presynaptic spikes vs. trials. The slope of the PR vs. trial was not significant for six out of seven conditions (1 pulse, p = 0.655; 2 pulses, p = 0.032; 3 pulses, p = 0.092; 4 pulses, p = 0.051; 5 pulses, p = 0.772; 6 pulses, p = 0.512; 7 pulses, p = 0.190). Linear fits were calculated for each cell individually and the obtained slopes were tested to differ significantly from 0 (t-test, α = 0.05). Yellow line indicates the average of the fits for all cells.

might also affect T cell spiking in an activity dependent manner. Additionally, we assumed that the kinetics of the slow K^+ channels were only voltage dependent. However, the activity of M-type K^+ channels was reported to be affected also by the intracellular concentration of ATP (Simmons and Schneider, 1998). Since ATP is consumed through Na^+/K^+-pump cycles, this additional mechanism could further modulate the spike rate adaptation.

One important discrepancy between our model and the experimentally measured neuronal response was the difference in spike amplitudes. This difference might imply that the spike initiation site of the real T cell, responding to somatic stimulation, is not located exactly in the cell body. The recorded somatic spikes may only reflect the propagated action potentials that are generated elsewhere. Non-uniform distribution of ion channels in the T cell was found in previous studies: for example, T cells do have calcium-dependent K^+ channels (Kleinhaus and Angstadt, 1995) while their cell bodies largely lack voltage-dependent calcium channels (Valkanov and Boev, 1988; Johansen, 1991). To replicate the observed membrane potential changes, we had to adopt different factors (κ_{chan} and κ_{pump} in **Table 2**) that convert Na^+ channel currents and Na^+/K^+-pump currents into the intracellular Na^+ concentration; the difference between the two conversion factors possibly implies that these current sources may exist in different locations. In addition, recorded spike heights did not decrease over trials (**Figure 2A**), making contrast to the naive expectation that the increased intracellular Na^+ concentration should lead to the decrease of the sodium reversal potential. Overall, these observations support the hypothesis that somatic spikes of the T cell may actually be generated not directly within the cell body but somewhere nearby in the cell processes.

In order to experimentally confirm the role of Na^+/K^+-pumps and M-type K^+ channels in the change of IR and the spike rate

adaptation of T cells, their pharmacological blockade would be necessary. Such an experiment might not be straightforward, because, in leech neurons, conventional blockers do not always suppress ionic currents as expected (Johansen and Kleinhaus, 1986). Furthermore, leech neurons are packed in segmental ganglia, where the extracellular space is limited. To better simulate the effect of limited resources, a model would need to consider both intracellular and extracellular ionic concentrations (Hübel and Dahlem, 2014). To theoretically investigate the possible roles of spatially distributed ion channels and pumps in neuronal information processing, multicompartment models would be required (Cataldo et al., 2005; Kretzberg et al., 2007). In the present study, however, we did not aim to create a multicompartment model for several reasons. First, the main focus of our modeling was to investigate the activity-dependent long-term activity change of T cells induced by repetitive somatic current injection. Second there is almost no information available on the spatial distribution of ion channel over the T cell membrane that can be used for creating a multicompartment model. Third, we have no data recorded from the dendritic processes of T cells, which are essential for testing the simulated initiation and conduction of peripherally induced spikes.

T Cell Function and Interaction in the Network

Leeches respond to identical stimulation with multiple distinct reactions, which inspired the discussion of behavioral choice in the leech (Kristan et al., 2005; Baljon and Wagenaar, 2015). These behavioral alternatives are triggered by different patterns in neuronal activity. Due to the small number of neurons, multifunctional cells play a particular role in shaping these patterns (Kristan et al., 2005; Briggman and Kristan, 2006; Frady et al., 2016). We assume that T cells are such multifunctional players in a network that controls the response to a light touch on the leech's skin. The activated segment produces shortening on the stimulated and lengthening on the opposite side of the body wall (Kristan, 1982; Kristan et al., 1982). This local bend response is one of the fastest behaviors of the leech, with muscle movements starting only 200 ms after stimulus onset (Kristan et al., 2005). T cells respond very fast to tactile stimulation and give input to several local bend interneurons before P cell neuron spikes arrive at the central ganglion (Kretzberg et al., 2016). However, T cells are not capable of eliciting a behavior on their own (Kristan, 1982; Fathiazar et al., 2018). We assume that they activate with their very fast responses a modulatory network that regulates the gain of behaviors. Frady et al. (2016) have identified such a "preparatory network" of neurons that starts to react with a very short latency prior to the production of multiple behaviors, including local bending and whole-body shortening. After repeated stimulation causing non-synaptic plasticity, the enhanced activity might enable the T cells to transfer the animal into a state that prepares the muscles for a rapid start of a behavioral response by shifting the threshold for firing action potentials.

T cells form synaptic connections with each other that have both an electrical and a chemical component (Nicholls and Baylor, 1968b; Li and Burrell, 2008). Electrical synapses have shorter latencies compared to chemical synapses (Nicholls and Purves, 1970), and such fast-acting synaptic inputs could facilitate rapid transmission of sensory information to the preparatory network. Our experiments revealed that the increase in SC by non-synaptic plasticity also increases the PR in other T cells, which may include postsynaptic spiking. These postsynaptic changes appear to be a mere reflection of the activity-dependent changes in the presynaptic T cell. This finding might be an alternative interpretation to the conclusion of previous studies that the Na^+/K^+-pump is involved in activity-dependent synaptic plasticity between two ipsilateral T neurons (Catarsi and Brunelli, 1991; Catarsi et al., 1993; Scuri et al., 2002, 2007; Lombardo et al., 2004). Additionally, T cells have a strong synaptic connection to the S cell, a prominent element of the preparatory network (Burrell and Sahley, 2004). Each ganglion contains a single unpaired S cell, which forms strong electrical connections to the S cells in adjacent ganglia (Sahley et al., 1994). This network is reminiscent of a fast-conducting system (Mistick, 1978), but its causal role in any behavior is unclear (Sahley et al., 1994). To determine more neurons and their interactions involved in this preparatory network, VSD imaging with a double-sided-microscope would be an appropriate method (Tomina and Wagenaar, 2018). It would allow us to directly analyze functional relationships between neurons located on opposite surfaces and detect both action potentials and sub-threshold excitatory and inhibitory synaptic potentials (Miller et al., 2012).

In many vertebrate neurons, spikes are generated in the axon hillock, the part of the cell body that connects to the axon (Clarac and Cattaert, 1999). However, many invertebrate neurons are unipolar, meaning that dendrites and the axon are not clearly separated, but form a continuum of processes (Rolls and Jegla, 2015). Leech T cells send several long-range touch-sensitive dendritic processes to their receptive fields in the skin several millimeters away (Nicholls and Baylor, 1968b). Additionally, they arborize centrally to also reach the skin via both adjacent ganglia, leading to an even more extended receptive field (Yau, 1976). When the skin is touched lightly, T cells respond to the rate of skin indentation generating transient, rapidly adapting responses at stimulus onset and offset (Carlton and McVean, 1995; Kretzberg et al., 2016; Pirschel and Kretzberg, 2016; Pirschel et al., 2018). The action potentials are generated in the periphery and propagate through the ipsilateral nerve roots toward the soma. Moreover, spikes induced by central synaptic input can also travel in the opposite direction toward the periphery (Yau, 1976). Burgin and Szczupak (2003) and Kretzberg et al. (2007) suggested that leech T neurons may have at least two spike initiation zones with the different computational tasks of encoding touch stimuli in the periphery and processing synaptic inputs in the central ganglion. A similar anatomy was found in the LG motor neuron of the stomatogastric nervous system of the crab. It has a large soma with a nearby spike initiation zone and projects via dendritic processes to the periphery, where it also can initiate spikes up to 2 cm away from the soma (Meyrand et al., 1992).

In addition to the mutual T cell connections, the central part of the T cells receives polysynaptic inputs from the

other mechanoreceptors, the P and N cells. The postsynaptic potentials induced by these mechanoreceptor inputs can be excitatory, inhibitory, or a combination of both, indicating two interneuron pathways between the other mechanoreceptors and the T cells (Burgin and Szczupak, 2003). Hence, Na^+/K^+-pump activation in the context of non-synaptic plasticity probably shifts the membrane potential relative to the reversal potentials of these synapses, which could lead to an increase of the excitatory and a decrease of the inhibitory components of these postsynaptic potentials. In consequence, two complementary mechanisms following repeated T cell stimulation could increase the probability for centrally elicited spike reactions to synaptic inputs from the other mechanoreceptors: The hyperpolarization could increase excitatory postsynaptic potential size and at the same time deactivate a slow K^+-current, leading to an increase in SC. Therefore, the activity-dependent non-synaptic plasticity we described in this study could act like a gain mechanism. It could serve the purpose of tuning the T cells – and maybe in consequence also postsynaptic cells in the preparatory network – in an activity-dependent way to the combination of two computational tasks. Depending on the previous activity, T cells could react more or less to the inputs from the other mechanorecepors, and combine these synaptic responses with the spikes that encode light skin stimulation, which are elicited by T cell processes in the periphery.

Outlook

The local bend, one of the fastest movements in the leech, is initiated by sensory stimulation of the body wall. The morphology and response properties of the mechanosensory touch (T) cells suggest that T cells have at least two spike initiation zones, one in the periphery and one in the central ganglion. While spikes generated in the periphery should faithfully represent mechanical skin stimulation, the central part of the T cell should integrate and react to synaptic inputs from all three mechanoreceptor types. The activity-dependent non-synaptic plasticity introduced in this study could serve as a mechanism to tune the interaction of both spike initiation zones and their computational tasks. To test this hypothesis, further experiments are necessary to study to which extend repeated skin stimulation also triggers non-synaptic plasticity and how both spike initiation zones interact in these situations. If our hypothesis is correct, this multi-tasking ability and its activity-dependent tuning could make the T cell a key player in a fast-conducting preparatory network that regulates the gain of behaviors. The leech nervous system allows to study such network effects by further voltage-sensitive dye imaging of the ganglion during repeated skin stimulation and/or current injection to the T cell soma (Kretzberg et al., 2016; Fathiazar et al., 2018). Hence, despite the small number of neurons, the leech tactile system might be suitable for studies on general mechanisms underlying the flexibility of neural activity and behavior. As mechanoreceptors of leeches and humans share several fundamental properties (Baca et al., 2005; Pirschel and Kretzberg, 2016), our results might inspire studies in the field of prosthetics and artificial skins (Kim et al., 2014).

DATA AVAILABILITY STATEMENT

The datasets generated for this study are available on request to the corresponding author.

AUTHOR CONTRIBUTIONS

JK and SM planned the study and designed the figures. SM performed the experiments, analyzed the data, and drafted the text. GA did the neuron modeling. All authors contributed to writing the manuscript and interpreting the results.

FUNDING

This work was supported by the Deutsche Forschungsgemeinschaft (DFG, German Research Foundation) under Germany's Excellence Strategy EXC 2177/1 (Project ID 390895286).

ACKNOWLEDGMENTS

We thank Birte Groos for fitting the properties of the single T cell spike within the neuron model and all members of the computational neuroscience division for critically reading the manuscript. We also thank Christiane Thiel, Karin Dedek, and Gerrit Hilgen for commenting the manuscript and Tina Gothner for literally fruitful discussions.

REFERENCES

Baca, S. M., Thomson, E. E., and Kristan, W. B. (2005). Location and intensity discrimination in the leech local bend response quantified using optic flow and principal components analysis. *J. Neurophysiol.* 93, 3560–3572. doi: 10.1152/jn.01263.2004

Baljon, P. L., and Wagenaar, D. A. (2015). Responses to conflicting stimuli in a simple stimulus-response pathway. *J. Neurosci.* 35, 2398–2406. doi: 10.1523/jneurosci.3823-14.2015

Barreto, E., and Cressman, J. R. (2011). Ion concentration dynamics as a mechanism for neuronal bursting. *J. Biol. Phys.* 37, 361–373. doi: 10.1007/s10867-010-9212-9216

Baylor, D. A., and Nicholls, J. G. (1969a). After−effects of nerve impulses on signalling in the central nervous system of the leech. *J. Physiol.* 203, 571–589. doi: 10.1113/jphysiol.1969.sp008880

Baylor, D. A., and Nicholls, J. G. (1969b). Chemical and electrical synaptic connexions between cutaneous mechnoreceptor neurones in the central nervous system of the leech. *J. Physiol.* 203, 591–609. doi: 10.1113/jphysiol.1969.sp008881

Benda, J., and Herz, A. V. M. (2003). A universal model for spike-frequency adaptation. *Neural. Comput.* 15, 2523–2564. doi: 10.1162/089976603322385063

Blackshaw, S. E. (1981). Morphology and distribution of touch cell terminals in the skin of the leech. *J. Physiol.* 320, 219–228. doi: 10.1113/jphysiol.1981.sp013945

Briggman, K. L., and Kristan, W. B. Jr. (2006). Imaging dedicated and multifunctional neural circuits generating distinct behaviors.

J. Neurosci. 26, 10925–10933. doi: 10.1523/jneurosci.3265-06.2006

Burgin, A. M., and Szczupak, L. (2003). Network interactions among sensory neurons in the leech. *J. Comp. Physiol. A* 189, 59–67. doi: 10.1007/s00359-002-0377-378

Burrell, B. D., and Sahley, C. L. (2004). Multiple forms of long-term potentiation and long-term depression converge on a single interneuron in the leech CNS. *J. Neurosci.* 24, 4011–4019. doi: 10.1523/JNEUROSCI.0178-04.2004

Calabrese, R. L. (1980). Control of multiple impulse-initiation sites in a leech interneuron. *J. Neurophysiol.* 44, 878–896. doi: 10.1152/jn.1980.44.5.878

Carlton, T., and McVean, A. (1995). The role of touch, pressure and nociceptive mechanoreceptors of the leech in unrestrained behaviour. *J. Comp. Physiol. A* 177, 781–791. doi: 10.1007/BF00187637

Cataldo, E., Brunelli, M., Byrne, J. H., Av-Ron, E., Cai, Y., and Baxter, D. A. (2005). Computational model of touch sensory cells (T cells) of the leech: role of the afterhyperpolarization (AHP) in activity-dependent conduction failure. *J. Comput. Neurosci.* 18, 5–24. doi: 10.1007/s10827-005-5477-5473

Catarsi, S., and Brunelli, M. (1991). Serotonin depresses the after-hyperpolarization through the inhibition of the Na+/K+ electrogenic pump in T sensory neurones of the leech. *J. Exp. Biol.* 155, 261–273.

Catarsi, S., Scuri, R., and Brunelli, M. (1993). Cyclic AMP mediates inhibition of the Na+-K+ electrogenic pump by serotonin in tactile sensory neurones of the leech. *J. Physiol.* 462, 229–242. doi: 10.1113/jphysiol.1993.sp019552

Clarac, F., and Cattaert, D. (1999). Functional multimodality of axonal tree in invertebrate neurons. *J. Physiol.* 93, 319–327. doi: 10.1016/S0928-4257(00)80060-80061

Deitmer, J. W., and Schlue, W. R. (1983). Intracellular Na+ and Ca2+ in leech Retzius neurones during inhibition of the Na+-K+ pump. *Pflügers Arch. Eur. J. Physiol.* 397, 195–201. doi: 10.1007/BF00584357

Duménieu, M., Fourcaud-Trocmé, N., Garcia, S., and Kuczewski, N. (2015). Afterhyperpolarization (AHP) regulates the frequency and timing of action potentials in the mitral cells of the olfactory bulb: role of olfactory experience. *Physiol. Rep.* 3:e12344. doi: 10.14814/phy2.12344

Fathiazar, E., Hilgen, G., and Kretzberg, J. (2018). Higher network activity induced by tactile compared to electrical stimulation of leech mechanoreceptors. *Front. Physiol.* 9:173. doi: 10.3389/fphys.2018.00173

Forrest, M. D. (2014). The sodium-potassium pump is an information processing element in brain computation. *Front. Physiol.* 5:472. doi: 10.3389/fphys.2014.00472

Frady, E. P., Kapoor, A., Horvitz, E., and Kristan, W. B. Jr. (2016). Scalable semisupervised functional neurocartography reveals canonical neurons in behavioral networks. *Neural. Comput.* 218, 1453–1497. doi: 10.1162/NECO_a_00852

Gerard, E., Hochstrate, P., Dierkes, P.-W., and Coulon, P. (2012). Functional properties and cell type specific distribution of I(h) channels in leech neurons. *J. Exp. Biol.* 215, 227–238. doi: 10.1242/jeb.062836

Goldman, M. S., Golowasch, J., Marder, E., and Abbott, L. F. (2001). Global structure, robustness, and modulation of neuronal models. *J. Neurosci.* 21, 5229–5238. doi: 10.1523/JNEUROSCI.21-14-05229.2001

Gulledge, A. T., Dasari, S., Onoue, K., Stephens, E. K., Hasse, J. M., and Avesar, D. (2013). A sodium-pump-mediated afterhyperpolarization in pyramidal neurons. *J. Neurosci.* 33, 13025–13041. doi: 10.1523/JNEUROSCI.0220-13.2013

Hakizimana, P., Brownell, W. E., Jacob, S., and Fridberger, A. (2012). Sound-induced length changes in outer hair cell stereocilia. *Nat. Commun.* 3:1094. doi: 10.1038/ncomms2100

Hodgkin, A. L., and Katz, B. (1949). The effect of sodium ions on the electrical activity of the giant axon of the squid. *J. Physiol.* 108, 37–77. doi: 10.1113/jphysiol.1949.sp004310

Hübel, N., and Dahlem, M. A. (2014). Dynamics from seconds to hours in Hodgkin-Huxley model with time-dependent ion concentrations and buffer reservoirs. *PLoS Comput. Biol.* 4:e1003941. doi: 10.1371/journal.pcbi.1003941

Jansen, J. K. S., and Nicholls, J. G. (1973). Conductance changes, an electrogenic pump and the hyperpolarization of leech neurones following impulses. *J. Physiol.* 229, 635–655. doi: 10.1113/jphysiol.1973.sp010158

Johansen, J. (1991). Ion conductances in identified leech neurons. *Comp. Biochem. Physiol. Part A Physiol.* 100, 33–40. doi: 10.1016/0300-9629(91)90180-K

Johansen, J., and Kleinhaus, A. (1986). Differential sensitivity of tetrodotoxin of nociceptive neurons in 4 species of leeches. *J. Neurosci.* 6, 3499–3504. doi: 10.1523/jneurosci.06-12-03499.1986

Johnson, K. O. (2001). The roles and functions of cutaneous mechanoreceptors. *Curr. Opin. Neurobiol.* 11, 455–461. doi: 10.1016/S0959-4388(00)00234-238

Kim, J., Lee, M., Shim, H. J., Ghaffari, R., Cho, H. R., Son, D., et al. (2014). Stretchable silicon nanoribbon electronics for skin prosthesis. *Nat. Commun.* 5:5747. doi: 10.1038/ncomms6747

Klees, G., Hochstrate, P., and Dierkes, P. W. (2005). Sodium-dependent potassium channels in leech P neurons. *J. Membr. Biol.* 208, 27–38. doi: 10.1007/s00232-005-0816-x

Kleinhaus, A. L., and Angstadt, J. D. (1995). Diversity and modulation of ionic conductances in leech neurons. *J. Neurobiol.* 27, 419–433. doi: 10.1002/neu.480270313

Kretzberg, J., Kretschmer, F., and Marin-Burgin, A. (2007). Effects of multiple spike-initiation zones in touch sensory cells of the leech. *Neurocomputing* 70, 1645–1651. doi: 10.1016/j.neucom.2006.10.048

Kretzberg, J., Pirschel, F., Fathiazar, E., and Hilgen, G. (2016). Encoding of tactile stimuli by mechanoreceptors and interneurons of the medicinal leech. *Front. Physiol.* 7:506. doi: 10.3389/fphys.2016.00506

Kristan, W. B., Calabrese, R. L., and Friesen, W. O. (2005). Neuronal control of leech behavior. *Prog. Neurobiol.* 76, 279–327. doi: 10.1016/j.pneurobio.2005.09.004

Kristan, W. B., McGirr, S. J., and Simpson, G. V. (1982). Behavioural and mechanosensory neurone responses to skin stimulation in leeches. *J. Exp. Biol.* 96, 143–160.

Kristan, W. B. J. (1982). Sensory and motor neurones responsible for the local bending response in leeches. *J. Exp. Biol.* 96, 161–180.

Larsson, H. P. (2013). What determines the kinetics of the slow afterhyperpolarization (sAHP) in neurons? *Biophys. J.* 104, 281–283. doi: 10.1016/j.bpj.2012.11.3832

Li, Q., and Burrell, B. D. (2008). CNQX and AMPA inhibit electrical synaptic transmission: a potential interaction between electrical and glutamatergic synapses. *Brain Res.* 1228, 43–57. doi: 10.1016/j.brainres.2008.06.035

Li, Q., and Burrell, B. D. (2009). Two forms of long-term depression in a polysynaptic pathway in the leech CNS: one NMDA receptor-dependent and the other cannabinoid-dependent. *J. Comp. Physiol. A* 195, 831–841. doi: 10.1007/s00359-009-0462-463

Li, Q., and Burrell, B. D. (2010). Properties of cannabinoid-dependent long-term depression in the leech. *J. Comp. Physiol. A* 196, 841–851. doi: 10.1007/s00359-010-0566-569

Lombardo, P., Scuri, R., Cataldo, E., Calvani, M., Nicolai, R., Mosconi, L., et al. (2004). Acetyl-L-carnitine induces a sustained potentiation of the afterhyperpolarization. *Neuroscience* 128, 293–303. doi: 10.1016/j.neuroscience.2004.06.028

Meyrand, P., Weimann, J., and Marder, E. (1992). Multiple axonal spike initiation zones in a motor neuron: serotonin activation. *J. Neurosci.* 12, 2803–2812. doi: 10.1523/JNEUROSCI.12-07-02803.1992

Miller, E. W., Lin, J. Y., Frady, E. P., Steinbach, P. A., Kristan, W. B., and Tsien, R. Y. (2012). Optically monitoring voltage in neurons by photo-induced electron transfer through molecular wires. *Proc. Natl. Acad. Sci. U.S.A.* 109, 2114–2119. doi: 10.1073/pnas.1120694109

Mistick, D. C. (1978). Neurones in the leech that facilitate an avoidance behaviour following nearfield water disturbances. *J. Exp. Biol.* 75, 1–23.

Muller, K. J., and Scott, S. A. (1981). Transmission at a 'direct' electrical connexion mediated by an interneurone in the leech. *J. Physiol.* 311, 565–583. doi: 10.1113/jphysiol.1981.sp013605

Nicholls, J. G., and Baylor, D. A. (1968a). Long-lasting hyperpolarization after activity of neurons in leech central nervous system. *Science* 162, 279–281. doi: 10.1126/science.162.3850.279-a

Nicholls, J. G., and Baylor, D. A. (1968b). Specific modalities and receptive fields of sensory neurons in CNS of the leech. *J. Neurophysiol.* 31, 740–756. doi: 10.1152/jn.1968.31.5.740

Nicholls, J. G., and Purves, D. (1970). Monosynaptic chemical and electrical connexions between sensory and motor cells in the central nervous system of the leech. *J. Physiol.* 209, 647–667. doi: 10.1113/jphysiol.1970.sp009184

Pinsker, H., and Kandel, E. R. (1969). Synaptic activation of an electrogenic sodium pump. *Science* 163, 931–935. doi: 10.1126/science.163.3870.931

Pirschel, F., Hilgen, G., and Kretzberg, J. (2018). Effects of touch location and intensity on interneurons of the leech local bend network. *Sci. Rep.* 8, 1–11. doi: 10.1038/s41598-018-21272-21276

Pirschel, F., and Kretzberg, J. (2016). Multiplexed population coding of stimulus properties by leech mechanosensory cells. *J. Neurosci.* 36, 3636–3647. doi: 10.1523/JNEUROSCI.1753-15.2016

Rolls, M. M., and Jegla, T. J. (2015). Neuronal polarity: an evolutionary perspective. *J. Exp. Biol.* 218, 572–580. doi: 10.1242/jeb.112359

Sahley, C. L., Modney, B. K., Boulis, N. M., and Muller, K. J. (1994). The S cell: an interneuron essential for sensitization and full dishabituation of leech shortening. *J. Neurosci.* 14, 6715–6721. doi: 10.1523/jneurosci.14-11-06715.1994

Scuri, R., Lombardo, P., Cataldo, E., Ristori, C., and Brunelli, M. (2007). Inhibition of Na+/K+ATPase potentiates synaptic transmission in tactile sensory neurons of the leech. *Eur. J. Neurosci.* 25, 159–167. doi: 10.1111/j.1460-9568.2006.05257.x

Scuri, R., Mozzachiodi, R., and Brunelli, M. (2002). Activity-dependent increase of the AHP amplitude in T sensory neurons of the leech. *J. Neurophysiol.* 88, 2490–2500. doi: 10.1152/jn.01027.2001

Simmons, M. A., and Schneider, C. R. (1998). Regulation of M-Type potassium current by intracellular nucleotide phosphates. *J. Neurosci.* 18, 6254–6260.

Smith, E. S. J., and Lewin, G. R. (2009). Nociceptors: a phylogenetic view. *J. Comp. Physiol. A. Neuroethol. Sens. Neural. Behav. Physiol.* 195, 1089–1106. doi: 10.1007/s00359-009-0482-z

Thomson, E. E., and Kristan, W. B. (2006). Encoding and decoding touch location in the leech CNS. *J. Neurosci.* 26, 8009–8016. doi: 10.1523/JNEUROSCI.5472-05.2006

Tomina, Y., and Wagenaar, D. A. (2018). Dual-sided voltage-sensitive dye imaging of leech ganglia. *Bio protocol* 8:e2751. doi: 10.21769/BioProtoc.2751

Valkanov, M., and Boev, K. (1988). Ionic currents in the somatic membrane of identified T-mechanosensory neurons isolated from segmental ganglia of the medicinal leech. *Gen. Physiol. Biophys.* 7, 643–649.

Vogalis, F., Storm, J. F., and Lancaster, B. (2003). SK channels and the varieties of slow after-hyperpolarizations in neurons. *Eur. J. Neurosci.* 18, 3155–3166. doi: 10.1111/j.1460-9568.2003.03040.x

Wagenaar, D. A. (2015). A classic model animal in the 21st century: recent lessons from the leech nervous system. *J. Exp. Biol.* 218, 3353–3359. doi: 10.1242/jeb.113860

Wyse, A. T., Bavaresco, C. S., Reis, E. A., Zugno, A. I., Tagliari, B., Calcagnotto, T., et al. (2004). Training in inhibitory avoidance causes a reduction of Na+,K+-ATPase activity in rat hippocampus. *Physiol. Behav.* 80, 475–479. doi: 10.1016/J.PHYSBEH.2003.10.002

Yamada, W., Koch, C., and Adams, P. (1998). "Multiple channels and calcium dynamics," in *Methods in Neuronal Modeling: From Ions to Networks*, 2nd Edn, eds C. Koch, and I. Segev, (Cambridge, MA: MIT Press).

Yau, K. W. (1976). Receptive fields, geometry and conduction block of sensory neurones in the central nervous system of the leech. *J. Physiol.* 263, 513–538. doi: 10.1113/jphysiol.1976.sp011643

Conflict of Interest: The authors declare that the research was conducted in the absence of any commercial or financial relationships that could be construed as a potential conflict of interest.

Copyright © 2019 Meiser, Ashida and Kretzberg. This is an open-access article distributed under the terms of the Creative Commons Attribution License (CC BY). The use, distribution or reproduction in other forums is permitted, provided the original author(s) and the copyright owner(s) are credited and that the original publication in this journal is cited, in accordance with accepted academic practice. No use, distribution or reproduction is permitted which does not comply with these terms.

Contributions of collaborators

Herewith, I would like to thank to my collaborators for my PhD thesis.

Study: Cellular basics of non-synaptic plasticity in leech touch neurons

Hodgkin-Huyley-Type neuron modelling was done and kindly provided by Dr. Go Ashida, Research Associate in the Division Computational Neuroscience, University of Oldenburg.

Study: Tactile stimulation of leech T cells.

The lab work was done by Maren Prelle (Jan-March 2020), exchange student of the division Computational Neuroscience, University of Oldenburg, Germany; currently at University of Cologne, Cologne, Germany

Study: Pharmacological blocking of Na^+/K^+ pump

The lab work was done by M.Sc. Ihor Arkhypchuk (Juli-Sept 2020), Master's student of the program Neuroscience at University of Oldenburg.

Study: Different baseline recordings

Half of the lab work was done by M.Sc. Jens-Steffen Scherer (May-June 2020), Research Associate and PhD candidate in the Division Computational Neuroscience, at University of Oldenburg.

Study: VSD recordings

Data Analysis and figure generation was done by B.Sc. Jimin Roh (Sept-Okt. 2020), Master's student of the program Neuroscience at University of Oldenburg)

Curriculum Vitae

Personal information

Sonja Meiser

Leriguaweg 77 – D – 26131 Oldenburg

Phone: +49 1520 259 2011

Mail: sonja.meiser@uol.de

Birth Date; -Place: 04.08.1991 Heidelberg

Academic Education

PhD Studies in Neurosensory Science & Systems **10/2016 – 01/2021**

Doctoral Thesis: „Cell intrinsic plasticity in leech touch neurons"

Carl von Ossietzky Universität Oldenburg

Masterstudium Biologie (final grade 1,31) **10/2014 – 09/2016**

Master's thesis: „Anatomische, Physiologische und Funktionelle Charakterisierung der Anterior Pagoda Zelle des medizinischen Blutegels", Grade 1,27

Carl von Ossietzky Universität Oldenburg

Bachelorstudium Biologie (final grade 1,67) **10/2011 – 09/2014**

Bachelor's thesis: „Expression und Lokalisation von Connexin43 in der Retina von wildtypischen und Connexin57-defizienten Mäusen", Grade: 2,0

Carl von Ossietzky Universität Oldenburg

Abitur (final grade 2,3) **09/2002 – 05/2011**

Examination subject: Mathematics, german, french, sports, religion

Kurpfalz Gymnasium Schriesheim

Professional Experience

Research Associate 10/2016 – 09/2020

Computational Neuroscience - Carl von Ossietzky Universität Oldenburg

- Electrophysiological research and data analysis
- Individual supervision of students in projects and final theses
- Laboratory management and organization

Scientific Career

Journal Publications

Meiser, Sonja; Ashida, Go; Kretzberg, Jutta November 2019 Non-synaptic Plasticity in Leech Touch Cells. In: Frontiers in physiology 10, S. 1444. DOI: 10.3389/fphys.2019.01444.

Conference Talk

Meiser, Sonja (2019): Activity-dependent non-synaptic cellular plasticity in leech touch sensory neurons depends on Na+/K+ pump. Francis Crick Institute. European Neuroscience Conference for undergraduate students. London, 24.06.2019.

Published Poster Abstracts

Meiser, Sonja; Ashida, Go; Kretzberg, Jutta (2019): Hodgkin-Huxley type neuron model for activity-dependent non-synaptic plasticity of leech touch cells. Hg. v. Bernstein Center for Computational Neuroscience. Bernstein Conference. Berlin. DOI: 10.12751/nncn.bc2019.0176

Meiser, Sonja; Ashida, Go; Kretzberg, Jutta (2018): Repeated Mechanoreceptor Stimulation Causes Two Different Forms of Activity-Dependent Neuronal Plasticity in One Cell. Hg. v. Bernstein Center for Computational Neuroscience. Bernstein Conference. Berlin. DOI: 10.12751/nncn.bc2018.0241

Trende, Alexander; Ahmed, Zurna; Meiser, Sonja; Ashida, Go; Kretzberg, Jutta (2017): Which abstraction level to choose for the leech local bend network model? Hg. v. Bernstein Center for Computational Neuroscience. Bernstein Conference. Göttingen. DOI: 10.12751/nncn.bc2017.0185

Danksagungen

An dieser Stelle möchte ich mich bei allen Personen bedanken, die mich im Laufe meiner Doktorarbeit begleitet und unterstützt haben.

Mein ausdrückliches Dankeschön gilt Frau Prof. Dr. Jutta Kretzberg, die mir die Möglichkeit gab, im Rahmen meiner Doktorarbeit, ein sehr interessantes Projekt zu bearbeiten. Vielen Dank für die Betreuung während meiner Zeit in der Arbeitsgruppe, dem mir entgegengebrachten Vertrauen und der Möglichkeit für eigenständiges Arbeiten. Außerdem möchte ich mich für Dein kritisches Lesen der Arbeit bedanken.

Frau Apl. Prof. Dr. Karin Dedek danke ich herzlich für die Übernahme des Zweitgutachtens sowie die Begleitung meiner wissenschaftlichen Ausbildung vom Bachelorstudium über den Masterabschluss bis hin zur Promotion. Herzlichen Dank an Dr. Gerrit Hilgen für die Übernahme des externen Gutachtens und für den zahlreichen Input in den Promotionskomitees. Des Weiteren möchte ich mich bei Euch Karin und Gerrit dafür bedanken, dass Ihr mir immer mit Rat und Tat zur Seite standet, wenn eine Frage aufkam oder es darum ging ein experimentelles Problem zu lösen.

Den Mitgliedern der Abteilung Computational Neuroscience danke ich für die angenehme Atmosphäre während meiner Zeit in der Arbeitsgruppe.

Für die Hilfestellung und Unterstützung in jeglichen Fragen mit MATLAB, Mathematik und Statistik danke ich ganz besonders Dr. Lena Köpcke, Dr. Go Ashida und Jens-Steffen Scherer.

Tina Gothner gilt mein Dank für die schöne Zeit auf den gemeinsamen Konferenzen.

Ein ausdrückliches Dankeschön geht auch an meine Eltern und Großeltern, für die ständige Unterstützung während meines gesamten Studiums. Sie haben immer an mich geglaubt und mich in meinem Vorhaben unterstützt.

Ein besonderer Dank gilt Eric, der immer für mich da war und mich in jeglicher Hinsicht unterstützt hat.

Erklärung

Hiermit erkläre ich, dass ich die vorliegende Dissertation selbstständig angefertigt, nur die angegebenen Hilfsmittel und Quellen verwendet und sie in dieser oder ähnlicher Form noch nicht anderweitig eingereicht habe.

_____

Sonja Meiser

Oldenburg, den 17.11.2020